INVESTIGATING THE *IN VIVO* ROLE

OF WNT ACYLATION

Kelsey Foss Speer

A DISSERTATION

in

Cell and Molecular Biology

Presented to the Faculties of the University of Pennsylvania

in

Partial Fulfillment of the Requirements for the

Degree of Doctor of Philosophy

2017

Supervisor of Dissertation:

Peter Klein, M.D., Ph.D.
Professor of Medicine

Co-Supervisor of Dissertation:

Mark Lemmon, Ph.D.
Adjunct Professor of Biochemistry and Biophysics

Graduate Group Chairperson:

Dan Kessler, Ph.D.
Associate Professor of Cell and Developmental Biology

Dissertation Committee

Michael Granato, Ph.D., Professor of Cell and Developmental Biology

Dan Kessler, Ph.D., Associate Professor of Cell and Developmental Biology

Eric Witze, Ph.D., Assistant Professor of Cancer Biology

Kate Ferguson, Ph.D., Associate Professor of Pharmacology, Yale University

INVESTIGATING THE *IN VIVO* ROLE OF WNT ACYLATION

COPYRIGHT

2017

Kelsey Foss Speer

This work is licensed under the

Creative Commons Attribution-

NonCommercial-ShareAlike 3.0

License

To view a copy of this license, visit

https://creativecommons.org/licenses/by-nc-sa/3.0/us/

Acknowledgements

I am grateful for the many people who supported me in the completion of this dissertation. I would like to thank my thesis committee for their guidance over the past four years. I would additionally like to thank Paul Wileyto, Ph.D., for his help with the statistical analysis of the presented data. I am also grateful for the help and support of Andrea Stout and Jasmine Zhao of the CDB microscopy core for their support in the collection of confocal microscopy data.

I would like to thank my two advisors, Peter Klein and Mark Lemmon, for allowing me to start a brand-new collaborative project for my thesis. I heartily enjoyed the intellectual experience of having one foot in each lab. A special thanks to Peter Klein for showing me the ins and outs of working with *Xenopus laevis* as a model organism. I would also particularly like to thank Mark Lemmon for continuing to support my scientific growth even after his lab moved to Yale University.

The completion of this dissertation was made possible by the amazing network of scientists that supported my scientific and personal growth in both the Klein and Lemmon labs. I appreciate your friendship and advice more every day. I would also like to thank my parents Darsi Foss and Matthew Speer for teaching me how to persevere. I am also grateful for the support of my sisters, Madison and MacKenzie, and my husband Scott.

Abstract

INVESTIGATING THE *IN VIVO* ROLE OF WNT ACYLATION

Kelsey Foss Speer

Peter S. Klein

Mark A. Lemmon

Wnts are a family of morphogens that play diverse roles in embryonic patterning, the maintenance of adult stem cells, and the evolution of cancers. Mammalian genomes contain 19 unique Wnt proteins which undergo post-translational acylation at a highly-conserved serine residue. All Wnts bind to the Frizzled (Fz) family of seven-pass transmembrane receptor at an extracellular cysteine-rich domain (CRD). Recent crystallographic evidence suggests that interaction between Wnt and CRD is dependent upon the direct binding of an acyl group on the Wnt to a hydrophobic groove on the CRD. As all vertebrate Wnts are acylated at a conserved site, it is predicted that all Wnts will require acylation to recognize Fzs at the cell surface. However, this hypothesis has not been systematically tested. To address this gap in our understanding, I investigated the role of acylation in the signaling of Wnts *in vivo*. I hypothesized that if acylation were required for receptor binding, then preventing acylation would abolish the biological activity of these ligands. I tested my hypothesis in *Xenopus laevis* embryos competent to respond to the ectopic expression of Wnts. Surprisingly, I found that Wnt8 and Wnt3a were capable of robust signaling *in vivo* even when acylation was prevented. Both ligands also retained the ability to bind to the CRD of Fz8, suggesting that receptor recognition can occur through both acylation-dependent and acylation-independent mechanisms. In contrast, Wnts 1 and 5a required acylation to signal in *Xenopus* embryos. These findings challenge the assumption that acylation is absolutely required for the biological activity of Wnts. Furthermore, they reveal that Wnts have unique dependencies on acylation for their signaling roles *in vivo*, which may arise due to unique mechanisms of receptor activation.

Table of Contents

List of Figures

Chapter 1: Introduction

1.1. Wnts engage a diverse array of cell surface receptors

Wnts are an ancient family of extracellular ligands required for the patterning and maintenance of the vertebrate body plan. Nineteen Wnts, with different expression patterns and physiological roles, exist in the mammalian proteome (http://web.stanford.edu/group/nusselab/cgi-bin/wnt/). These ligands control cell identity, differentiation, proliferation, survival, polarity and migration in different contexts (Clevers, 2006). The regulation of such a wide range of cell processes is dependent upon the engagement of a diverse set of cell surface receptors (Niehrs, 2012). Unravelling Wnt signaling has proven challenging based upon the complexity of receptor interactions and technical limitations that have precluded the purification and study of components *in vitro.* However, our current understanding suggests that Wnts are multivalent proteins that physically crosslink unique receptors to form heterodimeric complexes at the cell surface (Bourhis et al., 2010; Janda et al., 2017). The ability of Wnts to "mix and match" these cell surface receptors appears to dictate which intracellular signaling responses occur.

Most Wnt signaling occurs through the Frizzled (Fz) family of seven-pass transmembrane receptor (Figure 1.1, Bhanot et al., 1996). The Fz family, consisting of ten members, shares the conserved domain architecture of the G-protein coupled receptor (GPCR) superfamily (Schulte and Bryja, 2007). Like GPCRs, the intracellular loops of the transmembrane domain and the C-tail serve as docking sites for intracellular effectors (MacDonald and He, 2012). Of particular importance is the highly-conserved KTXXW motif (Wong et al., 2003) that provides an essential binding site for the

intracellular effector Dishevelled (Cong et al., 2004). Fzs also contain a large N-terminal domain, called the cysteine-rich domain (CRD), that projects into the extracellular space (Vinson et al., 1989; Byrne et al., 2016) and is both necessary and sufficient for Wnt binding (Bhanot et al., 1996; Hsieh et al., 1999). The only crystallographic evidence we currently have for Wnt binding to a receptor is of *Xenopus laevis* (x)Wnt8 bound to the CRD of murine (m)Fz8 (Figure 1.4, Janda et al., 2012). The structure supports the hypothesis that Wnts are asymmetric ligands that may crosslink a CRD-containing receptor with a co-receptor. However, as of yet, there has been no *in vivo* validation of the observed binding interfaces and the significance of this structure to the biology of Wnts remains unclear.

The receptors LRP5 and 6, members of the low-density lipoprotein receptor (LDLR) family, are the most common co-receptors for Fzs (Figure 1.1, Wehrli et al., 2000; Tamai et al., 2000). We know a great deal more about the role of LRPs in the activation of cytoplasmic Wnt signaling than we do about the role of Fzs. LRP5/6 are single-pass transmembrane receptors with an intracellular domain that provides binding sites for Wnt effectors. Wnt stimulation drives the phosphorylation of five intracellular PPPSPxS repeats by the kinases CK1α and GSK-3α/β (Davidson et al., 2005). These phosphorylated motifs serve as binding sites for the scaffold protein Axin, whose membrane association releases the negative regulation of the transcriptional co-activator β-catenin (discussed further in Section 1.3) (Tamai et al., 2004) (Zeng et al., 2005) (Davidson et al., 2005).

How do Wnts engage LRPs? The field has yet to produce a crystal structure of a Wnt bound to an LRP, but both biochemical and cellular studies suggest that LRPs may have multiple Wnt binding sites. The extracellular domains of LRPs include four tandem

copies of a motif containing a β-propeller domain followed by an EGF repeat (MacDonald and He, 2012). Antibodies targeting the first (N-terminal) β-propeller domain of LRP6 block the signaling activity of most Wnts (1, 2, 2b, 6, 7a, 7b, 8a, 9a, 9b, 10a, 10b), with the exception of Wnts 3 and 3a (Gong et al., 2010; Ettenberg et al., 2010). In converse, antibodies recognizing the third β-propeller domain selectively inhibit Wnt3/3a signaling. Biochemical data suggests that LRPs may engage these two Wnt-binding sites concurrently, with the prediction that LRPs may form oligomers containing multiple Fzs and Wnts at the cell surface (Bourhis et al., 2010). However, the mechanisms by which Wnts recognize, and distinguish between, these two sites remain unknown.

Recently, both genetic and cellular data have come to support the role of receptor tyrosine kinases (RTKs) as alternative Wnt receptors. RTKs differ from Fzs and LRPs in that, even amongst those that play a role in Wnt signaling, they contain diverse extracellular domains (Lemmon and Schlessinger, 2010). Some RTKs, including Ror2 and MuSK, contain CRDs that are related by both structure and function to Fz CRDs (Lemmon, unpublished; Saldanha et al., 1998; Oishi et al., 2003; Jing et al., 2009; Strochlic et al., 2012). However, unlike Fzs, the CRDs of RTKs form only part of a complex extracellular architecture that includes Ig domains and other domains of unknown function. PTK7 (or CCK4) is another Wnt-binding member of the RTK family that contains only Ig domains in its extracellular region, suggesting that Ig domains may also be capable of direct binding to Wnts (Lu et al., 2004b; Yen et al., 2009; Peradziryi et al., 2011; Martinez et al., 2015). Ryk is an RTK that contains an extracellular Wnt-inhibitory factor (WIF) domain similar to the WIF family of secreted Wnt antagonists and binds Wnt ligands directly (Patthy, 2000; Lemmon, unpublished).

In the canonical view of RTK signaling, ligand-induced receptor dimerization releases autoinhibition of the intracellular kinase domains by phosphorylation *in trans* (Lemmon and Schlessinger, 2010). However, Wnt-binding RTKs seem to break the canon, as Ror2, PTK7, and Ryk are all pseudokinases (Murphy et al., 2014; Mendrola et al., 2013; Yoshikawa et al., 2001; Inoue et al., 2004). Although we do not yet understand the nature of the Wnt-dependent complexes formed by RTKs, these receptors may undergo homodimerization (Liu et al., 2007; Liu et al., 2008; Grumolato et al., 2010), heterodimerization (Martinez et al., 2015), or act as alternative co-receptors for Fzs (Oishi et al., 2003; Yamamoto et al., 2008; Lu et al., 2004a; Kim et al., 2008; Shnitsar and Borchers, 2008). In summary, these data suggest that Wnts may recognize a diverse array of receptor domains, including CRDs, β-propeller domains, Ig domains and WIF domains. However, we know very little about what structural features of Wnts are required for these receptor interactions. The goal of this thesis to contribute to our understanding of how Wnts recognize binding partners *in vivo*.

1.2. Wnts activate at least two intracellular signaling pathways

1.2.1. The β-catenin dependent pathway

The best-studied role of Wnt signaling is to regulate the stability of the transcriptional co-activator β-catenin. Under basal conditions, intracellular levels of β-catenin are kept low by the activity of a large molecular machine called the β-catenin destruction complex (Figure 1.2, Nusse and Clevers, 2017). The core of the destruction complex is composed of two regulatory proteins, Axin and the APC tumor suppressor, that scaffold interactions between β-catenin and the serine/threonine kinases CK1α and GSK3α/β

(Liu et al., 2002; Amit et al., 2002; Munemitsu et al., 1995; Behrens et al., 1998; Hart et al., 1998; Nakamura et al., 1998; Hinoi et al., 2000). Sequential phosphorylation of β-catenin by these two kinases, respectively, creates a phosphodegron that targets β-catenin to the proteasome (Liu et al., 2002; Amit et al., 2002).

Wnt binding to Fz and LRP5/6 at the cell surface increases the stability of cytoplasmic β-catenin (Figure 1.2, Cook et al., 1996; Hernández et al., 2012), which can then translocate into the nucleus and act as a transcriptional co-activator with the TCF/LEF family of transcription factors (Behrens et al., 1996; Molenaar et al., 1996; McKendry et al., 1997; Brunner et al., 1997). A recent kinetic study of the CK1α and GSK3α/β phosphosites on β-catenin provided strong evidence that Wnt binding at the cell surface influences β-catenin stabilization at or upstream of β-catenin phosphorylation, although the mechanistic explanation for these observations remains contentious (Hernández et al., 2012). Data from the Klein laboratory supports the hypothesis that the kinase activity of GSK3α/β is enhanced by association with APC within the destruction complex under basal conditions (Valvezan et al., 2012). Upon Wnt stimulation, Axin translocates to the membrane and binds the phosphorylated tail of LRP5/6 (Mao et al., 2001; Tamai et al., 2004), causing a conformational change which dissociates APC from the destruction complex and decreases the activity of GSK3α/β towards β-catenin (Valvezan et al., 2012; Tran and Polakis, 2012).

What is the role of Fz and Dishevelled in this process? The binding of Dishevelled to the intracellular domain of Fzs appears to be critical for the activation of the canonical pathway but its mechanism of action is not clear (Nusse and Clevers, 2017). A recent study observed interactions between the DIX domains of Dishevelled

and Axin by NMR spectroscopy, suggesting that the binding of these two proteins at the membrane could play a role in stabilizing the active receptor complex and maintaining the interaction between Axin and LRP5/6 (Fiedler et al., 2011).

The stoichiometry of Wnt-induced complexes containing both Fzs and LRP5/6 is also not yet clearly defined. Although it is assumed to contain a 1:1:1 ratio of ligand to receptors, LRPs contain multiple Wnt binding sites that might be occupied simultaneously (Bourhis et al., 2010), allowing a single co-receptor to stabilize many Wnt/Fz pairs. Furthermore, ligands structurally unrelated to Wnts, such as Norrin, bind Fzs with distinct stoichiometry. Norrin is a lipid-free ligand for Fz4 that binds to the first and second β-propeller domains of LRP6 and activates the canonical Wnt pathway during angiogenesis in the developing eye (Xu et al., 2004; Ke et al., 2013; Shen et al., 2015; Chang et al., 2015). Unlike Wnts, Norrin is a dimer that can engage multiple Fz4 CRDs simultaneously, arguing that Fz clustering may be important to forming an active signaling complex (Shen et al., 2015; Chang et al., 2015). In summary, although Fz and LRP5/6 heterodimers are sufficient to activate Wnt signaling, the endogenous complexes formed at the cell membrane may be large assemblies of many Wnts and Wnt receptors.

Another unresolved aspect of the Fz and LRP5/6 complex is how Wnt binding regulates the active conformations of these receptors. Chimeric ligands that link lipid-free Fz-binding and LRP-binding modules can activate canonical Wnt signaling *in vivo* (Janda et al., 2017; Yan et al., 2017). Therefore, bringing the two receptors into close proximity may be sufficient to activate intracellular signaling. Additionally, a recent crystal structure of full-length Smoothened, a Hedgehog pathway receptor closely related to Fzs, suggests that conformational coupling between the ligand-binding module and the

intracellular motifs may be important for adopting the active signaling conformation of this class of receptors (Byrne et al., 2016). Although the purification and crystallization of Wnt/receptor complexes has proven difficult, structural studies performed with these new, chimeric ligands may yield insights into the conformation changes at the level of the receptor that induce active Wnt signaling.

The earliest evolutionary function of β-catenin dependent Wnt signaling was to provide a mechanism for patterning the the multicelluar embryo (Holstein, 2012). Key proteins in the pathway, including Wnts, Fzs, APC, and Axin, are absent from the genomes of protozoans but appear in primitive metazoans (Guder et al., 2006). β-catenin dependent signaling is responsible for establishing the anterior-posterior, or primary, body axis of almost all extant bilaterian and non-bilaterian metazoans (Petersen and Reddien, 2009a). These data demonstrate that specification of the primary body axis by β-catenin dependent Wnt signaling is a unifying principle of multicellular development.

Regeneration studies in planarians have proven to be an excellent system to study the conserved mechanisms of axis polarity. Transverse bisection of planaria initiates the regeneration of both anterior and posterior structures in the two resulting organisms. The treatment of regenerating planaria with siRNA targeting β-catenin or Wnt (WntP-1) results in the regeneration of only anterior structure (Petersen and Reddien, 2008; Gurley et al., 2008; Petersen and Reddien, 2009b). In contrast, siRNA knockdown of APC results in the regeneration of only posterior structures (Gurley et al., 2008). These data suggest that the patterning of the posterior pole requires high levels of Wnt signaling whereas the anterior pole requires low Wnt signaling. Indeed, the formation of

a posterior-high to anterior-low (or no) Wnt gradient is the conserved mechanism of establishing axis polarity from cnidarians to mammals (Petersen and Reddien, 2009a).

In both frogs and fish, the β-catenin dependent pathway also plays an important role in patterning the dorsal-ventral axis. Shortly after fertilization, frog embryos undergo a mechanical rearrangement during which the cell cortex shifts 30^{o} relative to the cytoplasm (Vincent et al., 1986). This rotation brings Wnt11 (Tao et al., 2005), originally associated with the vegetal cortical cytoplasm, in contact with the equatorial band of mesoderm on one side of the embryo (Rowning et al., 1997). Focal activation of the β-catenin dependent pathway within the mesoderm induces the transcription of dorsal determinants, includng *Siamois* and *Xnr3* (Lemaire et al., 1995; Brannon and Kimelman, 1996; Kessler, 1997; Smith et al., 1995; McKendry et al., 1997; Fan and Sokol, 1997). These cells give rise to the dorsal organizing center, originally identified by Hans Spemann and Hilde Mangold, which is necessary and sufficient for dorsalizing the three germ layers of the embryo (De Robertis et al., 2000).

The examples illustrated here represent only a small fraction of the patterning events that Wnts control during development. Murine knockout studies of components of the β-catenin dependent pathway show many tissue- and organ-specific defects (Logan and Nusse, 2004). One of the overarching themes that arises from these studies, however, is that the β-catenin dependent pathway is a master regulator of cell identity, survival and proliferation.

The β-catenin dependent pathway also plays important roles in adult tissue homeostasis and disease. Wnt signals are critical for the maintenance of stem cell identity in blood (Willert et al., 2003; Huang et al., 2012), skin (Lim et al., 2013), small

intestine (Korinek et al., 1998), and many other organs. Furthermore, Wnt stimulation has also proven critical to the culture of organoids derived from these tissues (Nusse and Clevers, 2017).

Unsurprisingly, the misregulation of this pro-proliferative, pro-survival signaling pathway often leads to human disease. Mammalian Wnt genes were first discovered as a common site of proviral insertion for the mouse mammary tumor virus (Nusse and Varmus, 1982). The most frequent disease-causing mutations in the pathway occur at the level of the β-catenin destruction complex, particularly APC (Anastas and Moon, 2012). Patients heterozygous for a loss-of-function allele of APC develop familial adenomatous polyposis, a disease characterized by the development of many hundreds of non-cancerous polyps throughout the intestine. With loss of heterozygosity, these polyps progress to colon cancer (Kinzler and Vogelstein, 1996). More recently, it was discovered that Wnt expression becomes upregulated in various human cancers, making them a potentially valuable therapeutic target (Yu et al., 2012; Madan et al., 2016; Tammela et al., 2017). However, the field lacks the mechanistic understanding of the interactions between Wnts and their respective receptors that might be used for the design of targeted therapeutics.

1.2.2. The planar cell polarity pathway

The planar cell polarity (PCP) pathway is a signaling cascade that induces the synchronized polarity of cells across the surface of a developing tissue. Our understanding of what this polarity looks like, with regards to both the composition and the asymmetric distribution of receptor complexes across a cell, originates from studies

of the *Drosophila* wing epithelium. In this tissue, the PCP pathway polarizes the apical surface of the epithelial cell layer to orient the uniform directional growth of wing hairs. The pathway consists of a core set of effectors that include both transmembrane (e.g., Fz/Fz1, Van Gogh/Strabismus, Flamingo) and intracellular (e.g., Dishevelled, Prickle, Diego) proteins (Gray et al., 2011). When a polarity signal is sensed by cells, the effectors are redistributed in an asymmetric fashion so that Van Gogh/Prickle complexes associate with the proximal apical membrane and Fz/Dishevelled/Diego complexes associate with the distal (Gray et al., 2011). PCP signaling also activates the small GTPase Rho and the Rho-associated kinase (ROK). The downstream consequences of activating these proteins have not been clearly elucidated in this system, but they likely play an important role in cytoskeletal remodeling and the establishment of cytoskeletal polarity (Amano et al., 2010).

Although Wnts are predicted to provide a polarity cue that initiates PCP signaling across a tissue, evidence for their involvement in *Drosophila* PCP remains limited. A recent study used both loss-of-function and gain-of-function analysis to suggest that gradients of Wingless (Wg, *Drosophila* homolog of Wnt1) and Wnt4 may bind Fz and provide directional cues for hair cell orientation in the *Drosophila* wing imaginal disc (Wu et al., 2013). However, the β-catenin dependent pathway and PCP pathway often work in tandem, first to establish cell identity and subsequently to induce cell polarity (Swarup and Verheyen, 2012), and therefore separating the contributions of these two pathways to tissue patterning has made interpretation of PCP phenotypes difficult. Furthermore, Wnt/Fz complexes activating the PCP pathway are thought to be LRP5/6 independent (van Amerongen and Nusse, 2009) and the question of which (if any) co-receptor stabilizes these interactions remains one of the key unanswered questions in the field.

The vertebrate planar cell polarity pathway appears to be a far more complicated signaling system, both requiring the core components identified in *Drosophila* as well as a much wider variety of Wnt receptors (Kikuchi et al., 2009). The polarization of the hair bundles on vestibular sensory cells within the mammalian inner ear has become a model system for studying the components of vertebrate PCP signaling. Mice null for both Fz3 and Fz6 display a pronounced misorientation of hair sensory cells, phenotypes analogous to the disruptions of polarity caused by Fz loss-of-function in the *Drosophila* wing (Wang et al., 2006b; Gubb and García-Bellido, 1982). Knockouts of Ryk, Ror2 and PTK7 all display similar defects in sensory cell polarity (Andre et al., 2012; Yamamoto et al., 2008; Lu et al., 2004b), suggesting that multiple types of Wnt-dependent receptor complexes may drive vertebrate PCP signaling (Figure 1.3). Genetic studies in zebrafish provide clear evidence that Wnts 5a and 11 control vertebrate PCP signaling (Heisenberg et al., 2000; Kilian et al., 2003). However, we do not yet understand what types of complexes assemble or how Wnt signals control their polarity.

Planar cell polarity signaling contributes to many tissue patterning events during embryogenesis. In vertebrates, the PCP pathway shapes at least two distinct types of morphological outcomes. The first outcome, as seen in the patterning of the hair cells of the inner ear, is to establish an architectural symmetry across the surface of a tissue. The second outcome is to link cell polarity with directed cell migration and/or cell rearrangement. The best-studied example of this patterning is the control of convergent extension movements in gastrulating frog and fish embryos (Skoglund and Keller, 2010). Convergent extension is a series of coordinated cellular rearrangements that result in the thinning and elongation of the tissues of the dorsal mesoderm and neuroectoderm (Keller and Tibbetts, 1989; Keller et al., 1989; Wallingford et al., 2000; Smith et al.,

2000). The cells within these tissues must be synchronously polarized for this rearrangement to occur correctly, and overexpression or depletion of PCP components results in neural tube closure defects and a shortened, curved axis (Sokol, 1996; Deardorff et al., 1998; Djiane et al., 2000; Wallingford et al., 2000; Smith et al., 2000; Wallingford et al., 2002). The role of PCP signaling in convergent extension movements is conserved in mammals (Wang et al., 2006a; Mahaffey et al., 2013) and disruption of this pathway similarly results in defects in neural tube closure in mice (Hamblet et al., 2002; Wang et al., 2006b; Etheridge et al., 2008; Yamamoto et al., 2008; Lu et al., 2004b). Genetic knockouts of PCP pathway components also show phenotypes in other morphogenic processes, most notably in cardiogenesis and limb bud elongation (Hamblet et al., 2002; Oishi et al., 2003; Halford et al., 2000).

Specific components of the PCP pathway have been implicated in both human congenital disorders and cancer phenotypes. Vangl1/2 (mammalian homolog of Strabismus) mutations were identified in a small subset of patients with neural tube defects (Kibar et al., 2007). Loss-of-function mutations in *Ror2*, *Wnt5a* and *Dishevelled1* cause both dominant and recessive forms of Robinow Syndrome, a congenital dwarfism (van Bokhoven et al., 2000; Afzal et al., 2000; Person et al., 2010; White et al., 2015). Ror2 signaling through Wnt5a also appears to contribute to the invasive phenotypes of many metastatic cancers (Enomoto et al., 2009; O'Connell et al., 2010; Yamamoto et al., 2009). Ror2 may prove to be an effective therapeutic target due to its low expression in adult tissues (Oishi et al., 1999), but to date, its mechanism of activation remains poorly understood.

1.2.3. Structural determinants of pathway specificity

Early studies searched for a one-to-one code of Wnts and Fzs whose relative expression would determine cell responsiveness and pathway activation. However, in cell-based assays, Wnts bind Fzs with highly-overlapping affinities (Hsieh et al., 1999; Deardorff et al., 2001; Ring et al., 2014; Dijksterhuis et al., 2015). The perceived promiscuity of Wnts has led to the hypothesis that selective pathway activation may be entirely determined by the cohort of receptors expressed by a given cell (Mikels and Nusse, 2006; He et al., 1997; Umbhauer et al., 2000). In support of this argument, Fz/Fz1 and Fz2 in *Drosophila* demonstrate structurally-encoded signaling specificity: although both receptors are capable of binding Wg (Rulifson et al., 2000), ectopic expression of either Fz1 or Fz2 in the wing imaginal disc of the *Drosophila* embryo causes strikingly different phenotypes. Whereas Fz1 overexpression disrupts PCP-dependent hair cell polarity (Krasnow and Adler, 1994; Boutros et al., 2000), Fz2 causes the formation of ectopic hairs by activating β-catenin dependent signaling (Cadigan et al., 1998; Zhang and Carthew, 1998). Through the use of Fz1/2 chimeras, researchers determined that the C-tail and intracellular loops of the transmembrane domain strongly influence the type of signaling response occurring downstream of a receptor (Boutros et al., 2000). In vertebrates, Fzs 3, 6 and 7 specifically signal through the PCP pathway (Gray et al., 2011), arguing that pathway selectivity is a highly-conserved, receptor-intrinsic property.

However, it seems undeniable that Wnts also contribute to signaling specificity. Similar to the functional differences observed between *Drosophila* Fzs 1 and 2, ectopic expression of Wnts in *Xenopus* embryos causes different phenotypic consequences. During the developmental window when the *Xenopus* dorsal-ventral axis is specified, the cells of the mesoderm remain competent to respond to the β-catenin dependent pathway

during cleavage stages (Heasman et al., 2000; Kao et al., 1986). A small subset of those cells is exposed to Wnt11 through the process of cortical rotation and becomes fated to form the dorsal organizing center (De Robertis et al., 2000). Ectopic expression of Wnts, or other positive regulators of β-catenin stability, within the naïve mesoderm induces the formation of a second organizing center (McMahon and Moon, 1989; Sokol et al., 1991; Funayama et al., 1995; Molenaar et al., 1996). These embryos develop two complete dorsal-anterior axes, including head, notochord, somites, and neural tube (Sokol et al., 1991).

However, only a subclass of Wnt ligands, including Wnts 1, 3a and 8, are capable of inducing axis duplication (McMahon and Moon, 1989; Sokol et al., 1991). The other subclass, which includes Wnt5a and Wnt4, does not readily induce second axes but can disrupt PCP-dependent convergence and extension movements when expressed from the dorsal tissues of the embryo (Du et al., 1995). Wnt11 appears to be a special case, as it is capable of inducing both phenotypes (Tao et al., 2005; Du et al., 1995). These data argue that Wnts have fundamentally different affinities for the Fzs (7 and 4), or Fz co-receptors, that are expressed in the *Xenopus* embryo during this developmental window (Medina et al., 2000; Shi and Boucaut, 2000). Furthermore, they demonstrate that the unique affinities of Wnts for receptors plays an important role in selective pathway activation.

Wnts engage a wide variety of receptors to regulate the activation of at least two distinct signaling outcomes *in vivo*. New research in the field continues to identify novel ways these complexes can be modified, such as through the regulation of Fz stability at the cell membrane by R-spondin signaling (Nusse and Clevers, 2017). However, our incomplete understanding of the core mechanisms by which Wnts control the formation

of different types of receptor complexes limits our interpretations of these novel pathway regulators. This thesis aims to address this gap in our knowledge by investigating the structural requirements for Wnt binding to receptors *in vivo*.

1.3. Receptor recognition by Wnts

One of the most important, and unanswered, questions in Wnt signaling is how Wnts recognize and engage different cell surface receptors. Our understanding of the biochemistry of Wnts and Wnt receptors has been stymied by technical difficulties associated with purifying and analyzing these ligands *in vitro*. Wnts are structurally complex proteins, sharing a nearly-invariant pattern of 22 cysteine residues that form 11 disulfide bonds (Janda et al., 2012). The polypeptide chain of Wnts also undergoes significant post-translational modification, including high levels of asparagine glycosylation (Komekado et al., 2007; Tanaka et al., 2002; Kurayoshi et al., 2007). Furthermore, most Wnts are post-translationally acylated at a highly-conserved serine residue (Willert et al., 2003; Takada et al., 2006; Kurayoshi et al., 2007; Najdi et al., 2012). The only exceptions to this rule are WntD (Ching et al., 2008) and DWnt5 (Lemmon lab, unpublished), both found in *Drosophila*.

Wnts are acylated by Porcupine, a membrane-bound O-acyltransferase. This hypothesis is primarily supported by *in vivo* data demonstrating that Porcupine inhibition or knockdown can reduce the hydrophobicity of Wnts, impair their secretion, and reduce their function (Zhai et al., 2004; Galli et al., 2007; Chen et al., 2009; van den Heuvel et al., 1993; Proffitt and Virshup, 2012; van den Heuvel et al., 1993; Chen et al., 2009; Biechele et al., 2013; Proffitt and Virshup, 2012). More recent biochemical data provides

support to the argument that Porcupine directly facilitates the chemical transfer of a fatty acid moiety to Wnt proteins (Takada et al., 2006; Gao and Hannoush, 2014; Rios-Esteves and Resh, 2013). The fatty acid itself is likely monounsaturated and between 13-16 carbons in length (Takada et al., 2006; Rios-Esteves and Resh, 2013) (Gao and Hannoush, 2014; Janda et al., 2012). Due to this modification, Wnts require detergents for solubilization *in vitro*, making them incompatible with many of the biochemical assays that might be used to determine the mechanisms of Wnt/receptor interactions (Willert et al., 2003; Kurayoshi et al., 2007).

Our current biochemical understanding of receptor recognition by Wnts is derived from a single crystal structure depicting xWnt8 bound to the mFz8 CRD (Janda et al., 2012). In this structure, xWnt8 adopts a crescent-like shape and engages the CRD with its extended arms, resembling the shape of a hand delicately grabbing an object with its thumb and index finger (Figure 1.4). The “thumb” represents the N-terminal arm of the Wnt, which interacts with the CRD at a surface called Site 1. The acylated serine sits at the tip of the thumb, and binding of the acyl group of the Wnt to a hydrophobic groove on the side of the CRD provides the primary driving force for Site 1 interaction (Janda et al., 2012). As all vertebrate Wnts are acylated at an equivalent residue, this binding mode may serve as a common mechanism for CRD recognition. However, this hypothesis has yet to be directly tested. The second crystallographic interface occurs almost 180^{o} away from Site 1, where the C-terminal “index finger” of the Wnt binds to the CRD through a protein-protein interface. This interface, called Site 2, is primarily stabilized by hydrophobic contacts between the two proteins. The amino acids on xWnt8 that engage in the Site 1 and Site 2 interactions are highly conserved across the Wnt family, strengthening the argument that they are likely to be bona fide binding interfaces *in vivo*

(Janda et al., 2012). Nevertheless, it is important to validate the biological predictions of a crystal structure to ensure that the interfaces do not represent a kinetically-trapped interaction or a binding intermediate. These assays have not been performed in the case of the xWnt8/mFz8 CRD structure. Therefore, while structure provides a useful starting point for our understanding of how Wnts bind CRDs, it also raises many questions about the nature of Wnt/receptor interactions *in vivo*.

1.4. The role of acylation in Wnt signaling

The xWnt8/mFz8 CRD crystal structure played an important role in resolving a decade-long controversy surrounding the site of acylation on Wnts. In 2003, the first study to report Wnt acylation used mass-spectrometry to identify the modified amino acid as the most N-terminal cysteine reside of Wnt3a (Willert et al., 2003). Many studies aiming to understand the role of acylation in Wnt signaling analyzed how mutations at this cysteine (also conserved across the Wnt family) changed the biological activity of Wnts (Willert et al., 2003; Komekado et al., 2007; Galli et al., 2007; Kurayoshi et al., 2007; Franch-Marro et al., 2008; Bänziger et al., 2006; Mulligan et al., 2012). However, a subsequent mass-spectrometry analysis of the same protein identified an alternative site of acylation at a serine residue (Takada et al., 2006) and the xWnt8/mFz8 CRD crystal structure has confirmed that this residue is the only site where covalent attachment of the acyl chain occurs (Janda et al., 2012). The previously implicated cysteine is, in fact, involved in a disulfide bond, suggesting that phenotypes caused by mutation of this cysteine, and attributed to acylation defects, were likely caused by protein misfolding. Thus, while the

crystal structure provided valuable information about the site of acylation, it also reopened many questions surrounding the role of acylation in Wnt signaling *in vivo.*

Acylation likely plays multiple roles in the signaling of Wnts. First, acylation appears to be required for the association of Wnts with Evi/Wntless, a cargo receptor that facilitates the trafficking of Wnts through the secretory pathway in many organisms (Bartscherer and Boutros, 2008). Second, acylation helps to shape extracellular Wnt gradients. Historically, Wnts were predicted to pattern tissues in the concentration-dependent manner of classic morphogens. The patterning of the *Drosophila* wing imaginal disc by Wg was the prototypical example of long-range Wnt signaling. In this tissue, Wnt-responsive genes *senseless* (high concentration threshold), *distal-less* (moderate concentration threshold) and *vestigial* (low concentration threshold) are activated at a distance from Wg-expressing cells (Lecuit and Cohen, 1997; Neumann and Cohen, 1997; Zecca et al., 1996; Swarup and Verheyen, 2012). However, it was recently demonstrated that a membrane-tethered version of Wg (NRT-Wg) can rescue Wg mutant embryos, suggesting that Wg gradients form through mechanisms independent of ligand diffusion (Alexandre et al., 2014). It is now well-accepted that, in most physiological contexts, Wnts signal by local cell-to-cell mechanisms (Papkoff and Schryver, 1990; Willert et al., 2003; Gao et al., 2011; Pfeiffer et al., 2002; Franch-Marro et al., 2008; Galli et al., 2007; Farin et al., 2016; Alexandre et al., 2014). The hydrophobic quality of the acyl tail may therefore “tether” Wnts to cell membranes in order to restrict their diffusion (Bartscherer and Boutros, 2008). Acylation also plays a tethering role in the biological activity of the EGFR ligand, Spitz (Miura et al., 2006). Lastly, the crystal structure of xWnt8 bound to the CRD of mFz8 predicts that acylation is required for Wnt recognition of Fzs at the cell surface (Janda et al., 2012). Based on this

evidence, there is a reasonable assumption in the field that Wnts require acylation for their biological activity. However, this prediction has not been systematically tested.

1.5. Research summary

This work directly examines the role of acylation in the *in vivo* signaling of Wnts. I began by analyzing the contributions of the Site 1 and Site 2 interfaces, predicted by the xWnt8/mFz8 CRD crystal structure, to the biological activity of xWnt8. I hypothesized that if these interfaces were critical for the ability of xWnt8 to engage CRDs, then mutating key amino acids at these sites would abolish the signaling of xWnt8 *in vivo*. xWnt8 is a potent activator of the β-catenin dependent pathway (Sokol et al., 1991). Therefore, I tested the signaling activity of xWnt8 mutants by evaluating their ability to cause dorsalization phenotypes in *Xenopus* embryos and to activate the transcription of the Wnt-responsive genes *Siamois* and *Xnr3.* I show that introducing point mutations to the predicted Site 2 interface abolishes the signaling of xWnt8 in *Xenopus* embryos. In contrast, mutating Site 1, including the acylated serine residue on xWnt8 (S187A), only caused a mild attenuation in signaling. These data suggested that xWnt8 might be capable of acylation-independent signaling. If true, I predicted that xWnt8 S187A would be capable of binding to Fz CRDs *in vivo*. To test this, I measured the association of xWnt8 S187A with the CRD of xFz8 by immunoprecipitation. I found that xWnt8 S187A was able to interact with the xFz8 CRD, providing support to the argument that acylation is not absolutely required for the signaling of xWnt8 *in vivo.* The data from these experiments are presented in Chapter 2.

In Chapter 3, I next asked whether other members of the Wnt family were also capable of acylation-independent signaling. I began these studies by analyzing the role of acylation in the signaling of Wnts 1 and 3a, which also activate the β-catenin dependent pathway and are considered functionally redundant with Wnt8. I mutated the respective sites of acylation on both Wnts and measured their ability to dorsalize *Xenopus* embryos and activate the transcription of *Siamois* and *Xnr3*. I discovered that Wnt3a, like xWnt8, can activate the β-catenin dependent pathway when acylation is prevented. In contrast, Wnt1 demonstrated no acylation-independent activity. Finally, I tested the role of acylation in the signaling of Wnt5a, a ligand that preferentially activates the planar cell polarity pathway. I discovered that Wnt5a, like Wnt 1, does not induce PCP dependent phenotypes in embryos when acylation is prevented. These data argue that neither acylation-dependence nor acylation-independence is a unique property of the Wnt family. Further a discussion of the implications of this work, with an emphasis on how these results affect our understanding of the structural relationships between Wnts and their receptors, is presented in Chapter 4.

Figure 1.1. Wnts bind a diverse set of cell surface receptors.

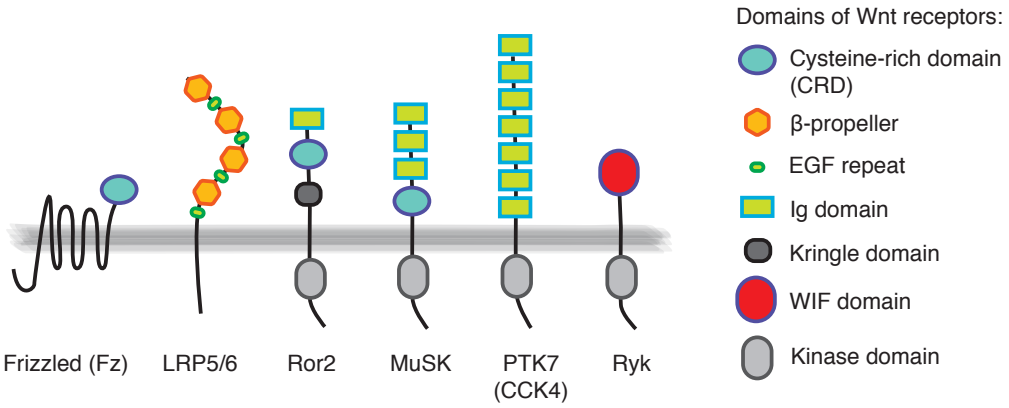

Figure 1.1. Wnts bind a diverse set of cell surface receptors. All Wnts bind the Frizzled (Fz) family of seven-pass transmembrane receptor (left) at their cysteine-rich domain (CRD). LRP5/6 (second left) act as co-receptors for Fzs. The LRP5/6 extracellular domain is composed of repeating β-propeller and EGF repeat elements. The first (top) and third β-propeller domains are thought to contain Wnt binding sites. Members of the receptor tyrosine kinase family, all containing intracellular kinase domains, may also act as Wnt receptors. Ror2 and MuSK also contain a CRD important for Wnt binding. Ror2 also has an extracellular Ig domain and Kringle domain of unknown function. MuSK contains two additional Ig domains in addition to the CRD. PTK7 (also known as CCK4) has seven tandem Ig domains in its extracellular domain. Ryk contains an extracellular Wnt-inhibitory factor (WIF) domain homologous to the WIF family of secreted Wnt antagonists.

Figure 1.2. The β-catenin dependent pathway.

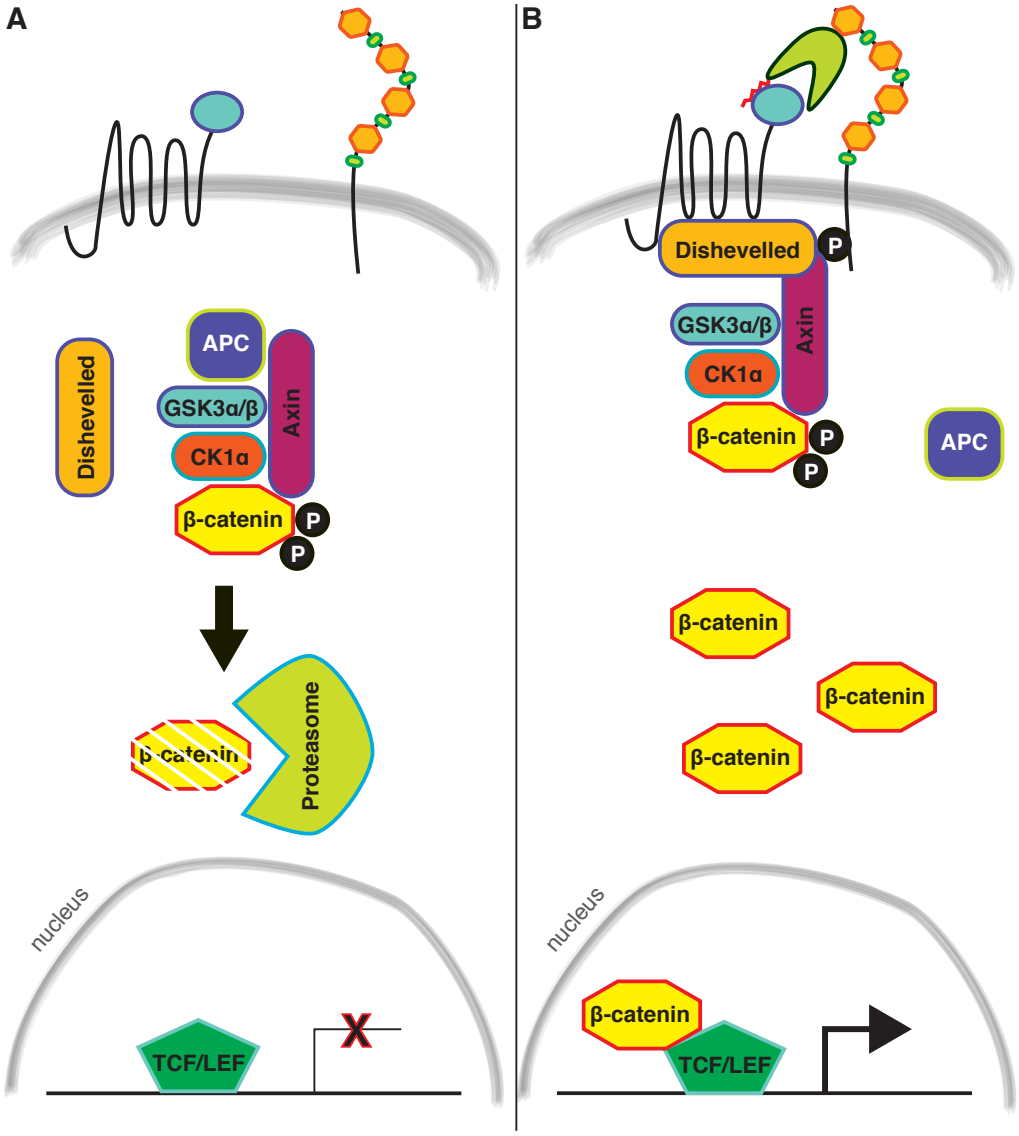

Figure 1.2 The β-catenin dependent pathway. (A) In the absence of Wnt, β-catenin levels are kept low by the β-catenin destruction complex, composed of Axin, APC, CK1α and GS3Kα/β. Sequential phosphorylation of β-catenin by CK1α and GS3Kα/β marks it for proteasomal degradation. (B) Upon Wnt binding to a Fz and LRP5/6 heterodimer at the cell surface, CK1α and GS3Kα/β phosphorylate PPPSPxS repeats on the intracellular domain of LRP5/6. Axin binds these phosphorylated motifs on LRP5/6, which induces the dissociation of APC from the complex. Dishevelled binds the intracellular C-tail of Fz and may also bind Axin. Without APC, the kinase activity of GS3Kα/β is reduced, and less β-catenin is marked for destruction. β-catenin is then able to translocate into the nucleus and bind to the TCF/LEF family of transcription factors to activate the transcription of target genes.

Figure 1.3. The Planar Cell Polarity pathway.

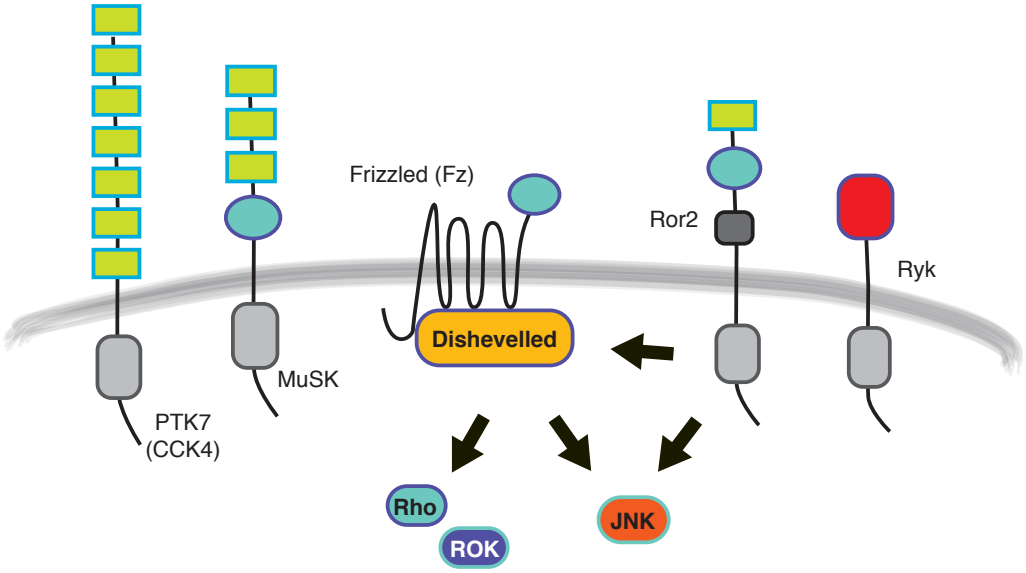

Figure 1.3. The Planar Cell Polarity pathway. The Planar Cell Polarity (PCP) pathway creates synchronized polarity across the surface of a tissue through the asymmetric redistribution of receptor complexes. In vertebrates, PCP signaling is activated by Wnts 5a and 11 through their interaction with a wide variety of cell surface receptors. Genetic evidence suggests Fzs, Ror2, Ryk, MuSK and PTK7 likely play a role in controlling polarity. However, how these receptors engage Wnts, and what types of complexes form, remain poorly understood. The pathway depends upon the intracellular effectors Dishevelled, the small GTPase Rho and the Rho-associated Kinase (ROK), and the kinase JNK. Current evidence points to these effectors having complex, cell type specific mechanisms of action.

Figure 1.4. The xWnt8/mFz8 CRD crystal structure.

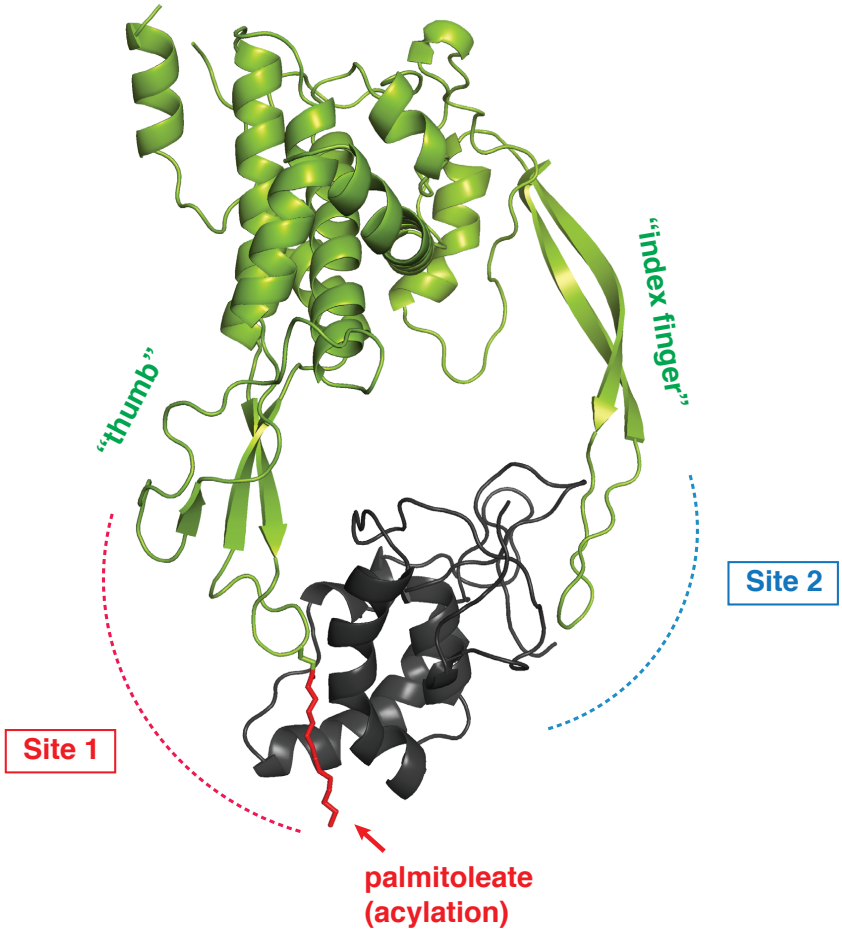

Figure 1.4. The xWnt8/mFz8 CRD crystal structure. Crystal structure of xWnt8 (green) bound to the mFz8 CRD (black) (PDB ID: 4F0A). The “thumb” and “index finger” arms of xWnt8 bind the CRD at interfaces Site 1 (red) and Site 2 (blue), respectively. The covalently attached palmitoleate moeity (red), also referred to as the “acyl tail,” on xWnt8 is the primary driver of Site 1 binding.

Chapter 2: Acylation in xWnt8 signaling

2.1 Introduction

Wnts are a family of 19 unique ligands that play key roles in the patterning and maintenance of the vertebrate organism. Wnt signaling regulates cell fate, proliferation, survival, polarity and migration under different physiological contexts (Kikuchi et al., 2009). The remarkable capacity for these ligands to control such a highly diverse set of cell processes is tied to their ability to engage and regulate many classes of cell surface receptor (Niehrs, 2012). However, the mechanisms by which Wnts recognize these receptors largely remains a mystery.

Binding studies using chimeric ligands have provided evidence that Wnts are multivalent proteins that crosslink a CRD-containing receptor to a co-receptor (Cong et al., 2004; Holmen et al., 2002; Janda et al., 2017). Most Wnt signaling occurs through the CRDs of Fzs, but members of the RTK family, including Ror2 and MuSK, also contain CRDs that are likely to be important for Wnt binding (Niehrs, 2012). Biochemical investigations into the interactions between Wnts and CRDs have been limited by technical difficulties associated with purifying active Wnt protein. Wnts are post-translationally acylated at a highly-conserved serine residue by the enzyme Porcupine (Willert et al., 2003; Takada et al., 2006; Gao and Hannoush, 2014). Unfortunately, the detergents required to stabilize this hydrophobic modification *in vitro* are incompatible with many of the biochemical assays that have been used to elucidate the binding mechanisms of other receptor and ligand families.

Our current understanding of the interactions of Wnts with CRDs is derived from a single crystal structure depicting the interaction of xWnt8 with the CRD of mFz8 (

Janda et al., 2012). In this structure, xWnt8 adopts a crescent-like shape and engages the CRD with two long projections called the thumb and index finger at interfaces named Site 1 and Site 2, respectively (Fig 1.4). The acylated serine residue on xWnt8 lies at the tip of the thumb, and the sequestration of this hydrophobic moiety within a binding groove on the side of the CRD is the primary driving force for the Site 1 interaction. At Site 2, which lies on the opposite side of the CRD, the index finger of xWnt8 engages the CRD primarily through a series of hydrophobic protein-protein contacts (Fig 1.4). The structural evidence presented in the xWnt8/mFz8 CRD crystal structure has led to the hypothesis that Wnts require acylation to recognize receptors. By extension, these data predict that a non-acylated Wnt will lack biologically activity. However, the interfaces engaged by xWnt8 in the crystal structure remain unverified *in vivo*, raising the possibility that they may not accurately represent the Wnt/CRD interactions occurring at the cell surface.

To determine the role of acylation in CRD binding, we assessed the relevance of the crystallographic Site 1 and Site 2 interfaces to the biological activity of xWnt8. Ectopic Wnt expression in the early *Xenopus* embryo causes the activation of the β-catenin dependent pathway, the formation of a second dorsal organizing center and the subsequent development of twinned dorsal structures (De Robertis et al., 2000; McMahon and Moon, 1989; Sokol et al., 1991). We hypothesized that introducing mutations to the protein surfaces required for CRD recognition would inhibit the ability of xWnt8 to activate the β-catenin dependent pathway and cause dorsalization phenotypes in embryos. To test this, we used site-directed mutagenesis to disrupt amino acids on the thumb and index finger of xWnt8 that make key interactions with the CRD at Site 1 and Site 2 (Figure 2.1). We demonstrate that mutations to the Site 2 interface inhibit the

signaling of xWnt8 *in vivo* (Figure 2.3), arguing that this binding surface plays an important role in the biology of the ligand. In contrast, our data reveal that xWnt8 activates the β-catenin dependent pathway and binds to the CRD of xFz8 even when Site 1 residues, in particular the site of acylation, are mutated (Figures 2.3 – 2.5). Our findings challenge the hypothesis that acylation is required for biological activity of Wnts and argue that acylation-independent CRD binding can occur *in vivo*.

2.2 Selection of xWnt8 point mutations

We began our study with the prediction that, if the Site 1 and Site 2 interfaces are required for xWnt8 binding to Fz CRDs, then mutating key amino acids on the thumb or index finger will abolish signaling *in vivo*. Mutations were chosen to disrupt interactions seen in the xWnt8/mFz8-CRD crystal structure (Figure 2.1, Janda et al., 2012). Three xWnt8 variants were designed to progressively disrupt Site 2 binding (W319A, W319A/F317A, and W319A/F317A/V323A) – the triple mutant altering all Site 2 contact residues in xWnt8 except C321 (where changes would likely cause misfolding). K182S, K182S/W196A, and K182S/W196A/I186A variants were also generated to interrogate side chain-mediated interactions at Site 1. Separately, we replaced the acylation site serine (S187: Figure 2.1) with alanine to prevent acylation and thus investigate the importance of acylation in Fz binding.

2.3 Development of a grading system for Wnt phenotypes

To assess the biological activity of the Site 1 and Site 2 mutants, we analyzed their ability to dorsalize *Xenopus laevis* embryos through the ectopic activation of the β-catenin dependent pathway (McMahon and Moon, 1989; Sokol et al., 1991). In our assays, xWnt8 wild-type ($xWnt8^{WT}$) was used as a positive control. Injection of mRNA encoding $xWnt8^{WT}$ into the equatorial region of a ventrally-fated cell (ventral marginal zone, VMZ) at the four-cell stage activates a gene signature, including the transcription *Siamois* and *Xnr3*, which causes the formation of an ectopic dorsal organizing center within the embryo (Lemaire et al., 1995; Brannon and Kimelman, 1996) (Kessler, 1997) (Smith et al., 1995) (McKendry et al., 1997; Fan and Sokol, 1997; De Robertis et al., 2000). At low doses, Wnt injection causes bifurcation of the dorsal axis, resulting in partial (incomplete) or full (complete) duplication of dorsoanterior structures (Figure 2.2). At high doses, ectopic Wnt injection causes radial dorsalization of the embryo, similar to activation of the β-catenin dependent pathway by lithium treatment (Klein and Melton, 1996), and characterized by severe shortening of the anterior-posterior axis. In extreme cases, embryos become completely cylindrical (Figure 2.2A, far right).

To compare the severity of phenotypes caused by the Site 1 and Site 2 mutants, we created a novel grading system that represents each phenotype with a numerical score. As indicated in Figure 2.2, tailbud-stage embryos with a normal phenotype where given a score of zero, partial axis duplications a score of one, full axis duplications a score of two and radial dorsalization a score of three. Full axis duplications can be distinguished from partial axis duplications by the formation of a cement gland at the most anterior surface of the ectopic head (Figure 2.2B). For each mutant and dose, we summed the phenotype scores observed across each biological replicate and divided by

the total number of individuals analyzed. The resulting value falls on a 0 – 3 scale and is termed the mean dorsal score.

2.4 Comparison of Site 1 and Site 2 mutations

We next tested the ability of the xWnt8 Site 2 mutants to dorsalize *Xenopus* embryos upon ectopic expression of either 50 or 500pg of mRNA. For each mutant and dose, we calculated a mean dorsal score at the tailbud stages (Figure 2.3A, B). To confirm that the observed phenotypes arose specifically from activation of the Wnt pathway, we collected injected embryos at the early gastrula stage (Nieuwkoop and Faber, NF, stage 10) and measured the transcription of Wnt-specific gene targets *Siamois* and *Xnr3* (Figure 2.3C). xWnt8^{WT} is highly active under these assay conditions, causing nearly complete radial dorsalization of embryos at both 50 and 500 pg doses of mRNA. The robust activation of the canonical pathway within these embryos is highlighted by the approximately ten-fold increase in the transcription of both *Siamois* and *Xnr3*.

Even under conditions when xWnt8^{WT} causes near-maximal dorsalization of embryos, we observed very little biological activity in our Site 2 mutants (Figure 2.3A-C). xWnt8^{W319A} caused weak phenotypes at both 50 and 500 pg doses, but its activity is less than 500-fold that of WT (compare Figure 2.3A and 2.5A). we detected no phenotypes in embryos injected with either xWnt8$^{W319A/F317A}$ or xWnt8$^{W319A/F317A/V323A}$. Furthermore, none of the Site 2 mutants induced Wnt-specific transcription of *Siamois* and *Xnr3* (Figure 2.3C). We reasoned that a decrease in total protein expression could account for the observed loss of activity of xWnt8. However, Western blotting analysis performed on whole embryo lysates demonstrated that all three Site 2 mutants are highly expressed in

the embryo (Figure 2.3D, bottom). These data argue that mutating even a single residue on the index finger of xWnt8 causes a near-total loss in biological activity.

In contrast, the Site 1 mutations had minimal effects on the signaling of Wnt8 *in vivo*. The serine substitution at K182 – predicted to form a salt bridge with the E64 side-chain in mFz8 (Janda et al., 2012) – had no effect on xWnt8 activity (Figure 2.3A). xWnt8$^{K182S/W196A}$ and xWnt8$^{K182S/W196A/I186A}$ variants failed to express (Figure 2.3D, top), making their lack of activity uninterpretable. Given the suggested importance of the S187-linked acyl chain for Wnt/Fz interactions, we were very surprised to find that replacing this residue with alanine had only a mild effect. Indeed, at 500 pg, xWnt8^{S187A} radially dorsalizes embryos as effectively as WT (Figure 2.3A, B). xWnt8^{S187A} also activates the transcription of Wnt-responsive genes *Siamois* and *Xnr3* (Figure 2.3C). However, a dose-response analysis of xWnt8 phenotypes revealed a shift in the activity xWnt8^{S187A} compared to xWnt8^{WT} at lower mRNA concentrations. These signaling differences may arise due to changes in protein expression, localization, receptor affinity or antagonist interaction. We therefore measured the total expression of xWnt8 S187A in embryo lysates and found that it was not impaired, and in fact consistently measured higher than WT (Figure 2.3D, top and bottom).

We next hypothesized that the S187A mutation may shift the cellular localization of xWnt8. A previous study demonstrated that mutating the site of acylation on Wnt3a (S209A) results in an accumulation of the ligand within the endoplasmic reticulum in both *Xenopus* embryos and cultured cells (Takada et al., 2006). To determine the localization of xWnt8 S187A in *Xenopus* tissues, we performed immunofluorescence staining on the animal hemisphere cells of blastula stage (NF stage 9) embryos expressing either

xWnt8WT or S187A. Surprisingly, our data do not support the hypothesis that preventing acylation causes ER retention. As shown in Figure 2.4, there is a similar distribution of $xWnt8^{WT}$ and $xWnt8^{S187A}$ between the nucleus and the cell periphery within *Xenopus* cells, which argues against a significant defect in intracellular trafficking of $Wnt8^{S187A}$.

The shift in activity we see between xWnt8WT and S187A may be a consequence of the role that acylation plays in shaping Wnt gradients. In many physiological contexts, Wnts remain tightly associated with the membranes of producing cells, which could promote local Wnt-responsiveness by restricting ligand diffusion (Papkoff and Schryver, 1990; Willert et al., 2003; Pfeiffer et al., 2002; Franch-Marro et al., 2008; Galli et al., 2007; Gao et al., 2011; Farin et al., 2016; Alexandre et al., 2014). The hydrophobicity of Wnts is dependent upon acylation, suggesting that the acyl tail may act to "anchor" Wnts within the cell membrane (Chen et al., 2009). In support of this argument, our immunofluorescence data show co-localization of xWnt8 and mem-GFP staining in cells expressing xWnt8WT but not S187A (Figure 2.4). These observations bear a striking resemblance to the role of acylation in the activity of the *Drosophila* EGFR ligand, Spitz. Like Wnts, inhibiting the acylation of Spitz significantly impairs its ability to pattern the eye imaginal disc of the *Drosophila* embryo (Miura et al., 2006). This defect arises not from changes in protein secretion or receptor binding, but a failure to tether ligands at the cell membrane and prevent their diffusion. The similarities between these two protein families highlights the importance of tethering in the function of acylated ligands and raises possibility that xWnt8 may be able to productively bind Fz/LRP complexes when acyl binding at Site 1 is prevented.

2.5 Acylation-independent signaling of xWnt8

To further characterize the signaling of xWnt8^{S187A} *in vivo*, we injected four-cell stage embryos at the VMZ with xWnt8^{WT} or xWnt8^{S187A} mRNA in doses ranging from 1 pg to 500 pg/embryo. We analyzed dorsalization phenotypes at tailbud stages (Figure 2.5A, B) and expression of *Siamois* and *Xnr3* at gastrula stage (Figure 2.5C). xWnt8^{S187A} again displayed highly similar activity to xWnt8^{WT}. Both proteins cause a dose-dependent increase in mean dorsal score and Wnt target gene expression (Figure 2.5A-C). Both proteins reach equivalent mean dorsal score and gene expression maxima at 500 pg injected mRNA. These data suggest that, at high doses, the biological activity of xWnt8^{WT} and xWnt8^{S187A} are highly similar. Confirming our observations in Figure 2.3A, xWnt8 S187A displayed approximately ten-fold weaker activity compared to WT. Yet, Western blotting of whole embryos showed that the proteins are expressed at a similar magnitude (Figure 2.5D). We predict that the apparent shift in activity is likely due to a change in the behavior of the ligand within the extracellular space. These behaviors may include changes in affinity for extracellular binding partners (including receptors) or changes in local concentration caused by a Spitz-like diffusion mechanism. Yet, as demonstrated, xWnt8WT and S187A cause a nearly-identical frequency of the three dorsalization phenotypes (partial axis duplications, full axis duplications and radial dorsalization) when this shift is taken into account (compare 5 pg of xWnt8^{WT} and 50 pg of xWnt8^{S187A} in Figure 2.5A). These data show that non-acylated xWnt8 can induce very similar signaling consequences to acylated xWnt8 within the *Xenopus* embryo.

2.6 Acylation-independent CRD binding of xWnt8

Since xWnt8 can signal in the absence of acylation, we next asked whether it could also bind to the CRDs of Fzs. As both biochemical (Hsieh et al., 1999; Janda et al., 2012) and *in vivo* (Deardorff et al., 1998) data support the hypothesis that Fz8 acts as a receptor for xWnt8, we chose to test the interaction of this receptor and ligand pair. A protein construct encoding only the CRD of Fz8 (Fz8 CRD) inhibits the dorsalizing activity of xWnt8^{WT} in *Xenopus* embryos (Deardorff et al., 1998). If xWnt8^{S187A} also binds Fzs, then we predicted that the co-expression of a soluble CRD construct should inhibit the signaling of both ligands. I tested this hypothesis by injecting 5 pg of xWnt8^{WT} or 50 pg of xWnt8^{S187A} mRNA, either alone or in the presence of *Xenopus* (x)Fz8 CRD mRNA, into the VMZ of four-cell stage *Xenopus* embryos. I collected embryos at the gastrula stage (NF stage 10) and analyzed expression of *Siamois* and *Xnr3*. As shown in Figure 2.6A, co-expression of the xFz8 CRD inhibits activation of the canonical Wnt pathway by either ligand. These data argue that acylation-independent signaling is equally sensitive to inhibition by the xFz8 CRD as wild-type.

We next asked whether the xFz8 CRD binds xWnt8^{S187A} *in vivo*. We co-expressed xWnt8^{WT} and xWnt8^{S187A} with a myc-tagged version of the xFz8 CRD in *Xenopus* embryos and assessed their interaction by co-immunoprecipitation. As demonstrated in Figure 2.6B, both xWnt8^{WT} and xWnt8^{S187A} associate, in a dose-dependent manner, with the xFz8 CRD. Interestingly, xWnt8^{WT} associated more efficiently with the xFz8 CRD than xWnt8^{S187A}. This shift could be a consequence of differences in receptor affinity or protein localization, and will require further study. Nevertheless, these data show that Wnts can bind Fzs in an acylation-independent manner and provide strong support to the argument that acylation at serine 187 is not required for xWnt8-dependent activation of the β-catenin dependent pathway.

2.7 Conclusion

An outstanding question in the Wnt signaling field is how ligands recognize and activate cell surface receptors. The crystal structure of xWnt8 bound to the CRD of mFz8 provided an important structural hypothesis for what receptor engagement might look like *in vivo*. Surprisingly, the structure predicted that the acyl tail on Wnts plays a direct, and essential, role in binding CRDs. While it has become accepted by many in the field that Wnt acylation is required for the biological activity of these ligands, the binding interfaces depicted in the crystal structure had not been validated *in vivo*. To address this gap in our knowledge, we investigated the contribution of the proposed crystallographic interfaces to the signaling of xWnt8 in *Xenopus* embryos. Our studies reveal that introducing point mutations at the Site 2 protein-protein interface potently interferes with the signaling of xWnt8. In contrast, mutating the site of acylation at Site 1 only results in a mild attenuation in the signaling of the ligand. Importantly, non-acylated xWnt8 still engages the xFz8 CRD *in vivo*, as measured by immunoprecipitation. These data demonstrate that Wnts are capable of acylation-independent CRD binding and activation of the β-catenin dependent pathway.

Our data support the hypothesis that the residues of the Site 2 protein-protein interface are essential to the activity of xWnt8. We demonstrate that introducing even a single point mutation at the predicted binding surface (W319A) reduces the signaling of xWnt8 by more than 500-fold. Western blotting analysis illustrates that these point mutations do not cause defects in protein expression. To our knowledge, our data represent the first *in vivo* validation of the importance of Site 2 in the activity of a Wnt. Although we cannot rule out that the Site 2 mutations may cause defects in Wnt folding

and/or trafficking, they clearly provide an illustration of how a single point mutation at a key residue on the surface of xWnt8 potently reduces the signaling activity of the ligand.

In contrast, our data reveal that acylation is not required for productive binding between Wnts and Fzs. We show that mutating the site of acylation (S187A) on xWnt8 does not cause the protein to become inactive, as predicted by the crystal structure. Instead, we observe an approximately ten-fold shift in activity of the non-acylated Wnt as compared to WT. However, if the ten-fold shift in activity is accounted for (comparing 5pg of $xWnt8^{WT}$ to 50pg of $xWnt8^{S187A}$ in Figure 2.5A-C), the patterns of dorsalization and transcription are strikingly similar between the two proteins. These observations led us to hypothesize that a non-acylated Wnt may retain the ability to bind CRDs and activate Fz/LRP complexes at the cell surface. We used a soluble form of the xFz8 CRD to demonstrate that xWnt8 S187A can associate with Fz CRDs *in vivo*. In sum, our data demonstrate that the Site 1 acyl-protein interface is not absolutely required for the biological activity of xWnt8.

Our data raise the important question of what CRD engagement by Wnts might look like in the absence of acylation. The question is difficult to answer as our understanding of Wnt structure is derived from a single, static, crystal structure and we therefore lack any information on the conformational flexibility of Wnts (Janda et al., 2012). With these restrictions in mind, we propose two simple possibilities for the mechanisms of acylation-independent Wnt/CRD binding. First, that acylation-independent binding to CRDs uses many of the same protein-protein interfaces seen in the crystal structure. Accumulating evidence in the field supports the hypothesis that the Site 2 interface on Fz CRDs may provide a common binding surface for both acylated and non-acylated ligands. The atypical ligand Norrin engages the CRD of Fz4 at Site 2

(Chang et al., 2015; Shen et al., 2015). Furthermore, binding studies performed using a "mini-Wnt," containing only the index finger domain of xWnt8, demonstrate that the Site 2 interaction can form independently of the acyl-protein interface at Site 1(Janda et al., 2012). In contrast, it is also quite possible that acylation-independent binding to CRDs requires protein-protein interfaces unrelated to those described in the crystal structure. Combining structural and *in vivo* studies will provide the most direct means for identifying the nature of these interactions.

A growing body of literature supports the essential role of Wnt acylation in protein secretion, extracellular distribution and receptor binding (Nusse and Clevers, 2017). We observe that the *in vivo* activity of xWnt8^{S187A} is approximately ten-fold weaker than its WT counterpart. Thus, our studies confirm that acylation plays an important role in the signaling of xWnt8 even though it is not essential for CRD binding. To investigate this shift in signaling further, we began with the hypothesis that xWnt8 may require acylation to exit the ER, as proposed in a previous study (Takada et al., 2006). However, our immunofluorescence data did not reveal a significant defect in intracellular trafficking of xWnt8^{S187A} (Figure 2.4). Although these data provide evidence that preventing acylation does not cause ER retention of Wnt ligands in *Xenopus* embryos, they do not directly address potential differences in the efficiency of Wnt secretion into the extracellular space. Indeed, performing direct measurements of the rates of secretion will be an important future direction for this project.

We next proposed that acylation may play a role in tethering Wnts, as demonstrated for the *Drosophila* EGFR ligand, Spitz (Miura et al., 2006). Wild-type Wnts are known to associate strongly with the cell membranes of producing cells (Papkoff and Schryver, 1990; Willert et al., 2003; Pfeiffer et al., 2002; Franch-Marro et al., 2008; Galli

et al., 2007; Gao et al., 2011). Similarly, we observed an accumulation of xWnt8 at the cell periphery of producing cells in *Xenopus* tissues and this association was dependent upon the presence of the acyl tail. However, could a defect in tethering be sufficient to cause a ten-fold shift in the apparent biological activity of a ligand? Studies of Spitz confirm that preventing acylation can cause significant attenuation of ligand signaling without affecting receptor affinity (Miura et al., 2006). However, in the case of Wnts, we cannot rule a that acylation may be also contributing to high-affinity interactions between Wnts and CRDs. In summary, we demonstrate that Wnts may engage CRDs and activate the β-catenin dependent pathway through acylation-independent mechanisms. Yet, the signaling differences we see between acylation and non-acylated Wnts argues that this modification is required for the full biological activity of these ligands. A biochemical approach will be necessary to understand the relative contributions of acylation to receptor engagement and membrane tethering.

Figure 2.1. Selection of Site 1 and Site 2 point mutations.

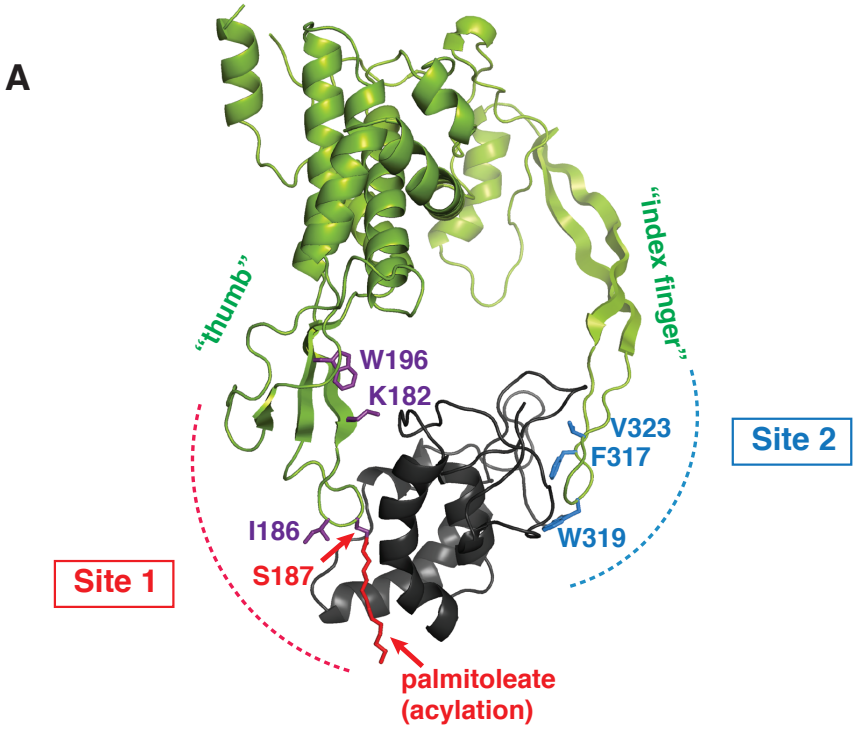

B

xWnt8	WT	CKCHGISGSCSIQTCW
xWnt8	S187A	CKCHGIAGSCSIQTCW
mWnt1	WT	CKCHGMSGSCTVRTCW
mWnt1	S224A	CKCHGMAGSCTVRTCW
hWnt3a	WT	CKCHGLSGSCEVKTCW
hWnt3a	S209A	CKCHGLAGSCEVKTCW
mWnt5a	WT	CKCHGVSGSCSLKTCW
mWnt5a	S244A	CKCHGVAGSCSLKTCW
		*****: *** ::***

Figure 2.1. Selection of Site 1 and Site 2 point mutations. (A) Point mutations were introduced into xWnt8 to perturb the Site 1 and Site 2. Amino acids on xWnt8 were selected based on their contributions to binding. Mutations K182S, K182S + W196A and K182S + W196A + I186A were made to abolish protein-protein interactions at Site 1. Serine 187 is the site of acylation on xWnt8, and a S187A mutation was introduced to disrupt protein-lipid interactions. The following constructs: W319A, W319A + F317A, W319A + F317A +V323A were created to abolish protein-protein interfaces at Site 2. (B) Sequence surrounding the highly-conserved serine acylation site in Wnt family members studied here. Site-directed mutagenesis was used to replace the acylated serine in xWnt8, mWnt1, hWnt3a, and mWnt5a with alanine. Other amino acids in the alignment correspond to residues on the “thumb” of xWnt8 immediately surrounding the acylated serine. DNA constructs were sequenced at the DNA Sequencing Facility at the University of Pennsylvania, translated using the Sequence Manipulation Suite (http://www.bioinformatics.org) and aligned using the Clustal Omega multiple sequence alignment tool (http://www.ebi.ac.uk/Tools/msa/clustalo).

Figure 2.2. A grading scale for Wnt phenotypes.

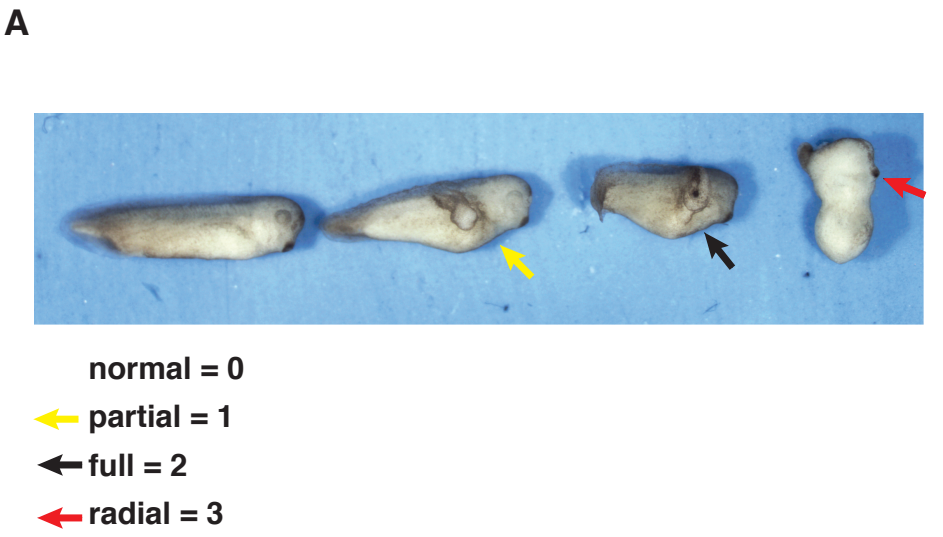

Figure 2.2. A grading scale for Wnt phenotypes. (A) The three categories of Wnt-dependent dorsalization phenotypes observed upon ectopic expression of Wnts from the VMZ of four-cell stage embryos. Pictures show representative tailbud-stage *Xenopus* embryos with their corresponding phenotype scores. Low levels of ectopic Wnt signaling cause the formation of a Siamese twin (extra tissue in foreground, indicated by arrows). Twins contain, at minimum, duplication of neural and dorsal mesodermal tissues ("partial", score = 1, yellow arrow). They may also contain a complete head, including the darkly-pigmented anterior cement gland ("full", score = 2, black arrow). High levels of ectopic Wnt signaling result in severe shortening of the anterior-posterior axis ("radial", score = 3, red arrow). (B) Calculating the mean dorsal score. Mean dorsal scores were calculated by summing the individual phenotype scores across all biological replicates and dividing by the total number of observations.

Figure 2.3. Comparing Site 1 and Site 2 mutations.

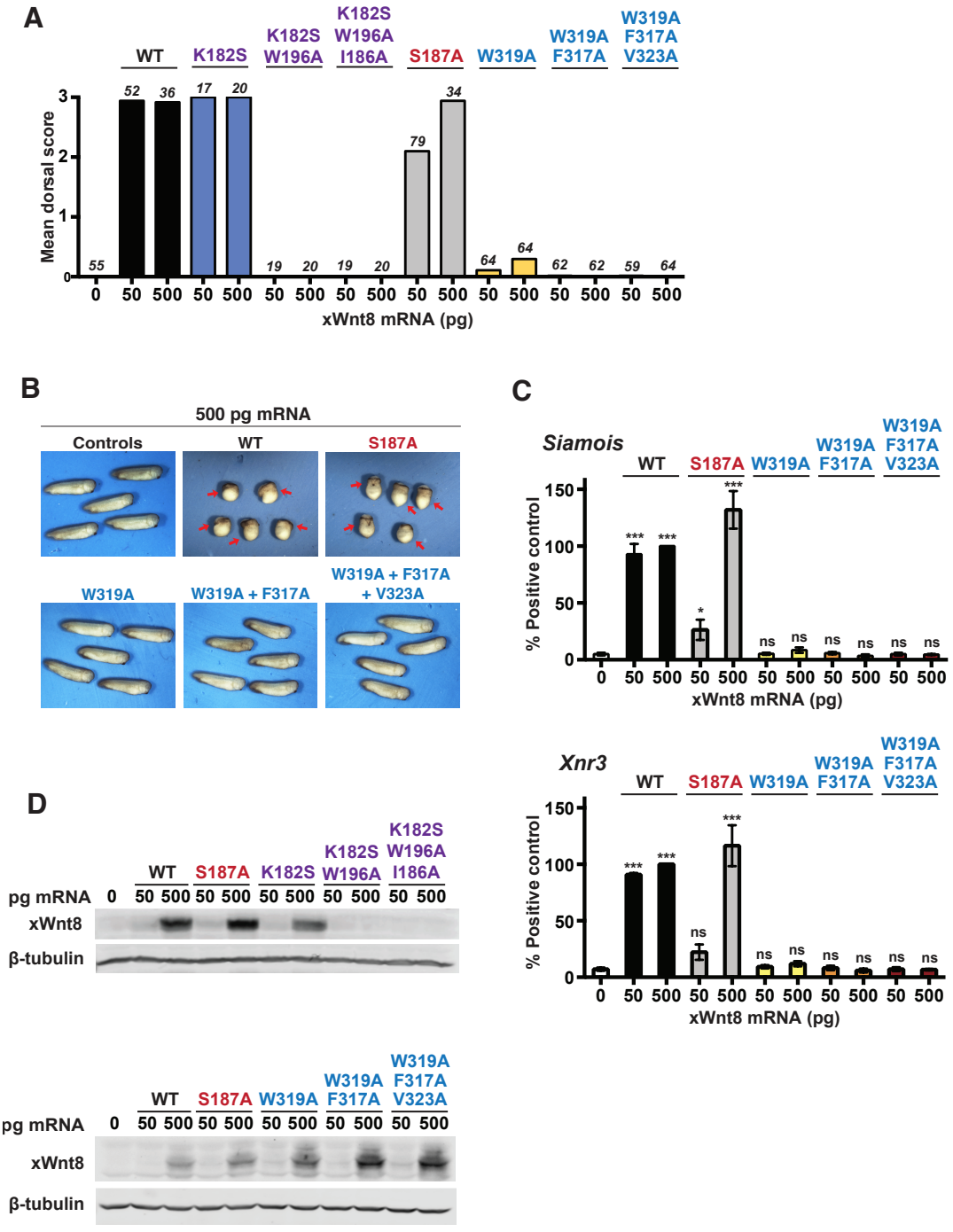

Figure 2.3. Comparing Site 1 and Site 2 mutations. (A) Site 2 mutants abolish signaling of xWnt8, but Site 1 mutations only cause a mild attenuation in activity. xWnt8 mRNA was injected into the VMZ of four-cell stage embryos. Mean dorsal scores were calculated at tailbud stages by summing individual phenotype scores (0-3 scale) within a treatment group and dividing by the population size. Numbers above bars indicate the total embryos scored across the biological replicates. N=3 for WT, S187A, W319A, W319A + F317A and W319A + F317A + V323A. N=1 for K182S, K182S + W196A and K182S + W196A + I186A. Mean dorsal scores for $xWnt8^{WT}$ and $xWnt8^{S187A}$ are from the data set shown in Figure 2.5A and are represented here for comparison. (B) Pictures show representative phenotypes caused by 0 pg or 500 pg injected mRNA. Red arrows = radial dorsalization. (C) Site 2 mutants do not activate the transcription of Wnt-responsive genes *Siamois* and *Xnr3*. xWnt8 mRNA was injected into the VMZ of four-cell stage embryos. At the early gastrula stage (stage 10), embryos were collected and the transcription of Wnt target genes assessed by RT-PCR. Each replicate was normalized to the 500 pg $xWnt8^{WT}$ treatment condition and are represented as mean ± SEM (n=3). Statistical significance was assessed using a fixed effects regression model with controls (0 pg) as a reference group. ns = $p \geq 0.05$, *$p \leq 0.05$, **$p \leq 0.01$ and ***$p \leq 0.001$. (D) Mutations at S187 and Site 2 do not decrease expression of xWnt8 protein. xWnt8 mRNA was injected into the VMZ of four-cell stage embryos. Embryos were collected at the gastrula stage (stage 10.5). Five embryos per treatment group were homogenized and one embryo equivalent of whole-embryo lysate was probed by Western blot for xWnt8 expression (n=1 for top Western, n=3 for bottom Western).

2.4. Immunofluorescence staining of xWnt8^{WT} and xWnt8^{S187A}.

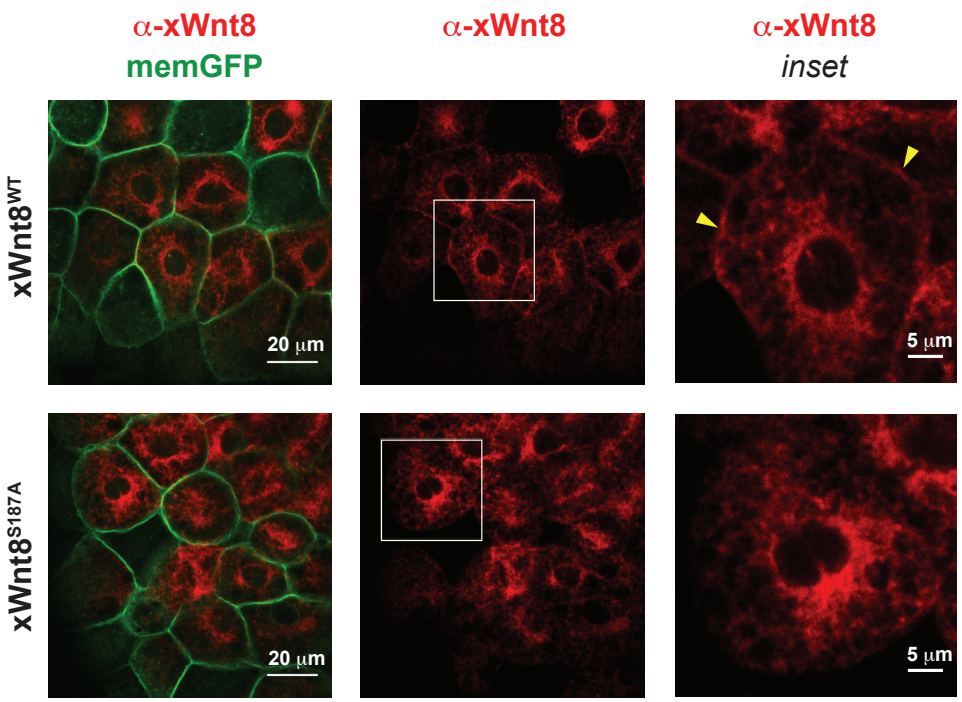

2.4. Immunofluorescence staining of xWnt8WT and S187A. xWnt8^{WT} and xWnt8^{S187A} have different distributions in *Xenopus* tissues. Two-cell stage embryos were first injected at both cells with 500 pg memGFP mRNA. Embryos were then allowed to develop until the 32-cell stage, when one animal pole cell was injected with 1 ng of *xWnt8^{WT}* or *xWnt8^{S187A}* mRNA. At the late blastula stage (stage 9), tissues of the animal pole were surgically removed, fixed, stained using standard protocols, and imaged by confocal microscopy (n=2). Far right images show magnification of boxed region in central panels. Scale bar, 20 μm (left and center panels) and 5 μm (right panels). Brightness and contrast were adjusted for clarity of viewing.

Figure 2.5. xWnt8 is biologically active in the absence of acylation.

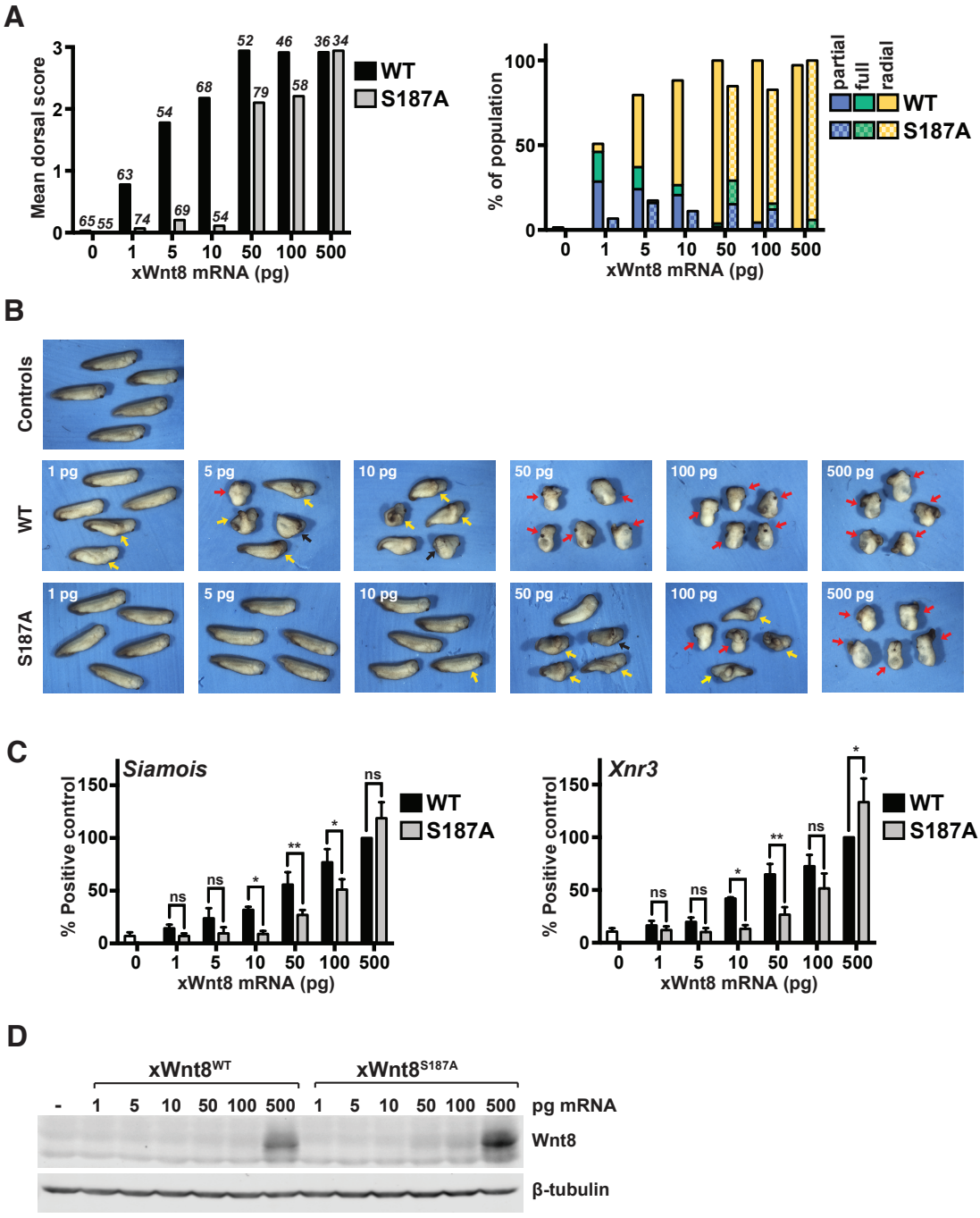

Figure 2.5. xWnt8 is biologically active in the absence of acylation. (A) xWnt8^{S187A} dorsalizes *Xenopus* embryos. xWnt8^{WT} or xWnt8^{S187A} mRNA was injected into the VMZ of four-cell stage embryos and embryos were scored at the tailbud stage. Numbers above bars (left) indicate the total embryos scored across (n=4) biological replicates. Data are represented as both mean dorsal score (left) and phenotype frequency (right) (B) Pictures show representative phenotypes from one biological replicate. Yellow arrows = partial duplication, black arrows = full duplication, red arrows = radial dorsalization. (C) xWnt8^{S187A} activates the transcription of Wnt-responsive genes. *xWnt8^{WT}* or *xWnt8^{S187A}* mRNA was injected into the VMZ of four-cell stage embryos. At early gastrula stage (stage 10), embryos were collected and *Siamois* and *Xnr3* transcript levels measured by RT-PCR. Each replicate was normalized to the 500 pg xWnt8^{WT} treatment condition and are represented as mean ± SEM (n=3). Statistical significance was assessed using a fixed effects regression model with controls (0pg) used as a reference group followed by a Wald chi-square test for pair-wise comparisons. ns = $p \geq 0.05$, *$p \leq 0.05$, **$p \leq 0.01$ and ***$p \leq 0.001$. (D) xWnt8^{WT} and xWnt8^{S187A} are expressed at a similar magnitude. *xWnt8^{WT}* and *xWnt8^{S187A}* mRNA were injected into the VMZ of four-cell stage embryos. Five embryos per treatment were collected at gastrula stage (stage 10.5), homogenized, and one embryo equivalent of whole cell lysate was probed by Western (n=3).

Figure 2.6. xWnt8^{WT} and xWnt8^{S187A} bind to the xFz8 CRD

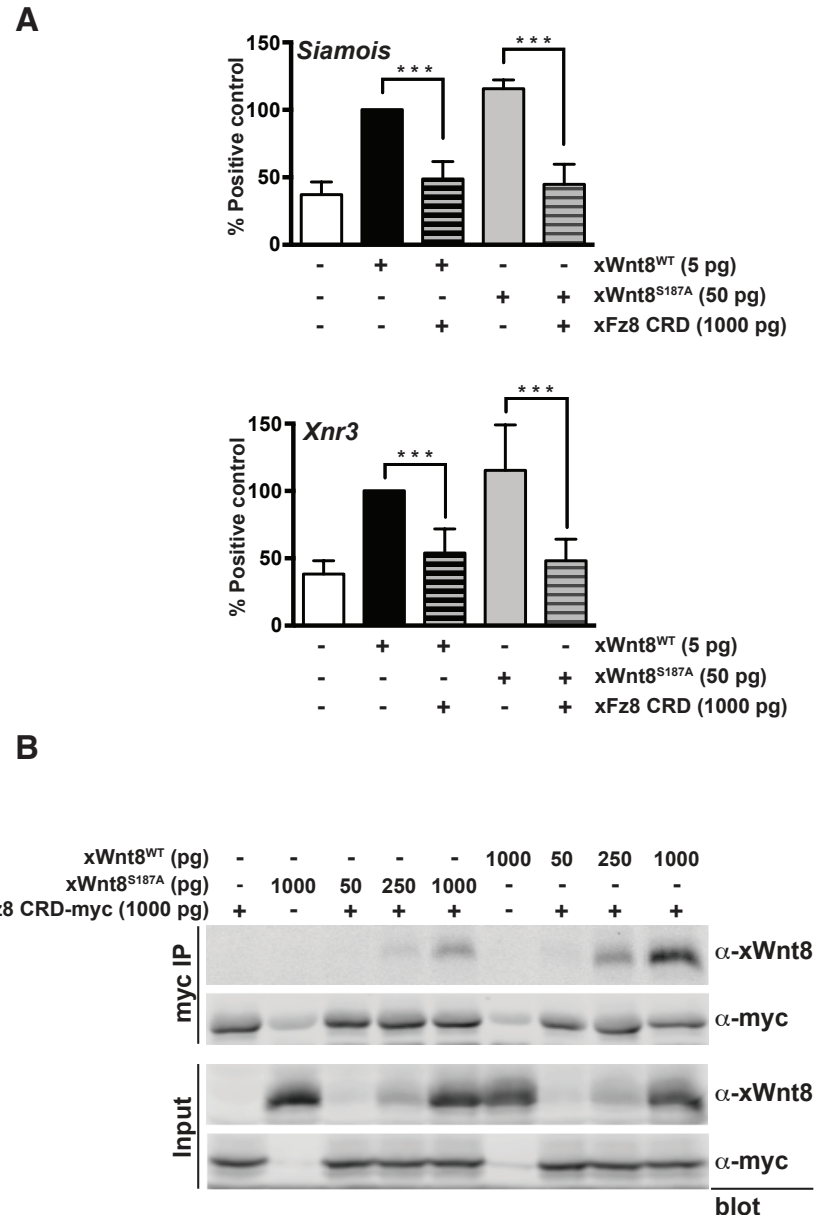

Figure 2.6. xWnt8^{WT} and xWnt8^{S187A} bind to the xFz8 CRD. (A) xWnt8^{WT} and xWnt8^{S187A} are sensitive to inhibition by the xFz8 CRD. *xWnt8* and *xFz8 CRD* mRNA were co-injected into the VMZ of four-cell stage embryos. At the early gastrula stage (stage 10), embryos were collected and *Siamois* and *Xnr3* levels measured by RT-PCR. Each replicate was normalized to the 5 pg xWnt8^{WT} treatment condition and are represented as mean ± SEM (n=4). Statistical significance was assessed using a fixed effects regression model with xWnt8^{WT} 5 pg as the reference group. (B) xWnt8^{WT} and xWnt8^{S187A} physically interact with the xFz8 CRD *in vivo*. *xWnt8* and *xFz8 CRD-myc* mRNA were co-injected into both cells of a two-cell stage embryo. Embryos were collected at the gastrula stage (stage 10.5). Precipitation of xFz8 CRD-myc was performed with an α-myc (9E10) antibody and Wnt interaction was detected by Western blotting. The band present in lanes 2 and 6 of the α-myc IP blot is likely a signal from the heavy chain of 9E10, as it runs at an identical molecular weight to the xFz8 CRD-myc protein (n=3).

Chapter 3: Acylation dependencies within the Wnt family

3.1 Introduction

Wnts are a family of morphogens that play diverse roles in embryonic patterning, the maintenance of adult stem cell populations, and the promotion of cancer. Interestingly, genetic studies of the ancient phylum Cnidaria reveal conservation of 11 of 12 mammalian Wnt subfamilies, suggesting that an almost full complement of Wnts arose early in the history of metazoans (Guder et al., 2006). Such high levels of conservation imply a strong evolutionary pressure to preserve diversity within this ligand family. Although our understanding of Wnt signaling has greatly advanced in the past decades, whether functional diversity exists within the many members of the Wnt family remains unclear.

Diversity within the Wnt family likely provides opportunities for both pre- and post-translational control of signaling outcomes. Transcriptional regulation of Wnt expression provides a mechanism for restricting when and where the different signaling pathways are activated (Logan and Nusse, 2004). At the post-transcriptional level, Wnts can be divided into two functional classes based on the phenotypes they elicit in *Xenopus* embryos. Wnts 1, 3a and 8 activate the β-catenin dependent pathway and cause ectopic dorsalization of embryos (McMahon and Moon, 1989; Sokol et al., 1991). In contrast, Wnts 5a and 11 selectively activate the PCP pathway and cause disruption of convergence and extension movements during gastrulation (Du et al., 1995). These simple assays argue that Wnts have significantly different affinities for receptors at the cell surface. However, the structural basis for these unique patterns of receptor interaction remain unclear.

Categorizing Wnts into two distinct functional classes is likely an oversimplification of structural differences between ligands, but biochemical studies have yet to yield information on what makes Wnts unique. Binding studies demonstrate that Wnts have overlapping affinities for Fzs (Hsieh et al., 1999; Deardorff et al., 2001; Ring et al., 2014; Dijksterhuis et al., 2015). Evidence from the xWnt8/mFz8 CRD crystal structure also reinforces the perceived redundancy in Wnt/Fz interactions. At Site 1, acylation is conserved throughout the vertebrate Wnt family, suggesting that all Wnts may rely on the acyl-protein interface for CRD binding (Janda et al., 2012). In addition, the amino acids on the thumb and forefinger of xWnt8 represent some of the most highly-conserved sequences in the entire protein. In sum, all evidence points to Wnts engaging Fzs through similar mechanisms.

The data presented in Chapter 2 challenges the assumption that all Wnts require acylation for their biological activity. An important question arising from these studies is whether all members of the Wnt family share the same capacity for acylation-independent signaling. To test this hypothesis, we introduced point mutations to the acylated serine residues on Wnts 1, 3a and 5a. For Wnts 1 and 3a, we analyzed their ability to activate the β-catenin dependent pathway and cause dorsalization of *Xenopus* embryos. For Wnt5a, we asked whether a non-acylated ligand could cause convergent extension phenotypes in *Xenopus* embryos.

Our results demonstrate that Wnts have unique dependencies on acylation for their biological activities. Wnt3a, like xWnt8, is capable of acylation-independent activation of the β-catenin dependent pathway and CRD binding. In contrast, both Wnts 1 and 5a demonstrate no detectable biological activity in *Xenopus* embryos when acylation was prevented. Our findings argue that Wnts have unique structural

requirements for signaling *in vivo* and we suggest that this structural diversity may translate into previously-unappreciated functional differences between individual ligands.

3.2 Acylation-dependent signaling of mWnt1

The observation that xWnt8 is capable of acylation-independent signaling prompted us to examine whether other canonical Wnts have the same capacity. In *Drosophila*, the signaling of Wg is strongly attenuated when acylation is prevented (Franch-Marro et al., 2008). Therefore, we asked whether murine (m)Wnt1 dorsalizes *Xenopus* embryos when its site of acylation is mutated (S224A, Figure 2.1B). We injected between 1 pg and 500 pg of mRNA encoding mWnt1^{WT} or mWnt1^{S224A} into the VMZ of four-cell stage *Xenopus* embryos and measured dorsalization phenotypes. mWnt1^{WT} caused the dorsalization of embryos at doses as low as 1 pg injected mRNA, similar to xWnt8^{WT} (compare Figure 2.5A, B and Figure 3.1A, B). However, we observed no phenotypes in mWnt1^{S224A}-expressing embryos up to 500 pg injected mRNA and very low frequency partial axis duplications at 1000 pg injected mRNA (data not shown). mWnt1^{S224A} also failed to induce the transcription of *Siamois* or *Xnr3* at any dose of mRNA tested (Figure 3.1C). Yet, we show by Western blot that mWnt1^{S224A} is expressed to a similar magnitude, even slightly higher, than its WT counterpart (Figure 3.1D). These data suggest that Wnt1, in contrast to Wnt8, is highly dependent upon acylation for its biological activity in *Xenopus* embryos.

The loss in signaling activity observed with the mWnt1^{S224A} mutation prompted us to examine whether acylation is required by mWnt1 for CRD binding. We first sought establish whether mWnt1^{WT}, like xWnt8, binds the xFz8 CRD. We co-expressed

mWnt1^{WT} with the soluble xFz8 CRD from the VMZ of four-cell stage embryos and measured levels of *Siamois* and *Xnr3* transcription. mWnt1 WT is also sensitive to inhibition by the xFz8 CRD, suggesting that the two proteins may bind *in vivo* (Figure 3.2A). We next asked whether the site of acylation on mWnt1 is required for xFz8 CRD binding. We co-expressed mWnt1^{WT} or mWnt1^{S209A} and xFz8 CRD-myc mRNA from the animal blastomeres of two-cell stage embryos and measured their interaction by co-immunoprecipitation. The xFz8 CRD binds to both mWnt1^{WT} and mWnt1^{S224A} in a dose-dependent manner (Figure 3.2B). These data argue that, while acylation is not absolutely required for Wnt1 binding to CRDs, it is necessary for the activation of intracellular signaling. Our experiments reveal striking differences between Wnts 1 and 8 and argue that canonical Wnts may be a structurally, and functionally, diverse group of ligands.

3.3 Acylation-independent signaling of hWnt3a

The distinct acyl dependencies of Wnts 1 and 8 prompted us to examine whether the activity of either ligand is unique amongst the Wnt family. We next performed experiments to determine whether Wnt3a, also an activator of the canonical signaling pathway, behaves in a more Wnt8-like or Wnt1-like manner when acylation is prevented. We expressed hWnt3a^{WT} and hWnt3a^{S209A} (Figure 2.1B) from the VMZ of four-cell stage embryos and measured the activation of the canonical Wnt pathway, as assessed by the transcription of Wnt-responsive genes and the dorsalization of tailbud stage embryos. Like xWnt8^{S187A}, hWnt3a^{S209A} caused dose-dependent dorsalization of *Xenopus* embryos and elevated the transcription of both *Siamois* and *Xnr3* (Figure 3.3A-C). However,

hWnt3a S209A induced fewer full axis duplications than hWnt3a WT (Figure 3.3A, right). Western blotting analysis performed on whole embryo lysates confirmed that mutating the site of acylation does not significantly change hWnt3a expression (Figure 3.3D). Yet, similar to xWnt8, hWnt3a^{S209A} displays approximately ten-fold weaker activity than hWnt3a^{WT} (compare 10 pg WT to 100 pg S209A in Figure 3.3A, B). These data suggest that both Wnts 8 and 3a can activate signaling through acylation-independent mechanisms but require acylation for full biological activity. We next examined whether hWnt3a^{S209A} could also interact with Fz CRDs, as seen for Wnts 8 and 1. We show that signaling by hWnt3a^{WT} and hWnt3a^{S209A} is inhibited by the soluble xFz8 CRD (Figure 3.4A). Furthermore, co-immunoprecipitation assays demonstrate that both hWnt3a^{WT} and hWnt3a^{S209A} physically bind the xFz8 CRD *in vivo* (Figure 3.4B).

3.4 Acylation-dependent signaling of mWnt5a

We next sought to address the role of acylation in Wnts regulating the non-canonical, or planar cell polarity, pathway. We chose to test the acylation-independent signaling of Wnt5a, which participates in the morphogenesis of many vertebrate tissues (Oishi et al., 2003), notably the convergent extension movements of the gastrulating *Xenopus* embryo (Figure 3.5A, Wallingford et al., 2001; Schambony and Wedlich, 2007). We therefore asked whether acylation is required for the ability of murine (m)Wnt5a to disrupt convergence extension movements in *Xenopus* embryos. We expressed mWnt5a^{WT} and acyl mutant (S244A, Figure 2.1B) from the upper dorsal marginal zone (DMZ) of four-cell stage embryos. By monitoring phenotypes at the neurula stage, we determined that ectopic expression of Wnt5a^{WT} resulted in a dose-dependent increase in

convergence extension phenotypes between 10 and 100 pg injected mRNA (Figure 3.5B,C). In contrast, mWnt5a^{S244A} did not induce significant convergence extension defects in this assay. Severe blastopore closure defects occurred upon injection of 500 pg or 1000 pg of mWnt5a^{WT} or mWnt5a^{S244A} mRNA, making it difficult to assess defects in convergence and extension at these mRNA concentrations. We note phenotypes were significantly distinct from those caused by mWnt5a^{WT} at lower concentrations and we conclude that they likely reflect toxicity (data not shown). Western blotting performed on whole embryo lysates indicated that both mWnt5a^{WT} and mWnt5a^{S244A} are expressed at equal magnitudes (Figure 3.5D). Although it remains unclear which receptors directly engage Wnt5a and which are involved in concurrent signaling events, these data suggest that Wnt5a, like Wnt1, is dependent upon acylation for signaling.

Although it appears that most functions of Wnt5a *in vivo* occur through the activation of the noncanonical Wnt pathway, Wnt5a also stimulates the canonical pathway when co-expressed with the certain Fzs (He et al., 1997; Mikels et al., 2006). This observation provided us with the opportunity to compare the role acylation in the activation of the canonical and noncanonical pathways, which have distinct receptor requirements. To measure the activation of the canonical pathway, we co-expressed 5 – 500pg of *Wnt5a^{WT}* or *Wnt5a^{S244A}* mRNA with 50pg of *Fz5* mRNA from the VMZ of a single cell in a four-cell stage embryo. At the tadpole stage, we analyzed the phenotypes arising from co-injections. We noted that, at low doses, the co-expression of *Wnt5a^{WT}* and *Fz5* mRNA caused dorsalization phenotypes, as seen for Wnts 8, 1 and 3a (Figure 3.5E, WT^{dorsal} and S244A^{dorsal} bars, and 3.5F Dorsal phenotypes). However, at higher doses (between 100 – 500pg of mRNA), we observed that the phenotypes became highly similar to the convergent extension phenotypes seen in Figure 3.5B (Figure 3.5E,

WT^{CE} and $S244A^{CE}$, and 3.5F CE phenotypes). Therefore, we chose to represent both phenotypes as a percentage of the total population. As we observed for our noncanonical assays, $Wnt5a^{WT}$ induced dose-dependent activation of the canonical pathway, whereas $Wnt5a^{S244A}$ caused no observable phenotypes. An important caveat of these data is that they represent only one biological replicate, and should be repeated before strong conclusions are drawn. Nevertheless, they argue that Wnt5a requires acylation to productively activate both the canonical and noncanonical pathways.

3.5 Conclusion

In Chapter 2, we demonstrated that xWnt8 was capable of acylation-independent activation of the β-catenin dependent pathway within the *Xenopus* embryo. Our data directly challenged the prediction from the xWnt8/mFz8 CRD crystal structure that acylation is required by Wnts for receptor recognition. There are 19 members of the Wnt family of ligands which are all predicted to bind to Fz CRDs *in vivo* (Niehrs, 2012). Furthermore, Fz-dependent signaling controls the activation of both the β-catenin dependent pathway and the PCP pathway. Therefore, an important question arising from the data presented in Chapter 2 was whether the acylation-independent signaling observed for xWnt8 represents a universal trait of all Wnts or specific characteristic of certain ligands.

In Chapter 3, we investigated the role of acylation in the signaling of unique Wnts. Wnts 1 and 3a, like Wnt8, activate the β-catenin dependent pathway and cause dorsalization phenotypes in *Xenopus* embryos. Furthermore, receptor synergy studies demonstrate that all three Wnts have highly-overlapping patterns of Fz binding *in vivo*

(Deardorff et al., 2001). Therefore, we predicted that all three ligands would have a similar dependency on acylation for their biological activities. On the contrary, we found that acylation-independent signaling is a unique characteristic even among Wnts with redundant signaling outcomes. Wnts 8 and 3a define a subclass of ligands that are capable of signaling through acylation-independent mechanisms. xWnt8^{S187A}, despite the ten-fold shift in its activity, is indistinguishable from xWnt8^{WT} in the quality and quantity of phenotypes it produces. Interestingly, ectopic hWnt3a^{S209A} expression yields quantities of phenotypes equal to hWnt3a^{WT}, but the quality, as measured by the number of full axis duplications induced in embryos, is markedly different. These data suggest that, even amongst Wnts capable of acylation-independent signaling, this modification may play ligand-specific roles.

In contrast, Wnt1 is dependent upon acylation for the activation of the canonical pathway. Although Wnt1^{S209A} was still capable of physically associating with the xFz8 CRD, it was unable to activate signaling *in vivo*. Wnt1 may be dependent upon acyl binding at the Site 1 interface to productively engage Fzs. Alternatively, Wnt1 may have lower affinity than Wnts 8 and 3a for the Fzs (7 and 4) expressed during the developmental window when ectopic dorsalization occurs (Medina et al., 2000; Shi and Boucaut, 2000). Thus, “untethering” of Wnt1 from the cell membrane would more efficiently reduce its concentration below the threshold required to activate signaling. Wnt5a, like Wnt1, also requires acylation for its ability to activate both the canonical and noncanonical pathways, thereby demonstrating that neither acylation-dependent nor acylation-independent signaling is unique amongst Wnts. Our data argue that Wnts have distinct structural characteristics that may play an important role in regulating receptor

recognition. Further discussion of the structural relationships between unique Wnts and Fzs and are presented in Chapter 4.

Figure 3.1. mWnt1 requires acylation for biological activity.

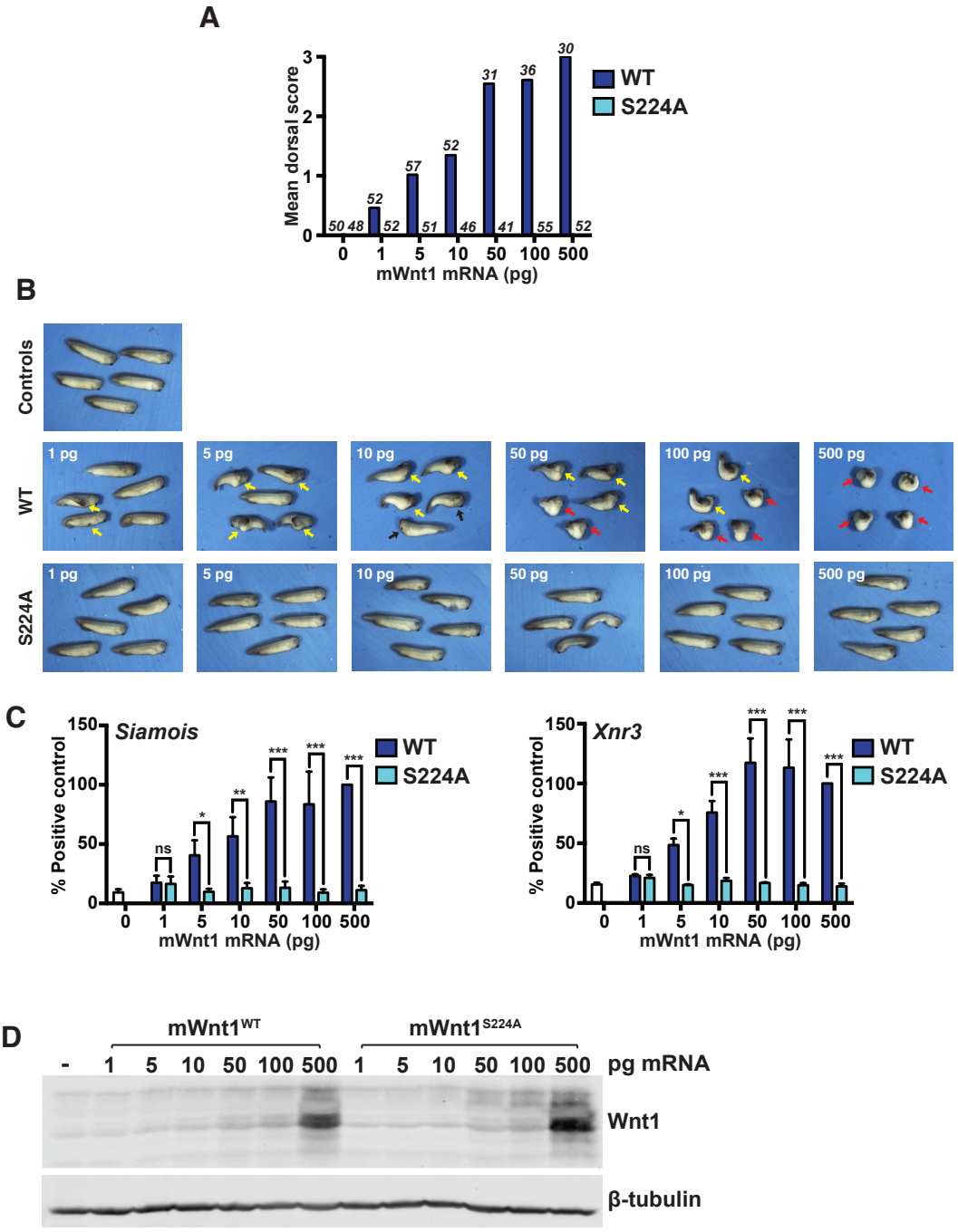

Figure 3.1. mWnt1 requires acylation for biological activity. (A) mWnt1^{S224A} does not dorsalize *Xenopus* embryos. *mWnt1*^{WT} or *mWnt1*^{S224A} mRNA was injected into the VMZ of four-cell stage embryos. Mean dorsal scores were calculated at the tailbud stage. Numbers above bars indicate the total embryos scored across (n=3) biological replicates. (B) Pictures show representative phenotypes from one biological replicate. Yellow arrows = partial duplication, black arrows = full duplication, red arrows = radial dorsalization. (C) mWnt1^{S224A} does not activate the transcription of Wnt-responsive genes. *mWnt1*^{WT} and *mWnt1*^{S224A} mRNA were injected into the VMZ of four-cell stage embryos. Embryos were collected at the early gastrula stage (stage 10) and transcription of *Siamois* and *Xnr3* were analyzed by RT-PCR. Each replicate was normalized to the 500 pg mWnt1^{WT} treatment condition and are represented as mean ± SEM (n=3). Statistical significance was assessed using a fixed effects regression model with controls (0pg) used as a reference group followed by a Wald chi-square test for pair-wise comparisons. ns = $p \geq 0.05$, *$p \leq 0.05$, **$p \leq 0.01$ and ***$p \leq 0.001$. (D) mWnt1^{WT} and mWnt1^{S224A} are expressed at similar levels within the embryo. mWnt1^{WT} or mWnt1^{S224A} mRNA was injected into the VMZ of four-cell stage embryos. At the gastrula stage (stage 10.5), five embryos per treatment group were collected, homogenized, and one embryo equivalent of whole embryo lysate was probed by Western blot (n=2). Wnt1 protein can be detected as four separate species which are indicated by black circles.

Figure 3.2. mWnt1^{WT} and mWnt1^{S224A} bind to the xFz8 CRD.

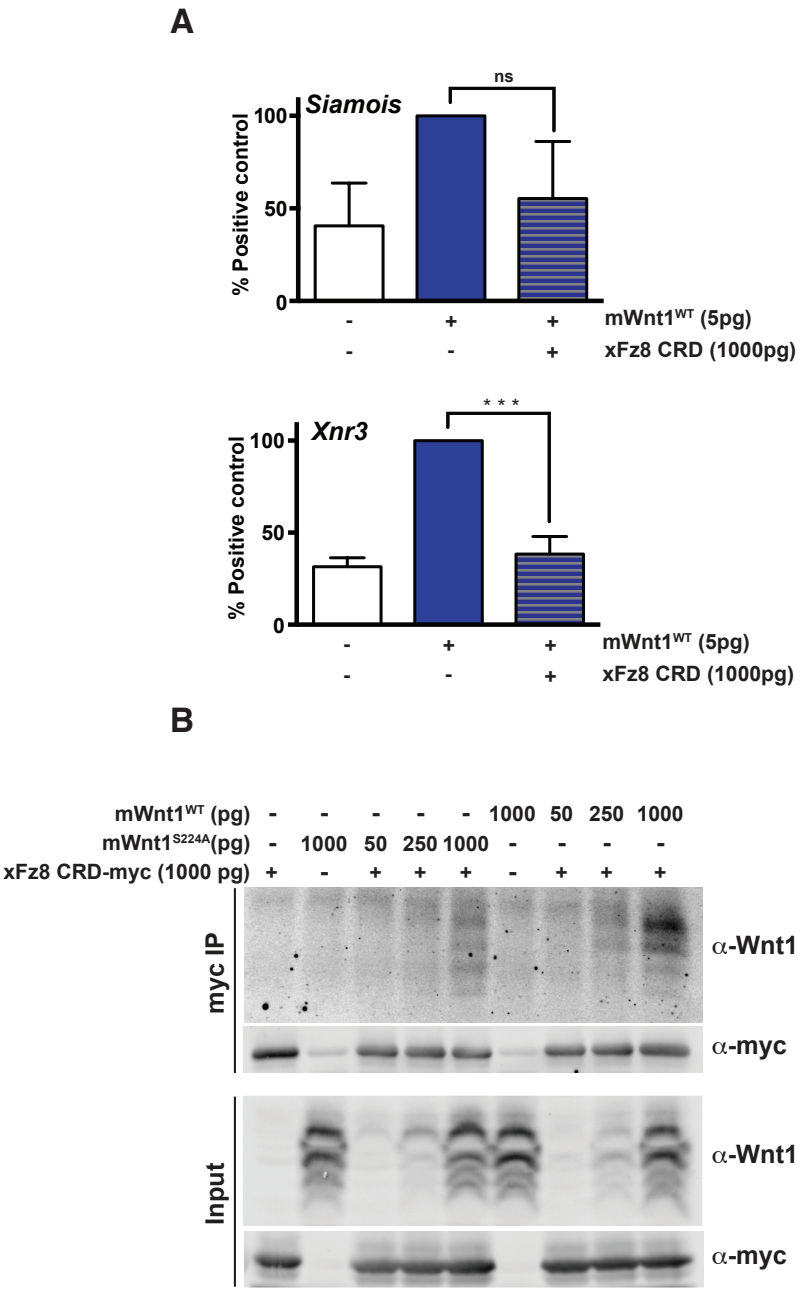

Figure 3.2. mWnt1^{WT} and mWnt1^{S224A} bind to the xFz8 CRD. (A) mWnt1^{WT} signaling is sensitive to inhibition by the xFz8 CRD. *mWnt1^{WT}* and *xFz8 CRD* mRNA were co-injected into the VMZ of four-cell stage embryos. Embryos were collected at the early gastrula stage (stage 10) and *Siamois* and *Xnr3* levels measured by RT-PCR. Each data set was normalized to the 5 pg mWnt1^{WT} treatment condition and are represented as mean $\pm$ SEM (n=3). Statistical significance was assessed using a fixed effects regression model with mWnt1^{WT} 5 pg as the reference group. (B) mWnt1^{WT} and mWnt1^{S224A} physically associate with the xFz8 CRD *in vivo*. *mWnt1* and *xFz8 CRD-myc* mRNA were co-injected into both cells of a two-cell stage embryo. Embryos were collected at gastrula stage (stage 10.5), precipitation of xFz8 CRD-myc was performed with an α-myc (9E10) antibody, and mWnt1 was detected by Western blotting. Wnt1 protein can be detected as four separate species which are indicated by the black circles. The band present in lanes 2 and 6 of the α-myc IP blot is likely a signal from the heavy chain of 9E10, as it runs at an identical molecular weight to xFz8 CRD-myc.

Figure 3.3. hWnt3a is biologically active in the absence of acylation.

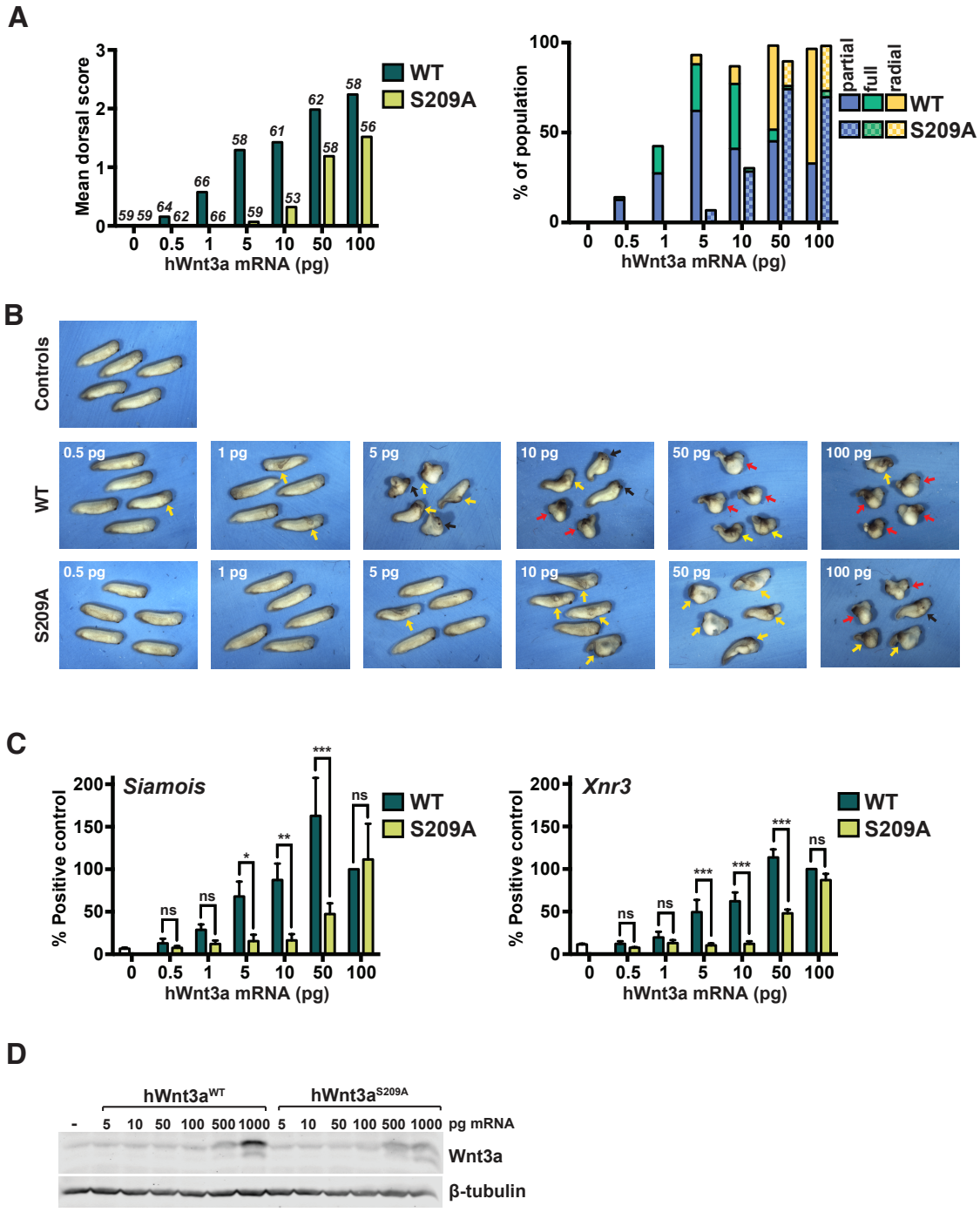

Figure 3.3. hWnt3a is biologically active in the absence of acylation. (A) hWnt3a^{S209A} dorsalizes *Xenopus* embryos. hWnt3a^{WT} and hWnt3a^{S209A} mRNA were injected into the VMZ of four-cell stage embryos and phenotypes were calculated at the tailbud stage. Data is represented as mean dorsal score (left) and phenotype frequency (right). Numbers above bars (left) indicate the total individuals scored across (n=3) biological replicates. (B) Pictures show representative embryos from one biological replicate. Yellow arrows = partial duplication, black arrows = full duplication, red arrows = radial dorsalization. (C) hWnt3a^{WT} and hWnt3a^{S209A} both upregulate the transcription of Wnt-responsive genes. *hWnt3a^{WT}* or *hWnt3a^{S209A}* mRNA were injected into the VMZ of four-cell stage embryos. Embryos were collected at early gastrula stage (stage 10) and the expression of *Siamois* and *Xnr3* analyzed by RT-PCR. Each replicate was normalized to the hWnt3a^{WT} 100 pg treatment condition and are represented as mean ± SEM (n=3). Statistical significance was assessed using a fixed effects regression model with controls (0pg) used as a reference group followed by a Wald chi-square test for pair-wise comparisons. ns = $p \geq 0.05$, *$p \leq 0.05$, **$p \leq 0.01$ and ***$p \leq 0.001$. (D) hWnt3a WT and S209A are expressed at similar magnitudes. *hWnt3a^{WT}* or *hWnt3a^{S209A}* mRNA was injected into the VMZ of four-cell stage embryos. Embryos were collected at gastrula stage (stage 10.5), homogenized, and two embryo equivalents of whole-embryo lysate were probed by Western blot for Wnt3a expression (n=3). hWnt3a runs at the same gel position as a ~40 kDa endogenous protein.

Figure 3.4. hWnt3a WT and S209A bind to the xFz8 CRD.

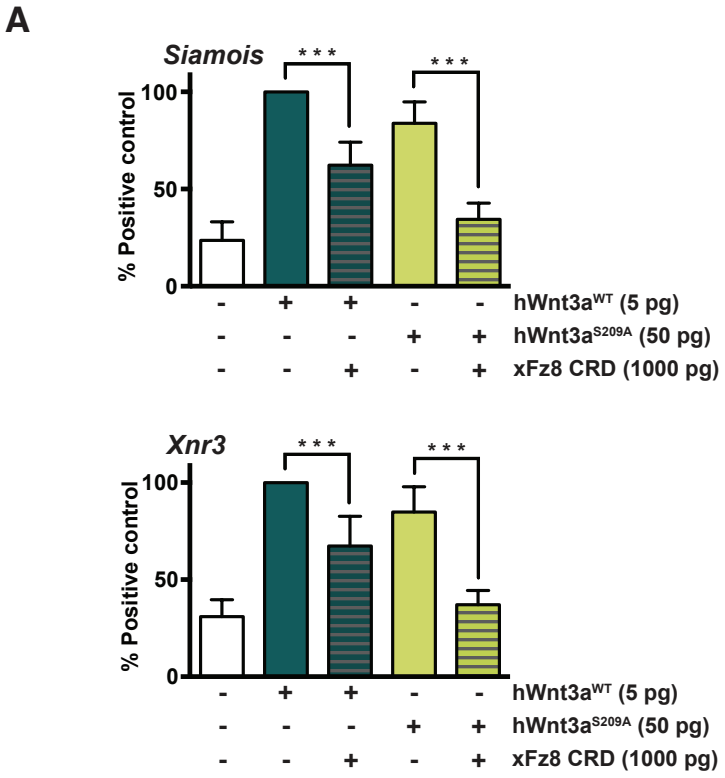

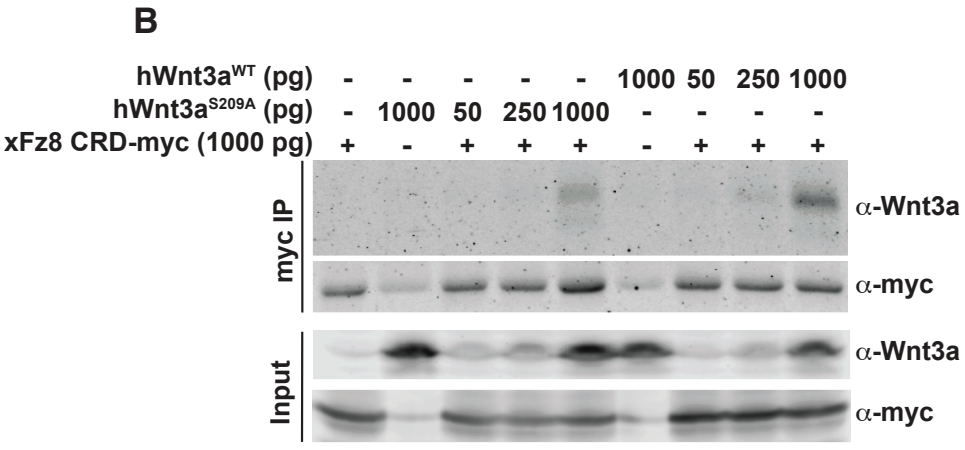

Figure 3.4. hWnt3a^{WT} and hWnt3a^{S209A} bind to the xFz8 CRD. (A) Both hWnt3a^{WT} and hWnt3a^{S209A} are sensitive to inhibition by the xFz8 CRD. *hWnt3a* and *xFz8 CRD* mRNA were co-injected into the VMZ of four-cell stage embryos. Embryos were collected at the early gastrula stage (stage 10) and the transcription of *Siamois* and *Xnr3* measured by RT-PCR. Each replicate was normalized to the 5 pg hWnt3a^{WT} treatment condition and are represented as mean ± SEM (n=3). Statistical significance was assessed using a fixed effects regression model with hWnt3a^{WT} 5 pg as the reference group. ns = $p \geq 0.05$, *$p \leq 0.05$, **$p \leq 0.01$ and ***$p \leq 0.001$. (B) hWnt3a^{S209A} binds the xFz8 CRD. hWnt3a and xFz8 CRD-myc mRNA were co-injected into both cells of a two-cell stage embryo. Embryos were collected at the gastrula stage (stage 10.5). Precipitation of the xFz8 CRD-myc was performed with an α-myc (9E10) antibody and Wnt interaction was detected by Western blotting (n=3). hWnt3a runs at the same gel position as a ~40 kDa endogenous protein in the Input blot. The band present in lanes 2 and 6 of the α-myc IP blot is likely a signal from the heavy chain of 9E10, as it runs at an identical molecular weight to the xFz8 CRD-myc protein.

Figure 3.5. mWnt5a requires acylation for its biological activity.

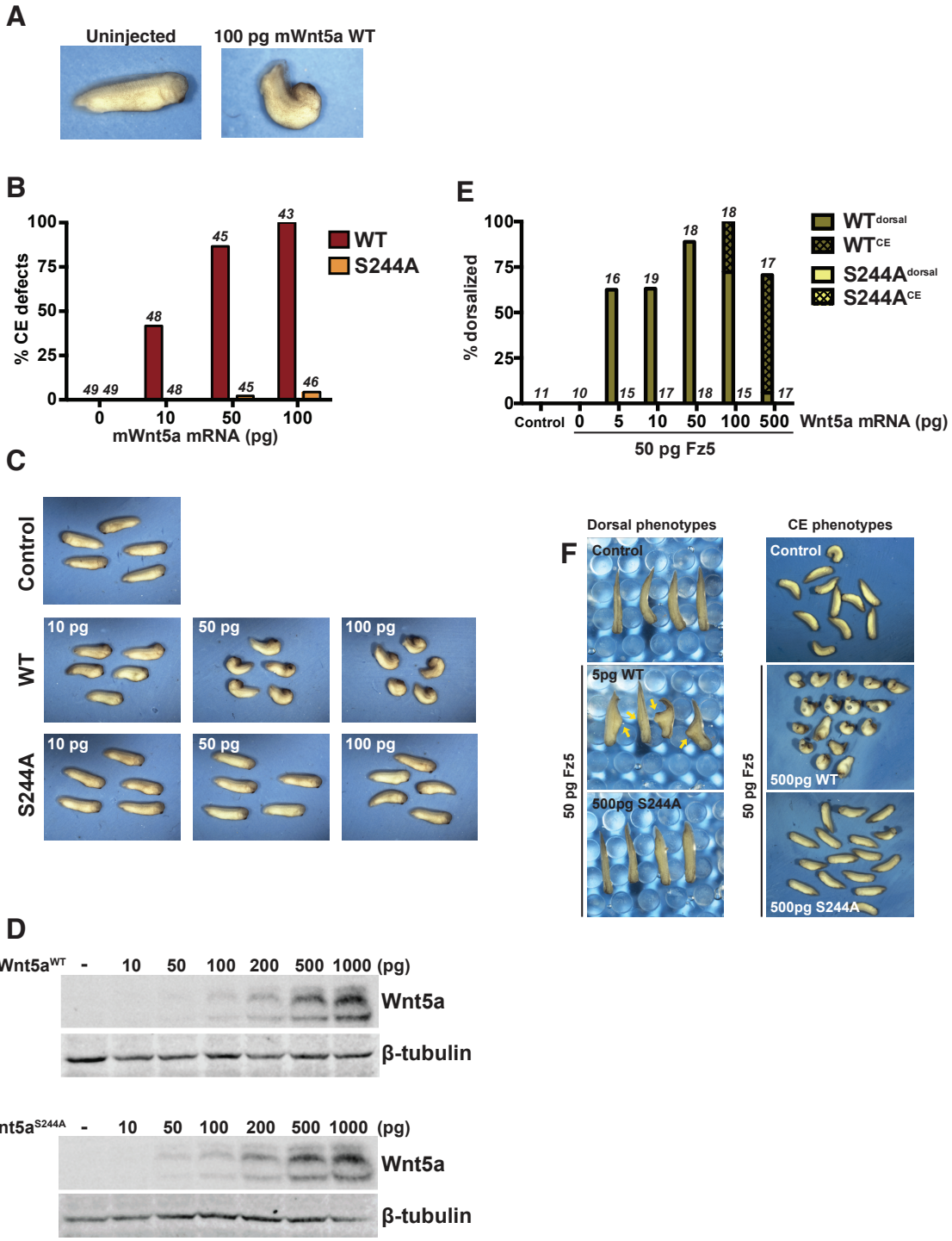

Figure 3.5. mWnt5a requires acylation for its biological activity. (A) Wnt5a causes convergent extension phenotypes in embryos. Ectopic expression of noncanonical Wnt5a from the DMZ of four-cell stage embryos causes the disruption of convergence and extension movements of the neural and dorsal mesodermal tissues of the embryo, resulting in a shortening and curvature to the anterior-posterior axis. (B) mWnt5a requires acylation to cause convergent extension defects in *Xenopus* embryos. *mWnt5a*^{WT} or *mWnt5a*^{S244A} mRNA was injected into the DMZ of four-cell stage embryos and convergent extension phenotypes were scored at neurula stages. Data is represented as the percentage of individuals displaying convergence and extension defects. Numbers above bars represent the total individuals scored across (n=3) biological replicates. (C) Pictures show representative phenotypes from one biological replicate. (D) Mutating the site of acylation does not decrease mWnt5a protein expression. *mWnt5a*^{WT} or *mWnt5a*^{S244A} mRNA was injected into the DMZ of four-cell stage embryos. At the gastrula stage (stage 10.5), embryos were collected, homogenized, and two embryo equivalents of whole cell lysate were probed by Western blot for the expression of Wnt5a. (E) Wnt5a requires acylation to cause dorsalization defects in *Xenopus* embryos. *mWnt5a*^{WT} or *mWnt5a*^{S244A} mRNA was co-injected with 50pg of *Fz5* mRNA into the VMZ of four-cell stage embryos and phenotypes were analyzed at the tailbud stages (n=1). Phenotype frequency, instead of mean dorsal score, is represented in order to illustrate that both dorsalization and convergent extension defects occur with Wnt5a^{WT} and Fz5 co-expression. (F) Representative embryos demonstrating the dorsalization phenotypes caused by low doses of Wnt5a^{WT} + Fz5 (right) and convergent extension (CE) phenotypes at high doses of Wnt5a^{WT} + Fz5 (left).

Chapter 4: Conclusions & Future directions

4.1. Introduction

The recent crystal structure of xWnt8 bound to the CRD of mFz8 led to a prediction in the field that Wnt acylation plays a direct, and essential, role in CRD recognition (Janda et al., 2012). However, without *in vivo* validation of the crystallographic binding interfaces, it remained unclear whether the structure was an accurate reflection of the interactions between Wnts and CRDs occurring at the cell surface. In this work, I investigated the role of acylation in the biological activity of unique Wnts. I introduced point mutations to the acylated serine residues on Wnts 8, 1, 3a and 5a and compared their abilities to activate well-established Wnt signaling outcomes within the early *Xenopus* embryo.

In Chapter 2, I first tested the ability of xWnt8 to activate the β-catenin dependent pathway when acylation was prevented. Surprisingly, I found that non-acylated xWnt8 (S187A) was capable dorsalizing *Xenopus* embryos as well as activating the transcription of the Wnt-responsive genes *Siamois* and *Xnr3.* These data argued that xWnt8 may be capable of acylation-independent signaling. Therefore, I next asked whether xWnt8^{S187A} were capable of interacting with Fz CRDs *in vivo*. I analyzed the interaction of xWnt8^{S187A} with the CRD of xFz8 by co-immunoprecipitation. This assay confirmed that xWnt8 retains the ability to interact with CRDs when acylation is prevented. My data argued that, contrary to the prediction from the xWnt8/mFz8 CRD crystal structure, acylation is not absolutely required for the biological activity of xWnt8.

Wnts are predicted to interact with Fzs through highly redundant mechanisms, which suggested that acylation-independent Wnt signaling might be a shared property of

the ligand family (Cong et al., 2004; Holmen et al., 2002; Janda et al., 2017). Therefore, in Chapter 3, I expanded my study to examine the role of acylation in activity of Wnts 1, 3a and 5a. Wnts 1 and 3a, like Wnt8, selectively activate the β-catenin dependent pathway (McMahon and Moon, 1989; Sokol et al., 1991). I observed that Wnt3a, like xWnt8, demonstrated acylation-independent signaling and CRD binding. In contrast, Wnt1 could not activate the β-catenin dependent pathway when acylation was prevented. My results argued that Wnts have unique dependencies on acylation for their biological activity. Furthermore, they suggested these Wnts with redundant functional outcomes are structurally unique and might have unique requirements for binding CRDs. Finally, I examined the role of acylation in the signaling of Wnt5a, and activator of the PCP pathway. Wnt5a, like Wnt1, required acylation for its biological activity, demonstrating that neither acylation-dependent nor acylation-independent signaling is unique amongst the Wnt family.

4.2. Structural requirements for acylation-independent Wnt/CRD binding

My data reveal that Wnts 8 and 3a do not require acylation to activate the β-catenin dependent pathway *in vivo*. Furthermore, I demonstrate that these ligands may productively engage the xFz8 CRD even when binding between the acyl tail on the Wnt and the hydrophobic groove on the CRD is prevented. My observations are not the first evidence that signaling through Fzs can occur via mechanisms independent of the Site 1 acyl/protein binding surface. The soluble ligands Norrin and WntD are both capable of engaging Fz4 *in vivo* (Xu et al., 2004; Ke et al., 2013; Shen et al., 2015; Chang et al., 2015; McElwain et al., 2011) (Ching et al., 2008). Additionally, artificial Wnt agonists that

contain lipid-free Fz-binding and LRP-binding modules potently activate canonical Wnt signaling through Fzs 1, 2, 5, 7, and 8 (Janda et al., 2017). In sum, accumulating evidence supports to the hypothesis that Fzs have the capacity to engage both acylated and non-acylated ligands.

What might an acylation-independent Wnt/Fz interaction look like? Evidence suggests that Site 2 may be a common ligand-binding interface on Fz CRDs. In Chapter 2, I demonstrate that Site 2 is necessary for the biological activity of xWnt8. Introducing even one mutation (W319A) to the index finger of xWnt8 decreased signaling of the ligand by more than 500-fold. Furthermore, a "mini-Wnt" comprising only this index finger domain is shown to bind independently to the mFz8 CRD *in vitro* (Janda et al., 2012), predicting that Site 2 interactions could stabilize Wnt binding in absence of the acyl/protein interface at Site 1. Lastly, crystallographic evidence reveals that Norrin also binds to the mFz4 CRD at the Site 2 interface (Shen et al., 2015; Chang et al., 2015). Thus, I predict that the protein-protein binding surface at Site 2 may play a role in the acylation-independent signaling of xWnt8 and hWnt3a observed in this study.

However, alone, the Site 2 interface is almost certainly insufficient for the stabilization of a heteromeric complex at the cell surface. xWnt8 binds at Site 2 with a buried surface area of ~400 Å and poor overall shape complementarity (Janda et al., 2012). In contrast, the dimeric ligand Norrin simultaneously engages two Fz4 CRDs, with each Site 2 interface containing twice (~800 Å) the buried surface area seen for xWnt8 (Chang et al., 2015). An examination of current Wnt structural data reveals that acylation-independent CRD binding may be stabilized at Site 1 through contacts involving the amino acids on the thumb of xWnt8. Structurally, the thumb is composed of a long β-hairpin, held together by disulfide bonds, with the acyl group attached at the tip

(Janda et al., 2012). In the xWnt8/mFz8 CRD crystal structure, the amino acids of the β-hairpin engage in important protein-protein contacts with a surface immediately above acyl-binding groove on the CRD (Figure 1.4) (Janda et al., 2012). In the context of a non-acylated Wnt, the binding of these thumb residues to the CRD may be sufficient to stabilize the Site 2 interface.

It is important to consider, however, that the character of the protein-protein interactions at Site 1 may differ significantly for the binding of a non-acylated Wnt. For wild-type xWnt8, the shape and orientation of the thumb are constrained by the interaction of the acyl tail with the hydrophobic pocket of the CRD. In contrast, a recent crystal structure of the thumb of WntD shows that this β-hairpin has significant conformational flexibility in its unbound, non-acylated state (Chu et al., 2013). Therefore, the binding of a non-acylated Wnt to a CRD may involve different, possibly even more extensive, protein-protein contacts at the Site 1 interface. Additionally, it is important to consider that the xWnt8/mFz8 crystal structure might represent a kinetically trapped structure or a ligand-binding intermediate and therefore not reflect the Wnt/CRD interactions occurring *in vivo.* Further structural characterization of acylation-independent Wnt binding will be required to understand which surfaces play key roles in these processes.

A combined *in vitro* and *in vivo* approach could be taken to test the role of protein-protein interfaces in acylation-independent Wnt binding. Previous efforts to purify and study wild-type Wnts have proven unsuccessful due to the requirement for detergent-solubilization of the acyl tail (Willert et al., 2003; Kurayoshi et al., 2007). However, biochemical studies may be successfully used to verify, and investigate the nature of, interactions between non-acylated Wnts and Fz CRDs. The Lemmon lab has

developed a successful protein purification method for DWnt5, a *Drosophila* Wnt that is not acylated when expressed from S2 cells (Lemmon, unpublished). The application of these methods to the purification of non-acylated mammalian Wnts could open an avenue to the biochemical study of Wnt/CRD interactions *in vitro.* These studies could also be expanded to include other Wnt-binding domains, such as the β-propeller motifs of LRP5/6 and the extracellular domains of RTKs. Using the *Xenopus*-based assay system developed in this thesis, future scientists would be able to translate structural predictions from biochemical assays into a physiological context. For example, mutating amino acids important for acylation-independent Wnt activity on xWnt8 S187A (or hWnt3a S209A) would be predicted to abolish the signaling of the ligand *in vivo.*

4.3. Updated roles for acylation in Wnt signaling

Acylation clearly plays an important role in Wnt signaling, even though our data argue that it is not absolutely required for productive receptor binding. Wnts 3a and 8, which are capable of robust acylation-independent activity, exhibit approximately ten-fold weaker signaling when acylation is prevented. The attenuated signaling of non-acylated Wnts explains why the biological activity of Wnt3a S209A was not detected in a previous study using a lower range of injected mRNA concentrations (Takada et al., 2006).

Acylation is predicted contribute to the signaling of Wnts through multiple mechanisms. In many physiological contexts, Wnt secretion requires acylation-dependent interactions with the cargo receptor Evi/Wntless (Herr and Basler, 2012). However, we were unable to verify a previous report which demonstrated that preventing acylation causes Wnts to accumulate in the endoplasmic reticulum of *Xenopus* embryos

(Figure 2.4, Takada et al., 2006). The early *Xenopus* embryo may provide a uniquely permissive environment for the secretion of non-acylated Wnts. The morpholino knockdown of xWntless affects the secretion and activity of Wnt4, but not Wnts 3a, 5a, 8 or 11 during *Xenopus* development (Kim et al., 2009). However, the authors failed to account for a possible contribution of maternal transcripts to protein levels within the embryo, and thus a role for xWntless cannot be entirely ruled out. As a continuation of the work presented in this thesis, it will be imperative to directly compare the secretion and extracellular activity of acylated and non-acylated Wnts. For example, if xWnt8 S187A is secreted and retains biological activity, these results would support to the hypothesis that non-acylated Wnts retain the ability productively engage Fz/LRP complexes. In contrast, if xWnt8 S187A is not secreted or not active in the extracellular space, then these data would argue that signaling may be occurring from the intracellular space through atypical mechanisms.

Interestingly, the only difference we were able to detect between the cellular distributions of $xWnt8^{WT}$ and $xWnt8^{S187A}$ was in the association of ligand with the cell periphery. $xWnt8^{WT}$ accumulates at the boundary of Wnt-producing cells but this staining was largely absent in tissues expressing $xWnt8^{S187A}$ (Figure 2.4). It is well-documented that Wnts signal primarily through local, cell-to-cell mechanisms (Willert et al., 2003; Pfeiffer et al., 2002; Franch-Marro et al., 2008; Galli et al., 2007; Farin et al., 2016; Gao et al., 2011). Could the changes in the extracellular distribution of xWnt8 S187A account for its ten-fold shift in activity? Preventing the acylation of the *Drosophila* EGFR ligand Spitz causes significant signaling defects *in vivo* without altering ligand secretion or receptor affinity (Miura et al., 2006). Spitz, like Wnts, requires acylation to restrict ligand diffusion in the extracellular space. In doing so, acylation provides an important

mechanism for defining Spitz gradients, as it allows local ligand concentrations to accumulate to the thresholds required for EGFR activation to drive the correct patterning of the photoreceptors in the eye imaginal disc (Miura et al., 2006). These studies highlight the importance of acylation-dependent tethering in ligands that signal through local mechanisms and suggest that a tethering defect may explain the ten-fold shift in activity seen for Wnts 8 and 3a.

However, defining the exact roles that acylation plays in Wnt signaling will prove to be quite a challenge. The fact that Spitz was amenable to purification and biochemical analysis allowed investigators to directly measure ligand affinities and conclude that acylation does not alter to the interaction of Spitz with *Drosophila* EGFR or other extracellular binding partners (Miura and Treisman, 2006). Thus, changes in extracellular distribution and tissue patterning of the ligand could reasonably be interpreted as pertaining to the role of acylation in gradient formation. Although the data presented in Chapters 2 and 3 argue that acylation is not absolutely required for productive CRD binding, we cannot rule out the possibility that acylation enhances the affinity of Wnts for CRDs. Receptor binding can also influence the diffusion of ligands within the extracellular space. For example, manipulating the levels of Fz expression alters the gradient of Wnt3a within the crypts of the small intestine (Farin et al., 2016). In sum, the diffusion of Wnts within the extracellular space may be influenced by their relative affinities for cell surface receptors as well as the tethering function of the acyl tail. Without the development of technologies that will allow for the direct measurement of the affinities of acylated Wnts for CRDs, we will not know the relative contributions of these processes to the biological activities of Wnts.

Alongside a clear requirement for continued biochemical analysis of Wnts, I suggest that future *in vivo* studies of Wnt acylation may benefit from the careful selection of biological systems. First, it is important to consider that chemical or mutagenesis-based methods for preventing Wnt acylation may create a "dilution effect" at the cell membrane that will vary based on the volume of the extracellular space. For example, we observe acylation-independent activity of Wnt3a in early *Xenopus* embryos which have highly-restrictive tissue architecture. In contrast, acylation-independent Wnt3a signaling has not been detected in cell culture models where "untethered" ligands may diffuse over great distances (Zhang et al., 2015; Kakugawa et al., 2015). Second, the secretion of non-acylated Wnts is attenuated in most model systems from *Drosophila* to mammals due to a requirement for the cargo receptor Evi/Wntless (van den Heuvel et al., 1993; Chen et al., 2009; Rios-Esteves and Resh, 2013; Herr and Basler, 2012). Therefore, selecting a system that is permissive for the secretion of non-acylated Wnts may be critical for detecting their activity. There is some evidence to suggest that the *Xenopus* embryo may be a system that naturally supports the secretion of non-acylated Wnts (Kim et al., 2009). However, it may also be possible to engineer such a system by using CRISPR/Cas9 technologies to knockout the cargo receptor Evi/Wntless in other contexts.

4.4 Structural differences between Wnts

The data we present in Chapters 2 and 3 demonstrate that Wnts have different dependencies on acylation for their biological activities. Wnts 8 and 3a define a novel subclass of ligands which are capable of acylation-independent signaling. In contrast,

Wnts 1 and 5a absolutely require acylation for signaling *in vivo*. It is particularly noteworthy that we observe signaling differences between Wnts 1, 3a and 8, as current evidence points to these ligands being both structurally and functionally redundant. All three Wnts selectively activate the β-catenin dependent pathway through the engagement of Fz and LRP5/6 heterodimers (Nusse and Clevers, 2017). Furthermore, synergy studies performed in *Xenopus* embryos reveal that the acylated versions of these ligands have highly-overlapping affinities for individual Fzs (Deardorff et al., 2001). Yet, in their non-acylated forms, Wnts 1, 3a and 8 have surprisingly different biological activities. These data argue that Wnts activating the β-catenin dependent pathway are structurally diverse and may have fundamentally unique mechanisms for engaging Fzs at the cell surface.

How might structural differences between Wnts give rise to the unique biological activities I observe *in vivo*? Biochemical studies will almost certainly provide the most direct answer to this question. Within the embryo, the acylation state of individual Wnts may affect a variety of intracellular and extracellular interactions both known and unknown. However, if one assumes that the unique structural characteristics of Wnts directly relate to their ability to bind CRD-containing receptors, then three different hypotheses could explain the distinct biological activities of Wnts 8, 1, 3a and 5a observed in our assays.

First, only select Wnts may contain the requisite structural features for acylation-independent CRD binding. If true, I would predict that Wnts 8 and 3a contain certain protein elements, discussed in Section 4.2, allowing them to engage CRDs through acylation-independent mechanisms. In contrast, Wnts 1 and 5a would likely depend upon the sequestration of the acyl tail at the Site 1 interface to engage CRD-containing

receptors. This hypothesis might be tested *in vivo* by creating chimeric ligands of Wnt1 and Wnt8, possibly by swapping thumb and index finger domains between the pair, in order to identify which parts of the protein are required for acylation-independent signaling.

Second, all Wnts may be capable of both acylation-dependent and acylation-independent CRD binding. Non-acylated Wnts may have different, possibly more specific, CRD affinities than their acylated counterparts. Under this hypothesis, I would predict that Wnt1 is also capable of acylation-independent signaling if it encounters the right receptor. This could be tested by examining the synergistic signaling of unique Wnt and Fz pairs in *Xenopus* embryos using both acylated and non-acylated versions of each ligand.

Lastly, it is possible that Wnts only bind CRDs through acylation-independent mechanisms. It is interesting to note that the authors of the xWnt8/mFz8 CRD crystal structure were only able to capture this protein interaction under conditions where the CRD was expressed as an Fc fusion construct (Janda et al., 2012). If the acyl tails of Wnts are normally sequestered within the outer layer of the cell membrane, then forcing Wnt association with a soluble, dimeric CRD-Fc may have caused the acyl tail to become sequestered away from the aqueous environment in a non-physiological manner. If acylation does not directly contribute to receptor binding, then the unique biological activities of non-acylated Wnts observed in this study are likely a manifestation of the different binding affinities of Wnts for endogenous Fzs. Although cell-based binding assays argue that Wnt/Fz interactions lack specificity (Hsieh et al., 1999; Deardorff et al., 2001; Dijksterhuis et al., 2015), I suggest that the ability of the acyl tail to "concentrate" ligands at the cell membrane may mask real differences in affinity between

Wnt and Fz pairs. Testing this prediction, as described for the ligand Spitz (Miura and Treisman, 2006), will require the direct biochemical comparison of the affinities of acylated and non-acylated Wnts for CRDs.

4.5 Signaling consequences of non-acylated Wnts

The unique structural requirements for acylation within the Wnt family may translate into distinct signaling outcomes *in vivo*. Several recent studies have demonstrated that the secreted deacylase, Notum, enzymatically removes the acyl tail from Wnt ligands within the extracellular space (Kakugawa et al., 2015; Zhang et al., 2015). Extracellular deacylation may provide an important mechanism for shaping Wnt gradients *in vivo*. Long-range transport of active Wnts, although uncommon, could be achieved through the Notum-dependent "untethering" of Wnts from membranes. Deacylation may also provide a mechanism for remodeling the spatial and temporal boundaries of Wnt gradients. Expression of Notum at tissue boundaries could effectively "turn off" the signaling of certain Wnts, as seen for Wnts 1 and 5a in this study. Alternatively, deacylation could reveal distinct patterns of Fz binding, which may help to shape the responsiveness of specific cells within a tissue to extracellular Wnt.

Notum is thought to bind to Wnts by specifically recognizing the unsaturated hydrophobic palmitoleic moiety covalently added to Wnts, suggesting that the enzyme will nonspecifically de-acylate all Wnts it encounters *in vivo* (Kakugawa et al., 2015). However, experiments I performed during my thesis argue that Notum likely also recognizes and engages Wnt proteins (Appendix, Figure 2). When I co-expressed Notum (both WT and an enzymatically dead S239A mutant) with $xWnt8^{WT}$ or $xWnt8^{S187A}$

from the same cell of the *Xenopus* embryo, I observed inhibition of xWnt8^{S187A}, which suggests a dominant-negative effect of Notum on Wnt function that is independent of lipid binding (Appendix Figure 2A, B). To investigate potential differences in the effect of Notum-mediated, extracellular deacylation on unique Wnts, I expressed Notum^{WT} and xWnt8^{WT} or mWnt1^{WT} from separate cells of the embryo (Notum was injected at the 4-cell stage, and Wnt at the 8-cell stage into an adjacent cell, Appendix Figure 2D, E). I observed very weak inhibition of both proteins in these assays, and was unable to draw any strong conclusions about the differential effect of extracellular deacylation on individual Wnts. In summary, the regulation of Wnt acylation by Notum may provide a mechanism to fine-tune Wnt gradients *in vivo*, but requires more study to determine the relative contributions of protein-binding and deacylation to its inhibitory effect on Wnts.

Targeting Wnt acylation for therapeutic purposes has become very attractive in the Wnt field. Particularly, inhibitors of the acyltransferase Porcupine demonstrate clinical promise in the treatment of cancers with Wnt-driven activation of the β-catenin dependent pathway (Proffitt et al., 2013; Chen et al., 2009; Kulak et al., 2015; Madan et al., 2016; Tammela et al., 2017). The inhibitor LGK974 is currently in phase one clinical trials for the treatment of triple negative breast cancer, pancreatic cancer, as well as many other malignancies (https://clinicaltrials.gov/ct2/show/NCT01351103). Although these drugs continue to show significant promise in the treatment of human disease, the work presented in this study urges a more nuanced evaluation of the effects of Porcupine inhibition on Wnt signaling. Although Porcupine inhibitors greatly reduce the secretion of Wnts, they do not completely abolish the transport of these ligands to the extracellular space (Proffitt et al., 2013; Chen et al., 2009). In Chapter 2, I demonstrate that Wnts lacking acylation are still able to productively bind CRDs and activate the β-

catenin dependent pathway. In Chapter 3, my studies of the acylation-independent signaling of unique Wnts further predict that the effects of Porcupine inhibition will depend on the specific structural properties of the Wnt(s) and Wnt receptors expressed by cancer cells. In sum, my work highlights that continued research into the mechanisms that govern Wnt/receptor interaction will be important for our understanding of vertebrate development and the treatment of human disease.

Chapter 5: Materials & Methods

5.1. Reagents

Antibodies		
β-tubulin	BD Pharmingen	556321
xWnt8	Cocalico Biologicals	Custom Ab 137 μM
Wnt1	abcam	15251
Wnt3a	abcam	28472
Wnt5a	Cell Signaling	C27E8
Myc 9E10	UPenn Cell Center	3207
Myc	Cell Signaling	2272
FLAG	Thermofisher	PA1-984B
GFP	abcam	13970
Donkey α-Mouse 680 secondary	Licor	925-68072
Donkey α-Rab 800CW secondary	Licor	925-32213
Alexa Fluor 488 Goat α-Chicken IgY (H+L) secondary	ThermoFisher	A-11039
Alexa Fluor 594 Goat α-Rabbit IgG (H+L) secondary	ThermoFisher	A-11012
Chemicals, Peptides, and Recombinant Proteins		
Protease Inhibitor Cocktail	Sigma	P8340
bløk™-FL Fluorescent Blocker	Millipore	WBAVDFL01
Recombinant Protein G Agarose	ThermoFisher	15920010
Critical Commercial Assays		
mMessage mMachine™ SP6 Transcription Kit	ThermoFisher	AM1340

RNeasy Mini Kit	QIAGEN	74106
M-MLV Reverse Transcriptase	ThermoFisher	28025013
Power SYBR™ Green PCR Master Mix	ThermoFisher	4367659
EpiMAX Affinity Purification Kit	abcam	ab138915
Oligonucleotides		
ODC_for: 5′ – GATCATGCACATGTCAAGCC – 3′	Skirkanich et al., 2011	*siamois* Forward
ODC_rev: 5′ – TCTACGATACGATCCAGCCC – 3′	Skirkanich et al., 2011	*siamois* Reverse
Siamois_for: 5′ – CTGTCCTACAAGAGACTCTG – 3′	Iwasaki and Thomsen, 2014	*siamois* U
Siamois_rev: 5′ – TGTTGACTGCAGACTGTTGA – 3′	Iwasaki and Thomsen, 2014	*siamois* D
Xnr3_for: 5′ – CTGGAGTCACCACAAATCTACCCAGA – 3′	Blythe et al., 2010	Xnr3 5' Forward 5'
Xnr3_rev: 5′ – AGGCATCGCCATCAGTGGGG – 3′	Blythe et al., 2010, #54228	Xnr3 5' Reverse 5'

5.2. Experimental model and vertebrate animal handling

In vitro fertilization, microinjection and culture of *Xenopus laevis* embryos were performed as previously described (Hazel et al., 2000). All *Xenopus* experiments were approved by the Institutional Animal Care and Use Committee at the University of Pennsylvania and conform to relevant regulatory standards.

5.3. Plasmid construction and *in vitro* translation

The pCS2-memGFP plasmid was a gift from the laboratory of John Wallingford and is described in (Wallingford et al., 2000). pCS2-Venus was constructed by cloning an

Nco1/EcoR1 fragment of pVENUS-C1 into pCS2. pCS2-xWnt8 is described in (Deardorff et al., 1998). pcDNA-Wnt3A was a gift from Marian Waterman (Addgene plasmid # 35908). The open reading frame (start to stop codon only) of Wnt3A was amplified by PCR and cloned into pCS2 using restriction enzymes BamHI and XbaI. pCS2-mWnt1 was a gift from the laboratory of Jean-Pierre Saint-Jeannet and is described in (Saint-Jeannet et al., 1997). The open reading frame was PCR amplified and re-cloned into pCS2 using restriction enzymes EcoRI and XbaI in order to remove the 3' and 5' UTRs. pcDNA-mWnt5a was a gift from the laboratory of Ed Morrisey and the open reading frame (start to stop codon only) was PCR amplified and cloned into pCS2 using the restriction enzymes BamHI and XhoI. Notum^{WT}-FLAG and Notum^{S239A}-FLAG cDNAs in pCS2 were a gift from the laboratory of Xi He and are cited here (Zhang et al., 2015). Site-directed mutagenesis was used to introduce point mutations to Site 1 and Site 2. Capped mRNA was synthesized using the mMessage mMachine™ SP6 Transcription Kit (ThermoFisher AM1340) and purified using an RNeasy Mini Kit (QIAGEN).

5.4. Analysis of Wnt phenotypes in *Xenopus laevis* embryos

Xenopus embryos were obtained by *in vitro* fertilization as previously described (Sive et al., 2000) and cultured at room temperature in 0.1 X Marc's Modified Ringer's (MMR) buffer unless otherwise stated. All buffer recipes are described in the handbook by Sive et al. (Sive et al., 2000). Ectopic expression of Wnt constructs was achieved by microinjection of mRNAs. Groups of 20-30 individual embryos were randomly grouped and placed in 0.5 X MMR, 3% Ficoll at 12˚C, and microinjected at the four-cell stage, with the exception of experiments where Notum and Wnts were expressed from

separate cells of the embryo (specific protocol described below). All mRNAs were co-injected with 300 pg of Venus YFP mRNA, and negative control groups were injected with YFP mRNA only. Biological replicates were obtained using embryos from unique parental crosses. At the gastrula stage, embryos were sorted for YFP expression (as a positive control for successful mRNA injection) under a fluorescence dissecting microscope. Discrepancies between sample sizes at the beginning and end of each analysis are due to attrition caused by either a failure of embryos to demonstrate YFP fluorescence (resulting in embryos being discarded from the analysis) or the death of embryos before phenotypes were analyzed.

For Wnts 1, 3a and 8, 10 nl of mRNA was injected into the lower marginal zone (4 o'clock) of one ventrally-fated blastomere (ventral marginal zone, VMZ). Wnt5a was co-injected with Fz5 mRNA at the same location. At the tailbud stages, a numerical score was assigned to individual embryo phenotypes (normal phenotype = 0, partial axis duplication = 1, full axis duplication = 2, radial duplication = 3). For each treatment, phenotype scores from individuals across three (or more) biological replicates were summed. Dividing by the total number of individuals analyzed yielded a mean dorsal score, which falls on a 0 – 3 scale.

Experiments with Wnt and Notum mRNA were carried out using an identical protocol except for what is noted here. For experiments where Wnts were co-expressed with Notum from the same cell, mRNAs were mixed and injected simultaneously into the VMZ of a four-cell stage embryo. For experiments where Wnt and Notum were expressed from separate cells, Notum mRNA was injected at the four-cell stage into the VMZ of one ventral blastomere. At the eight-cell stage, Wnt mRNA was injected into the

adjacent ventral blastomere, in the lower cell, in the same batch of embryos. Notum mRNA was co-injected with 500 pg of tdTomato (RFP) mRNA and Wnt was co-injected with 300 pg of YFP mRNA. At the neurula stage, embryos were evaluated for YFP and tdTomato expression (note that tdTomato expression is quite weak) and any embryos with significantly overlapping expression patterns were discarded. Phenotypes were analyzed as described above.

For mWnt5a-dependent convergent extension phenotypes, 5 nl of mRNA was injected in the upper marginal zone (2 o'clock) of both dorsally-fated blastomeres. Embryo phenotypes were analyzed for convergent extension defects at the mid-neurula stage. For each treatment, the number of embryos displaying convergent extension defects across three biological replicates was summed and represented as percent of the total individuals analyzed.

5.5. RT-PCR

Embryos used for the analysis of Wnt target gene transcription were cultured and microinjected using the methods described above. Ten YFP-positive embryos were flash-frozen at the early gastrula stage (Nieuwkoop and Faber stage 10). mRNA was isolated from all ten embryos using an RNeasy Mini Kit (QIAGEN). Reverse transcription was performed using M-MLV Reverse Transcriptase (ThermoFisher) with 2 μg template mRNA for 1 h at 42˚C. Real-time PCR was performed with *Power* SYBR™ Green PCR Master Mix (ThermoFisher) for 30 cycles using the primers listed below. *Ornithine decarboxylase* (*ODC*) served as a reference gene. All primers are listed in Section 5.1.

Data were analyzed using the Comparative C_T Method ($\Delta\Delta C_T$) of qPCR analysis. Due to variability in the magnitude of fold change across clutches from different parental crosses, $\Delta\Delta C_T$ values were calculated by normalizing our test samples to a positive control. For comparisons of wild-type and mutated Wnt activity, the ΔC_T value from the sample injected with the highest dose of WT mRNA was used as the calibrating sample (500 pg of $xWnt8^{WT}$ and $mWnt1^{WT}$, 100 pg of $hWnt3a^{WT}$). For co-injection of Wnt and xFz8 CRD mRNA, the ΔC_T value of the sample injected with 5 pg Wnt^{WT} mRNA was used as the calibrating sample for all three Wnts.

5.6. xWnt8 antibody development

Peptides A (aa21 – 119) and B (aa197 – 308) from xWnt8 were expressed as MBP fusion proteins from the pMAL-c2X vector. Fusion proteins were grown in *E. coli* and purified using standard methods. Immunization of rabbits with both peptides A and B was performed by Cocalico Biologicals. The resulting antisera reacted with peptide B only. The antibody was purified and concentrated from antisera with the EpiMAX Affinity Purification Kit (Abcam) using immobilized Peptide B GST fusion protein as bait. The antibody recognizes *Xenopus* Wnt8 but not murine Wnt8. Representative Western blots demonstrating the specificity of the antibody are included in Appendix Figure 1.

5.7. Western blotting

Embryos used for the analysis of Wnt protein expression were cultured and microinjected using the methods described above. Five YFP-positive embryos were

flash-frozen at the mid gastrula stage (stage 10.5). Embryos were homogenized through a P200 pipet tip in 10 μl/embryo Lysis Buffer (20 mM Tris, pH 7.5, 1% Triton X-100, 140 mM NaCl, 10% glycerol, 10 mM EDTA, 1 mM DTT) supplemented with protease inhibitor cocktail (Sigma P8340, 1:100 dilution). Lysates were centrifuged at 1000 x g for 5 min to remove yolk protein, and subsequently at 14,000 rpm for 10 minutes to remove cellular debris. The lipid-free layer of supernatant was recovered and 1-2 embryo equivalents were loaded on to a 10% SDS-PAGE gel. Protein gels were run at 100V and transferred to a nitrocellulose membrane for 2 h at 350 mA. Membranes were blocked for 1 h in bløk™-FL Fluorescent Blocker (Millipore), and probed with antibodies against β-tubulin (BD Pharmingen 556321, 1:1000), FLAG (1:500), xWnt8 (see above, 0.14 μg/ml), Wnt1 (Abcam 15251, 1:1000), Wnt3a (Abcam 28472, 20 μg/mL) and Wnt5a (Cell Signaling Technology C27E8, 1:1000). Blots were incubated with fluorescently-conjugated secondary antibodies (LI-COR, 1:50,000) for 1 h, washed for at least 2 h (optimally overnight) in TBS-T, and visualized on a LI-COR Odyssey scanner.

5.8. Immunoprecipitations

5 nl of a mixture of mRNAs encoding the relevant Wnt variant and xFz8 CRD-myc was injected into both animal blastomeres of two-cell stage embryos with YFP mRNA as a control. For studies with xWnt8, 10 YFP-positive embryos were frozen for processing from each treatment group at the gastrula stage (stage 10.5). Embryos were resuspended in 100 μl immunoprecipitation (IP) buffer (25 mM Tris-HCl, pH 7.4, 150 mM NaCl, 1% Triton X-100 and 2 mM EDTA) supplemented with protease inhibitor cocktail (Sigma, 1:100 dilution) and homogenized through a P200 pipet tip. Lysates were

centrifuged at 1000 x g for 5 min to remove yolk protein, transferred to a new Eppendorf tube, and subsequently centrifuged at 14,000 rpm for 10 min to remove cellular debris. One embryo equivalent of whole cell lysate was collected as an 'Input' sample and 7 embryo equivalents were used for IP. Each IP sample was pre-cleared for one hour with 10 μl settled protein-G agarose (ThermoFisher Scientific) and incubated, rotating, overnight at 4˚C with 1 μg 9E10 α-myc antibody (UPenn Cell Center). Lysates were subsequently incubated for 2 h at 4˚C with 10 μl settled protein-G agarose. Beads were washed for 10 min in 700 μl cold IP buffer three times. Beads were subsequently resuspended in 15 μl of standard 2 X SDS loading buffer, and incubated for 5 min on a 95˚C heat block. 12 μl of IP eluate was then run on a 10% SDS-PAGE gel alongside Input samples. Gels were run and transferred as described above. For hWnt3a IPs, twice the volume of Input and IP samples were loaded on gels. For Wnt1 IPs, 2 μg of 9E10 α-myc antibody was used for the overnight immunoprecipitation. Both protocols were otherwise identical to that described for xWnt8. Membranes were blocked for 1 h in bløk™-FL Fluorescent Blocker (Millipore), and probed with antibodies against xWnt8 (see above, 0.14 μg/ml), Wnt1 (Abcam 15251, 1:250), Wnt3a (Abcam 28472, 40 μg/ml). The mouse 9E10 α-myc antibody (UPenn Cell Center, 1:1000) was used to detect xFz8 CRD-myc expression in Input samples. A rabbit α-myc antibody (Cell Signaling 2272, 1:1000) was used to detect xFz8 CRD-myc in IP samples, as this protein runs at the same molecular weight as the 9E10 heavy chain. Blots were incubated with fluorescently-conjugated secondary antibodies (LI-COR, 1:20,000) for 1 h, washed for at least 2 h in TBS-T, and visualized using a LI-COR Odyssey scanner.

5.9. Immunofluorescence

Two-cell stage embryos were injected with 5 nl of 100 ng/μl memGFP mRNA in both blastomeres. At the 32-cell stage, embryos were again injected with 5 nl of 200 ng/μl mRNA encoding $xWnt8^{WT}$ or $xWnt8^{S187A}$ in one cell closest to the animal pole. At the late blastula stage (stage 9), the animal tissues of the embryo were surgically removed, fixed, bleached and stained (Lee et al., 2008). Antibodies were used to detect GFP (Abcam 13970, 1:2000) and xWnt8 (see above, 6.9 μg/ml), with secondary antibodies Alexa Fluor 488 Goat α-Chicken for GFP (ThermoFisher Scientific A-11039) and Alexa Fluor 594 Goat α-Rabbit for xWnt8 (ThermoFisher Scientific A-11012). Imaging was performed using a Leica TCS SP8 Confocal microscope. Negative control embryos (not shown) were neither injected with xWnt8 nor memGFP but were processed alongside experimental samples and were used to determine the data acquisition parameters on the confocal microscope. The 'levels' function in Adobe Photoshop was used to perform linear contrast stretching equally in all images for clarity of viewing.

5.10. Statistical Analysis

Gene expression data were analyzed with STATA software (https://www.stata.com/). To analyze the relationship between mRNA treatment and gene expression, a fixed effects regression model treating the X variable (mRNA treatment type) as categorical was employed to account for clutch-to-clutch variation in gene expression values in all analyses. Two-tailed P values were used to determine significance. Statistical significance was set as follows: 'ns' denotes $p \geq 0.05$, *$p \leq 0.05$, **$p \leq 0.01$ and ***$p \leq 0.001$. Activation of Wnt-specific gene expression by the Site 1- and Site 2-mutated proteins was analyzed using control samples (YFP mRNA-injected embryos) as

the reference group. Wnt 8, 1 and 3a dose curves were also analyzed using the control samples as a reference group. Subsequent pair-wise comparisons were performed using a Wald chi-squared test with (1, 24) degrees of freedom. To determine the effect of xFz8 CRD co-expression on Wnt-dependent transcription, each data set was first analyzed for interaction between the two treatment variables – Wnt type (WT or acyl mutant) and inhibitor (CRD) presence – but no significant interaction was found. Final analysis was performed using a regression model without interaction with the WT alone treatment group serving as a reference group.

Bibliography

Afzal, A. R., Rajab, A., Fenske, C. D., Oldridge, M., Elanko, N., Ternes-Pereira, E., Tuysuz, B., Murday, V. A., Patton, M. A., Wilkie, A. O., and Jeffery, S. (2000). Recessive Robinow syndrome, allelic to dominant brachydactyly type B, is caused by mutation of ROR2. Nat Genet *25*, 419-422.

Alexandre, C., Baena-Lopez, A., and Vincent, J. P. (2014). Patterning and growth control by membrane-tethered Wingless. Nature *505*, 180-185.

Amano, M., Nakayama, M., and Kaibuchi, K. (2010). Rho-kinase/ROCK: A key regulator of the cytoskeleton and cell polarity. Cytoskeleton (Hoboken) *67*, 545-554.

Amit, S., Hatzubai, A., Birman, Y., Andersen, J. S., Ben-Shushan, E., Mann, M., Ben-Neriah, Y., and Alkalay, I. (2002). Axin-mediated CKI phosphorylation of beta-catenin at Ser 45: a molecular switch for the Wnt pathway. Genes Dev *16*, 1066-1076.

Anastas, J. N., and Moon, R. T. (2012). WNT signalling pathways as therapeutic targets in cancer. Nat Rev Cancer *13*, 11-26.

Andre, P., Wang, Q., Wang, N., Gao, B., Schilit, A., Halford, M. M., Stacker, S. A., Zhang, X., and Yang, Y. (2012). The Wnt coreceptor Ryk regulates Wnt/planar cell polarity by modulating the degradation of the core planar cell polarity component Vangl2. J Biol Chem *287*, 44518-44525.

Bänziger, C., Soldini, D., Schütt, C., Zipperlen, P., Hausmann, G., and Basler, K. (2006). Wntless, a conserved membrane protein dedicated to the secretion of Wnt proteins from signaling cells. Cell *125*, 509-522.

Bartscherer, K., and Boutros, M. (2008). Regulation of Wnt protein secretion and its role in gradient formation. EMBO Rep *9*, 977-982.

Behrens, J., Jerchow, B. A., Würtele, M., Grimm, J., Asbrand, C., Wirtz, R., Kühl, M., Wedlich, D., and Birchmeier, W. (1998). Functional interaction of an axin homolog, conductin, with beta-catenin, APC, and GSK3beta. Science *280*, 596-599.

Behrens, J., von Kries, J. P., Kuhl, M., Bruhn, L., Wedlich, D., Grosschedl, R., and Birchmeier, W. (1996). Functional interaction of beta-catenin with the transcription factor LEF-1. Nature *382*, 638-642.

Bhanot, P., Brink, M., Samos, C. H., Hsieh, J. C., Wang, Y., Macke, J. P., Andrew, D., Nathans, J., and Nusse, R. (1996). A new member of the frizzled family from Drosophila functions as a Wingless receptor. Nature *382*, 225-230.

Biechele, S., Cockburn, K., Lanner, F., Cox, B. J., and Rossant, J. (2013). Porcn-dependent Wnt signaling is not required prior to mouse gastrulation. Development *140*, 2961-2971.

Blythe, S. A., Cha, S. W., Tadjuidje, E., Heasman, J., and Klein, P. S. (2010). beta-Catenin primes organizer gene expression by recruiting a histone H3 arginine 8 methyltransferase, Prmt2.

Bourhis, E., Tam, C., Franke, Y., Bazan, J. F., Ernst, J., Hwang, J., Costa, M., Cochran, A. G., and Hannoush, R. N. (2010). Reconstitution of a frizzled8.Wnt3a.LRP6 signaling complex reveals multiple Wnt and Dkk1 binding sites on LRP6. J Biol Chem *285*, 9172-9179.

Boutros, M., Mihaly, J., Bouwmeester, T., and Mlodzik, M. (2000). Signaling specificity by Frizzled receptors in Drosophila. Science *288*, 1825-1828.

Brannon, M., and Kimelman, D. (1996). Activation of Siamois by the Wnt pathway. Dev Biol *180*, 344-347.

Brunner, E., Peter, O., Schweizer, L., and Basler, K. (1997). pangolin encodes a Lef-1 homologue that acts downstream of Armadillo to transduce the Wingless signal in Drosophila. Nature *385*, 829-833.

Byrne, E. F. X., Sircar, R., Miller, P. S., Hedger, G., Luchetti, G., Nachtergaele, S., Tully, M. D., Mydock-McGrane, L., Covey, D. F., Rambo, R. P., Sansom, M. S. P., Newstead, S., Rohatgi, R., and Siebold, C. (2016). Structural basis of Smoothened regulation by its extracellular domains. Nature *535*, 517-522.

Cadigan, K. M., Fish, M. P., Rulifson, E. J., and Nusse, R. (1998). Wingless repression of Drosophila frizzled 2 expression shapes the Wingless morphogen gradient in the wing. Cell *93*, 767-777.

Chang, T. H., Hsieh, F. L., Zebisch, M., Harlos, K., Elegheert, J., and Jones, E. Y. (2015). Structure and functional properties of Norrin mimic Wnt for signalling with Frizzled4, Lrp5/6, and proteoglycan. Elife *4*,

Chen, B., Dodge, M. E., Tang, W., Lu, J., Ma, Z., Fan, C. W., Wei, S., Hao, W., Kilgore, J., Williams, N. S., Roth, M. G., Amatruda, J. F., Chen, C., and Lum, L. (2009). Small molecule-mediated disruption of Wnt-dependent signaling in tissue regeneration and cancer. Nat Chem Biol *5*, 100-107.

Ching, W., Hang, H. C., and Nusse, R. (2008). Lipid-independent secretion of a Drosophila Wnt protein. J Biol Chem *283*, 17092-17098.

Chu, M. L., Ahn, V. E., Choi, H. J., Daniels, D. L., Nusse, R., and Weis, W. I. (2013). structural Studies of Wnts and identification of an LRP6 binding site. Structure *21*, 1235-1242.

Clevers, H. (2006). Wnt/beta-catenin signaling in development and disease. Cell *127*, 469-480.

Cong, F., Schweizer, L., and Varmus, H. (2004). Wnt signals across the plasma membrane to activate the beta-catenin pathway by forming oligomers containing its receptors, Frizzled and LRP. Development *131*, 5103-5115.

Cook, D., Fry, M. J., Hughes, K., Sumathipala, R., Woodgett, J. R., and Dale, T. C. (1996). Wingless inactivates glycogen synthase kinase-3 via an intracellular signalling pathway which involves a protein kinase C. EMBO J *15*, 4526-4536.

Davidson, G., Wu, W., Shen, J., Bilic, J., Fenger, U., Stannek, P., Glinka, A., and Niehrs, C. (2005). Casein kinase 1 gamma couples Wnt receptor activation to cytoplasmic signal transduction. Nature *438*, 867-872.

De Robertis, E. M., Larrain, J., Oelgeschlager, M., and Wessely, O. (2000). The establishment of Spemann's organizer and patterning of the vertebrate embryo. Nat Rev Genet *1*, 171-181.

Deardorff, M. A., Tan, C., Conrad, L. J., and Klein, P. S. N. (1998). Frizzled-8 is expressed in the Spemann organizer and plays a role in early morphogenesis. Development *125*, 2687-2700.

Deardorff, M. A., Tan, C., Saint-Jeannet, J. P., and Klein, P. S. (2001). A role for frizzled 3 in neural crest development. Development *128*, 3655-3663.

Dijksterhuis, J. P., Baljinnyam, B., Stanger, K., Sercan, H. O., Ji, Y., Andres, O., Rubin, J. S., Hannoush, R. N., and Schulte, G. (2015). Systematic mapping of WNT-FZD protein interactions reveals functional selectivity by distinct WNT-FZD pairs. J Biol Chem *290*, 6789-6798.

Djiane, A., Riou, J., Umbhauer, M., Boucaut, J., and Shi, D. (2000). Role of frizzled 7 in the regulation of convergent extension movements during gastrulation in Xenopus laevis. Development *127*, 3091-3100.

Du, S. J., Purcell, S. M., Christian, J. L., McGrew, L. L., and Moon, R. T. (1995). Identification of distinct classes and functional domains of Wnts through expression of wild-type and chimeric proteins in Xenopus embryos. Mol Cell Biol *15*, 2625-2634.

Enomoto, M., Hayakawa, S., Itsukushima, S., Ren, D. Y., Matsuo, M., Tamada, K., Oneyama, C., Okada, M., Takumi, T., Nishita, M., and Minami, Y. (2009). Autonomous regulation of osteosarcoma cell invasiveness by Wnt5a/Ror2 signaling. Oncogene *28*, 3197-3208.

Etheridge, S. L., Ray, S., Li, S., Hamblet, N. S., Lijam, N., Tsang, M., Greer, J., Kardos, N., Wang, J., Sussman, D. J., Chen, P., and Wynshaw-Boris, A. (2008). Murine dishevelled 3 functions in redundant pathways with dishevelled 1 and 2 in normal cardiac outflow tract, cochlea, and neural tube development. PLoS Genet *4*, e1000259.

Ettenberg, S. A., Charlat, O., Daley, M. P., Liu, S., Vincent, K. J., Stuart, D. D., Schuller, A. G., Yuan, J., Ospina, B., Green, J., Yu, Q., Walsh, R., Li, S., Schmitz, R., Heine, H., Bilic, S., Ostrom, L., Mosher, R., Hartlepp, K. F., Zhu, Z., Fawell, S., Yao, Y. M., Stover, D., Finan, P. M., Porter, J. A., Sellers, W. R., Klagge, I. M., and Cong, F. (2010). Inhibition of tumorigenesis driven by different Wnt proteins requires blockade of distinct ligand-binding regions by LRP6 antibodies. Proc Natl Acad Sci U S A *107*, 15473-15478.

Fan, M. J., and Sokol, S. Y. (1997). A role for Siamois in Spemann organizer formation. Development *124*, 2581-2589.

Farin, H. F., Jordens, I., Mosa, M. H., Basak, O., Korving, J., Tauriello, D. V., de Punder, K., Angers, S., Peters, P. J., Maurice, M. M., and Clevers, H. (2016). Visualization of a short-range Wnt gradient in the intestinal stem-cell niche. Nature *530*, 340-343.

Fiedler, M., Mendoza-Topaz, C., Rutherford, T. J., Mieszczanek, J., and Bienz, M. (2011). Dishevelled interacts with the DIX domain polymerization interface of Axin to interfere with its function in down-regulating β-catenin. Proc Natl Acad Sci U S A *108*, 1937-1942.

Franch-Marro, X., Wendler, F., Griffith, J., Maurice, M. M., and Vincent, J. P. (2008). In vivo role of lipid adducts on Wingless. J Cell Sci *121*, 1587-1592.

Funayama, N., Fagotto, F., McCrea, P., and Gumbiner, B. M. (1995). Embryonic axis induction by the armadillo repeat domain of beta-catenin: evidence for intracellular signaling. J Cell Biol *128*, 959-968.

Galli, L. M., Barnes, T. L., Secrest, S. S., Kadowaki, T., and Burrus, L. W. (2007). Porcupine-mediated lipid-modification regulates the activity and distribution of Wnt proteins in the chick neural tube. Development *134*, 3339-3348.

Gao, X., Arenas-Ramirez, N., Scales, S. J., and Hannoush, R. N. (2011). Membrane targeting of palmitoylated Wnt and Hedgehog revealed by chemical probes. FEBS Lett *585*, 2501-2506.

Gao, X., and Hannoush, R. N. (2014). Single-cell imaging of Wnt palmitoylation by the acyltransferase porcupine. Nat Chem Biol *10*, 61-68.

Gong, Y., Bourhis, E., Chiu, C., Stawicki, S., DeAlmeida, V. I., Liu, B. Y., Phamluong, K., Cao, T. C., Carano, R. A., Ernst, J. A., Solloway, M., Rubinfeld, B., Hannoush, R. N., Wu, Y., Polakis, P., and Costa, M. (2010). Wnt isoform-specific interactions with coreceptor specify inhibition or potentiation of signaling by LRP6 antibodies. PLoS One *5*, e12682.

Gray, R. S., Roszko, I., and Solnica-Krezel, L. (2011). Planar cell polarity: coordinating morphogenetic cell behaviors with embryonic polarity. Dev Cell *21*, 120-133.

Grumolato, L., Liu, G., Mong, P., Mudbhary, R., Biswas, R., Arroyave, R., Vijayakumar, S., Economides, A. N., and Aaronson, S. A. (2010). Canonical and noncanonical Wnts use a common mechanism to activate completely unrelated coreceptors. Genes Dev *24*, 2517-2530.

Gubb, D., and García-Bellido, A. (1982). A genetic analysis of the determination of cuticular polarity during development in Drosophila melanogaster. J Embryol Exp Morphol *68*, 37-57.

Guder, C., Philipp, I., Lengfeld, T., Watanabe, H., Hobmayer, B., and Holstein, T. W. (2006). The Wnt code: cnidarians signal the way. Oncogene *25*, 7450-7460.

Gurley, K. A., Rink, J. C., and Sánchez Alvarado, A. (2008). Beta-catenin defines head versus tail identity during planarian regeneration and homeostasis. Science *319*, 323-327.

Halford, M. M., Armes, J., Buchert, M., Meskenaite, V., Grail, D., Hibbs, M. L., Wilks, A. F., Farlie, P. G., Newgreen, D. F., Hovens, C. M., and Stacker, S. A. (2000). Ryk-deficient mice exhibit craniofacial defects associated with perturbed Eph receptor crosstalk. Nat Genet *25*, 414-418.

Hamblet, N. S., Lijam, N., Ruiz-Lozano, P., Wang, J., Yang, Y., Luo, Z., Mei, L., Chien, K. R., Sussman, D. J., and Wynshaw-Boris, A. (2002). Dishevelled 2 is essential for cardiac outflow tract development, somite segmentation and neural tube closure. Development *129*, 5827-5838.

Hart, M. J., de los Santos, R., Albert, I. N., Rubinfeld, B., and Polakis, P. (1998). Downregulation of beta-catenin by human Axin and its association with the APC tumor suppressor, beta-catenin and GSK3 beta. Curr Biol *8*, 573-581.

Hazel, L. S., Robert, M. G., and Richard, M. H. (2000). Early Development of Xenopus Laevis.

He, X., Saint-Jeannet, J. P., Wang, Y., Nathans, J., Dawid, I., and Varmus, H. (1997). A member of the Frizzled protein family mediating axis induction by Wnt-5A. Science *275*, 1652-1654.

Heasman, J., Kofron, M., and Wylie, C. (2000). Beta-catenin signaling activity dissected in the early Xenopus embryo: a novel antisense approach. Dev Biol *222*, 124-134.

Heisenberg, C. P., Tada, M., Rauch, G. J., Saude, L., Concha, M. L., Geisler, R., Stemple, D. L., Smith, J. C., and Wilson, S. W. (2000). Silberblick/Wnt11 mediates convergent extension movements during zebrafish gastrulation. Nature *405*, 76-81.

Hernández, A. R., Klein, A. M., and Kirschner, M. W. (2012). Kinetic responses of β-catenin specify the sites of Wnt control. Science *338*, 1337-1340.

Herr, P., and Basler, K. (2012). Porcupine-mediated lipidation is required for Wnt recognition by Wls. Dev Biol *361*, 392-402.

Hinoi, T., Yamamoto, H., Kishida, M., Takada, S., Kishida, S., and Kikuchi, A. (2000). Complex formation of adenomatous polyposis coli gene product and axin facilitates glycogen synthase kinase-3 beta-dependent phosphorylation of beta-catenin and down-regulates beta-catenin. J Biol Chem *275*, 34399-34406.

Holmen, S. L., Salic, A., Zylstra, C. R., Kirschner, M. W., and Williams, B. O. (2002). A novel set of Wnt-Frizzled fusion proteins identifies receptor components that activate beta -catenin-dependent signaling. J Biol Chem *277*, 34727-34735.

Holstein, T. W. (2012). The evolution of the Wnt pathway. Cold Spring Harb Perspect Biol *4*, a007922.

Hsieh, J. C., Rattner, A., Smallwood, P. M., and Nathans, J. (1999). Biochemical characterization of Wnt-frizzled interactions using a soluble, biologically active vertebrate Wnt protein. Proc Natl Acad Sci U S A *96*, 3546-3551.

Huang, J., Nguyen-McCarty, M., Hexner, E. O., Danet-Desnoyers, G., and Klein, P. S. (2012). Maintenance of hematopoietic stem cells through regulation of Wnt and mTOR pathways. Nat Med *18*, 1778-1785.

Inoue, T., Oz, H. S., Wiland, D., Gharib, S., Deshpande, R., Hill, R. J., Katz, W. S., and Sternberg, P. W. (2004). C. elegans LIN-18 is a Ryk ortholog and functions in parallel to LIN-17/Frizzled in Wnt signaling. Cell *118*, 795-806.

Iwasaki, Y., and Thomsen, G. H. (2014). The splicing factor PQBP1 regulates mesodermal and neural development through FGF signaling. Development *141*, 3740-3751.

Janda, C. Y., Dang, L. T., You, C., Chang, J., de Lau, W., Zhong, Z. A., Yan, K. S., Marecic, O., Siepe, D., Li, X., Moody, J. D., Williams, B. O., Clevers, H., Piehler, J., Baker, D., Kuo, C. J., and Garcia, K. C. (2017). Surrogate Wnt agonists that phenocopy canonical Wnt and β-catenin signalling. Nature *545*, 234-237.

Janda, C. Y., Waghray, D., Levin, A. M., Thomas, C., and Garcia, K. C. (2012). Structural basis of Wnt recognition by Frizzled. Science *337*, 59-64.

Jing, L., Lefebvre, J. L., Gordon, L. R., and Granato, M. (2009). Wnt signals organize synaptic prepattern and axon guidance through the zebrafish unplugged/MuSK receptor. Neuron *61*, 721-733.

Kakugawa, S., Langton, P. F., Zebisch, M., Howell, S. A., Chang, T. H., Liu, Y., Feizi, T., Bineva, G., O'Reilly, N., Snijders, A. P., Jones, E. Y., and Vincent, J. P. (2015). Notum deacylates Wnt proteins to suppress signalling activity. Nature *519*, 187-192.

Kao, K. R., Masui, Y., and Elinson, R. P. (1986). Lithium-induced respecification of pattern in Xenopus laevis embryos. Nature *322*, 371-373.

Ke, J., Harikumar, K. G., Erice, C., Chen, C., Gu, X., Wang, L., Parker, N., Cheng, Z., Xu, W., Williams, B. O., Melcher, K., Miller, L. J., and Xu, H. E. (2013). Structure and function of Norrin in assembly and activation of a Frizzled 4-Lrp5/6 complex. Genes Dev *27*, 2305-2319.

Keller, R., Cooper, M. S., Danilchik, M., Tibbetts, P., and Wilson, P. A. (1989). Cell intercalation during notochord development in Xenopus laevis. J Exp Zool *251*, 134-154.

Keller, R., and Tibbetts, P. (1989). Mediolateral cell intercalation in the dorsal, axial mesoderm of Xenopus laevis. Dev Biol *131*, 539-549.

Kessler, D. S. (1997). Siamois is required for formation of Spemann's organizer. Proc Natl Acad Sci U S A *94*, 13017-13022.

Kibar, Z., Torban, E., McDearmid, J. R., Reynolds, A., Berghout, J., Mathieu, M., Kirillova, I., De Marco, P., Merello, E., Hayes, J. M., Wallingford, J. B., Drapeau, P., Capra, V., and Gros, P. (2007). Mutations in VANGL1 associated with neural-tube defects. N Engl J Med *356*, 1432-1437.

Kikuchi, A., Yamamoto, H., and Sato, A. (2009). Selective activation mechanisms of Wnt signaling pathways. Trends Cell Biol *19*, 119-129.

Kilian, B., Mansukoski, H., Barbosa, F. C., Ulrich, F., Tada, M., and Heisenberg, C. P. (2003). The role of Ppt/Wnt5 in regulating cell shape and movement during zebrafish gastrulation. Mech Dev *120*, 467-476.

Kim, G. H., Her, J. H., and Han, J. K. (2008). Ryk cooperates with Frizzled 7 to promote Wnt11-mediated endocytosis and is essential for Xenopus laevis convergent extension movements. J Cell Biol *182*, 1073-1082.

Kim, H., Cheong, S. M., Ryu, J., Jung, H. J., Jho, E. H., and Han, J. K. (2009). Xenopus Wntless and the retromer complex cooperate to regulate XWnt4 secretion. Mol Cell Biol *29*, 2118-2128.

Kinzler, K. W., and Vogelstein, B. (1996). Lessons from hereditary colorectal cancer. Cell *87*, 159-170.

Klein, P. S., and Melton, D. A. (1996). A molecular mechanism for the effect of lithium on development. Proc Natl Acad Sci U S A *93*, 8455-8459.

Komekado, H., Yamamoto, H., Chiba, T., and Kikuchi, A. (2007). Glycosylation and palmitoylation of Wnt-3a are coupled to produce an active form of Wnt-3a. Genes Cells *12*, 521-534.

Korinek, V., Barker, N., Moerer, P., van Donselaar, E., Huls, G., Peters, P. J., and Clevers, H. (1998). Depletion of epithelial stem-cell compartments in the small intestine of mice lacking Tcf-4. Nat Genet *19*, 379-383.

Krasnow, R. E., and Adler, P. N. (1994). A single frizzled protein has a dual function in tissue polarity. Development *120*, 1883-1893.

Kulak, O., Chen, H., Holohan, B., Wu, X., He, H., Borek, D., Otwinowski, Z., Yamaguchi, K., Garofalo, L. A., Ma, Z., Wright, W., Chen, C., Shay, J. W., Zhang, X., and Lum, L. (2015). Disruption of Wnt/β-Catenin Signaling and Telomeric Shortening Are Inextricable Consequences of Tankyrase Inhibition in Human Cells. Mol Cell Biol *35*, 2425-2435.

Kurayoshi, M., Yamamoto, H., Izumi, S., and Kikuchi, A. (2007). Post-translational palmitoylation and glycosylation of Wnt-5a are necessary for its signalling. Biochem J *402*, 515-523.

Lecuit, T., and Cohen, S. M. (1997). Proximal-distal axis formation in the Drosophila leg. Nature *388*, 139-145.

Lee, C., Kieserman, E., Gray, R. S., Park, T. J., and Wallingford, J. (2008). Whole-mount fluorescence immunocytochemistry on Xenopus embryos. CSH Protoc *2008*, pdb.prot4957.

Lemaire, P., Garrett, N., and Gurdon, J. B. (1995). Expression cloning of Siamois, a Xenopus homeobox gene expressed in dorsal-vegetal cells of blastulae and able to induce a complete secondary axis. Cell *81*, 85-94.

Lemmon, M. A., and Schlessinger, J. (2010). Cell signaling by receptor tyrosine kinases. Cell *141*, 1117-1134.

Lim, X., Tan, S. H., Koh, W. L., Chau, R. M., Yan, K. S., Kuo, C. J., van Amerongen, R., Klein, A. M., and Nusse, R. (2013). Interfollicular epidermal stem cells self-renew via autocrine Wnt signaling. Science *342*, 1226-1230.

Liu, C., Li, Y., Semenov, M., Han, C., Baeg, G. H., Tan, Y., Zhang, Z., Lin, X., and He, X. (2002). Control of beta-catenin phosphorylation/degradation by a dual-kinase mechanism. Cell *108*, 837-847.

Liu, Y., Ross, J. F., Bodine, P. V., and Billiard, J. (2007). Homodimerization of Ror2 tyrosine kinase receptor induces 14-3-3(beta) phosphorylation and promotes osteoblast differentiation and bone formation. Mol Endocrinol *21*, 3050-3061.

Liu, Y., Rubin, B., Bodine, P. V., and Billiard, J. (2008). Wnt5a induces homodimerization and activation of Ror2 receptor tyrosine kinase. J Cell Biochem *105*, 497-502.

Logan, C. Y., and Nusse, R. (2004). The Wnt signaling pathway in development and disease. Annu Rev Cell Dev Biol *20*, 781-810.

Lu, W., Yamamoto, V., Ortega, B., and Baltimore, D. (2004a). Mammalian Ryk is a Wnt coreceptor required for stimulation of neurite outgrowth. Cell *119*, 97-108.

Lu, X., Borchers, A. G., Jolicoeur, C., Rayburn, H., Baker, J. C., and Tessier-Lavigne, M. (2004b). PTK7/CCK-4 is a novel regulator of planar cell polarity in vertebrates. Nature *430*, 93-98.

MacDonald, B. T., and He, X. (2012). Frizzled and LRP5/6 receptors for Wnt/β-catenin signaling. Cold Spring Harb Perspect Biol *4*,

Madan, B., Ke, Z., Harmston, N., Ho, S. Y., Frois, A. O., Alam, J., Jeyaraj, D. A., Pendharkar, V., Ghosh, K., Virshup, I. H., Manoharan, V., Ong, E. H., Sangthongpitag, K., Hill, J., Petretto, E., Keller, T. H., Lee, M. A., Matter, A., and Virshup, D. M. (2016). Wnt addiction of genetically defined cancers reversed by PORCN inhibition. Oncogene *35*, 2197-2207.

Mahaffey, J. P., Grego-Bessa, J., Liem, K. F. J., and Anderson, K. V. (2013). Cofilin and Vangl2 cooperate in the initiation of planar cell polarity in the mouse embryo. Development *140*, 1262-1271.

Mao, J., Wang, J., Liu, B., Pan, W., Farr, G. H., Flynn, C., Yuan, H., Takada, S., Kimelman, D., Li, L., and Wu, D. (2001). Low-density lipoprotein receptor-related protein-5 binds to Axin and regulates the canonical Wnt signaling pathway. Mol Cell *7*, 801-809.

Martinez, S., Scerbo, P., Giordano, M., Daulat, A. M., Lhoumeau, A. C., Thomé, V., Kodjabachian, L., and Borg, J. P. (2015). The PTK7 and ROR2 Protein Receptors Interact in the Vertebrate WNT/Planar Cell Polarity (PCP) Pathway. J Biol Chem *290*, 30562-30572.

McElwain, M. A., Ko, D. C., Gordon, M. D., Fyrst, H., Saba, J. D., and Nusse, R. (2011). A suppressor/enhancer screen in Drosophila reveals a role for wnt-mediated lipid metabolism in primordial germ cell migration. PLoS One *6*, e26993.

McKendry, R., Hsu, S. C., Harland, R. M., and Grosschedl, R. (1997). LEF-1/TCF proteins mediate wnt-inducible transcription from the Xenopus nodal-related 3 promoter. Dev Biol *192*, 420-431.

McMahon, A. P., and Moon, R. T. (1989). Ectopic expression of the proto-oncogene int-1 in Xenopus embryos leads to duplication of the embryonic axis. Cell *58*, 1075-1084.

Medina, A., Reintsch, W., and Steinbeisser, H. (2000). Xenopus frizzled 7 can act in canonical and non-canonical Wnt signaling pathways: implications on early patterning and morphogenesis. Mech Dev *92*, 227-237.

Mendrola, J. M., Shi, F., Park, J. H., and Lemmon, M. A. (2013). Receptor tyrosine kinases with intracellular pseudokinase domains. Biochem Soc Trans *41*, 1029-1036.

Mikels, A. J., and Nusse, R. (2006). Purified Wnt5a protein activates or inhibits beta-catenin-TCF signaling depending on receptor context. PLoS Biol *4*, e115.

Miura, G. I., Buglino, J., Alvarado, D., Lemmon, M. A., Resh, M. D., and Treisman, J. E. (2006). Palmitoylation of the EGFR ligand Spitz by Rasp increases Spitz activity by restricting its diffusion. Dev Cell *10*, 167-176.

Miura, G. I., and Treisman, J. E. (2006). Lipid modification of secreted signaling proteins. Cell Cycle *5*, 1184-1188.

Molenaar, M., van de Wetering, M., Oosterwegel, M., Peterson-Maduro, J., Godsave, S., Korinek, V., Roose, J., Destree, O., and Clevers, H. (1996). XTcf-3 transcription factor mediates beta-catenin-induced axis formation in Xenopus embryos. Cell *86*, 391-399.

Mulligan, K. A., Fuerer, C., Ching, W., Fish, M., Willert, K., and Nusse, R. (2012). Secreted Wingless-interacting molecule (Swim) promotes long-range signaling by maintaining Wingless solubility. Proc Natl Acad Sci U S A *109*, 370-377.

Munemitsu, S., Albert, I., Souza, B., Rubinfeld, B., and Polakis, P. (1995). Regulation of intracellular beta-catenin levels by the adenomatous polyposis coli (APC) tumor-suppressor protein. Proc Natl Acad Sci U S A *92*, 3046-3050.

Murphy, J. M., Zhang, Q., Young, S. N., Reese, M. L., Bailey, F. P., Eyers, P. A., Ungureanu, D., Hammaren, H., Silvennoinen, O., Varghese, L. N., Chen, K., Tripaydonis, A., Jura, N., Fukuda, K., Qin, J., Nimchuk, Z., Mudgett, M. B., Elowe, S., Gee, C. L., Liu, L., Daly, R. J., Manning, G., Babon, J. J., and Lucet, I. S. (2014). A robust methodology to subclassify pseudokinases based on their nucleotide-binding properties. Biochem J *457*, 323-334.

Najdi, R., Proffitt, K., Sprowl, S., Kaur, S., Yu, J., Covey, T. M., Virshup, D. M., and Waterman, M. L. (2012). A uniform human Wnt expression library reveals a shared secretory pathway and unique signaling activities. Differentiation *84*, 203-213.

Nakamura, T., Hamada, F., Ishidate, T., Anai, K., Kawahara, K., Toyoshima, K., and Akiyama, T. (1998). Axin, an inhibitor of the Wnt signalling pathway, interacts with beta-catenin, GSK-3beta and APC and reduces the beta-catenin level. Genes Cells *3*, 395-403.

Neumann, C. J., and Cohen, S. M. (1997). Long-range action of Wingless organizes the dorsal-ventral axis of the Drosophila wing. Development *124*, 871-880.

Niehrs, C. (2012). The complex world of WNT receptor signalling. Nat Rev Mol Cell Biol *13*, 767-779.

Nusse, R., and Clevers, H. (2017). Wnt/β-Catenin Signaling, Disease, and Emerging Therapeutic Modalities. Cell *169*, 985-999.

Nusse, R., and Varmus, H. E. (1982). Many tumors induced by the mouse mammary tumor virus contain a provirus integrated in the same region of the host genome. Cell *31*, 99-109.

O'Connell, M. P., Fiori, J. L., Xu, M., Carter, A. D., Frank, B. P., Camilli, T. C., French, A. D., Dissanayake, S. K., Indig, F. E., Bernier, M., Taub, D. D., Hewitt, S. M., and Weeraratna, A. T. (2010). The orphan tyrosine kinase receptor, ROR2, mediates Wnt5A signaling in metastatic melanoma. Oncogene *29*, 34-44.

Oishi, I., Suzuki, H., Onishi, N., Takada, R., Kani, S., Ohkawara, B., Koshida, I., Suzuki, K., Yamada, G., Schwabe, G. C., Mundlos, S., Shibuya, H., Takada, S., and Minami, Y. (2003). The receptor tyrosine kinase Ror2 is involved in non-canonical Wnt5a/JNK signalling pathway. Genes Cells *8*, 645-654.

Oishi, I., Takeuchi, S., Hashimoto, R., Nagabukuro, A., Ueda, T., Liu, Z. J., Hatta, T., Akira, S., Matsuda, Y., Yamamura, H., Otani, H., and Minami, Y. (1999). Spatio-temporally regulated expression of receptor tyrosine kinases, mRor1, mRor2, during mouse development: implications in development and function of the nervous system. Genes Cells *4*, 41-56.

Papkoff, J., and Schryver, B. (1990). Secreted int-1 protein is associated with the cell surface. Mol Cell Biol *10*, 2723-2730.

Patthy, L. (2000). The WIF module. Trends Biochem Sci *25*, 12-13.

Peradziryi, H., Kaplan, N. A., Podleschny, M., Liu, X., Wehner, P., Borchers, A., and Tolwinski, N. S. (2011). PTK7/Otk interacts with Wnts and inhibits canonical Wnt signalling. EMBO J *30*, 3729-3740.

Person, A. D., Beiraghi, S., Sieben, C. M., Hermanson, S., Neumann, A. N., Robu, M. E., Schleiffarth, J. R., Billington, C. J., van Bokhoven, H., Hoogeboom, J. M., Mazzeu, J. F., Petryk, A., Schimmenti, L. A., Brunner, H. G., Ekker, S. C., and Lohr, J. L. (2010). WNT5A mutations in patients with autosomal dominant Robinow syndrome. Dev Dyn *239*, 327-337.

Petersen, C. P., and Reddien, P. W. (2008). Smed-betacatenin-1 is required for anteroposterior blastema polarity in planarian regeneration. Science *319*, 327-330.

Petersen, C. P., and Reddien, P. W. (2009a). Wnt signaling and the polarity of the primary body axis. Cell *139*, 1056-1068.

Petersen, C. P., and Reddien, P. W. (2009b). A wound-induced Wnt expression program controls planarian regeneration polarity. Proc Natl Acad Sci U S A *106*, 17061-17066.

Pfeiffer, S., Ricardo, S., Manneville, J. B., Alexandre, C., and Vincent, J. P. (2002). Producing cells retain and recycle Wingless in Drosophila embryos. Curr Biol *12*, 957-962.

Proffitt, K. D., Madan, B., Ke, Z., Pendharkar, V., Ding, L., Lee, M. A., Hannoush, R. N., and Virshup, D. M. (2013). Pharmacological inhibition of the Wnt acyltransferase PORCN prevents growth of WNT-driven mammary cancer. Cancer Res *73*, 502-507.

Proffitt, K. D., and Virshup, D. M. (2012). Precise regulation of porcupine activity is required for physiological Wnt signaling. J Biol Chem *287*, 34167-34178.

Ring, L., Neth, P., Weber, C., Steffens, S., and Faussner, A. (2014). β-Catenin-dependent pathway activation by both promiscuous “canonical” WNT3a-, and specific “noncanonical” WNT4- and WNT5a-FZD receptor combinations with strong differences in LRP5 and LRP6 dependency. Cell Signal *26*, 260-267.

Rios-Esteves, J., and Resh, M. D. (2013). Stearoyl CoA desaturase is required to produce active, lipid-modified Wnt proteins. Cell Rep *4*, 1072-1081.

Rowning, B. A., Wells, J., Wu, M., Gerhart, J. C., Moon, R. T., and Larabell, C. A. (1997). Microtubule-mediated transport of organelles and localization of beta-catenin to the future dorsal side of Xenopus eggs. Proc Natl Acad Sci U S A *94*, 1224-1229.

Rulifson, E. J., Wu, C. H., and Nusse, R. (2000). Pathway specificity by the bifunctional receptor frizzled is determined by affinity for wingless. Mol Cell *6*, 117-126.

Saint-Jeannet, J. P., He, X., Varmus, H. E., and Dawid, I. B. (1997). Regulation of dorsal fate in the neuraxis by Wnt-1 and Wnt-3a. Proc Natl Acad Sci U S A *94*, 13713-13718.

Saldanha, J., Singh, J., and Mahadevan, D. (1998). Identification of a Frizzled-like cysteine rich domain in the extracellular region of developmental receptor tyrosine kinases. Protein Sci *7*, 1632-1635.

Schambony, A., and Wedlich, D. (2007). Wnt-5A/Ror2 regulate expression of XPAPC through an alternative noncanonical signaling pathway. Dev Cell *12*, 779-792.

Schulte, G., and Bryja, V. (2007). The Frizzled family of unconventional G-protein-coupled receptors. Trends Pharmacol Sci *28*, 518-525.

Shen, G., Ke, J., Wang, Z., Cheng, Z., Gu, X., Wei, Y., Melcher, K., Xu, H. E., and Xu, W. (2015). Structural basis of the Norrin-Frizzled 4 interaction. Cell Res *25*, 1078-1081.

Shi, D. L., and Boucaut, J. C. (2000). Xenopus frizzled 4 is a maternal mRNA and its zygotic expression is localized to the neuroectoderm and trunk lateral plate mesoderm. Mech Dev *94*, 243-245.

Shnitsar, I., and Borchers, A. (2008). PTK7 recruits dsh to regulate neural crest migration. Development *135*, 4015-4024.

Skirkanich, J., Luxardi, G., Yang, J., Kodjabachian, L., and Klein, P. S. (2011). An essential role for transcription before the MBT in Xenopus laevis. Dev Biol *357*, 478-491.

Skoglund, P., and Keller, R. (2010). Integration of planar cell polarity and ECM signaling in elongation of the vertebrate body plan. Curr Opin Cell Biol *22*, 589-596.

Smith, J. C., Conlon, F. L., Saka, Y., and Tada, M. (2000). Xwnt11 and the regulation of gastrulation in Xenopus. Philos Trans R Soc Lond B Biol Sci *355*, 923-930.

Smith, W. C., McKendry, R., Ribisi, S., and Harland, R. M. (1995). A nodal-related gene defines a physical and functional domain within the Spemann organizer. Cell *82*, 37-46.

Sokol, S., Christian, J. L., Moon, R. T., and Melton, D. A. (1991). Injected Wnt RNA induces a complete body axis in Xenopus embryos. Cell *67*, 741-752.

Sokol, S. Y. (1996). Analysis of Dishevelled signalling pathways during Xenopus development. Curr Biol *6*, 1456-1467.

Strochlic, L., Falk, J., Goillot, E., Sigoillot, S., Bourgeois, F., Delers, P., Rouvière, J., Swain, A., Castellani, V., Schaeffer, L., and Legay, C. (2012). Wnt4 participates in the formation of vertebrate neuromuscular junction. PLoS One *7*, e29976.

Swarup, S., and Verheyen, E. M. (2012). Wnt/Wingless signaling in Drosophila. Cold Spring Harb Perspect Biol *4*,

Takada, R., Satomi, Y., Kurata, T., Ueno, N., Norioka, S., Kondoh, H., Takao, T., and Takada, S. (2006). Monounsaturated fatty acid modification of Wnt protein: its role in Wnt secretion. Dev Cell *11*, 791-801.

Tamai, K., Semenov, M., Kato, Y., Spokony, R., Liu, C., Katsuyama, Y., Hess, F., Saint-Jeannet, J. P., and He, X. (2000). LDL-receptor-related proteins in Wnt signal transduction. Nature *407*, 530-535.

Tamai, K., Zeng, X., Liu, C., Zhang, X., Harada, Y., Chang, Z., and He, X. (2004). A mechanism for Wnt coreceptor activation. Mol Cell *13*, 149-156.

Tammela, T., Sanchez-Rivera, F. J., Cetinbas, N. M., Wu, K., Joshi, N. S., Helenius, K., Park, Y., Azimi, R., Kerper, N. R., Wesselhoeft, R. A., Gu, X., Schmidt, L., Cornwall-Brady, M., Yilmaz, Ö. H., Xue, W., Katajisto, P., Bhutkar, A., and Jacks, T. (2017). A Wnt-producing niche drives proliferative potential and progression in lung adenocarcinoma. Nature *545*, 355-359.

Tanaka, K., Kitagawa, Y., and Kadowaki, T. (2002). Drosophila segment polarity gene product porcupine stimulates the posttranslational N-glycosylation of wingless in the endoplasmic reticulum. J Biol Chem *277*, 12816-12823.

Tao, Q., Yokota, C., Puck, H., Kofron, M., Birsoy, B., Yan, D., Asashima, M., Wylie, C. C., Lin, X., and Heasman, J. (2005). Maternal wnt11 activates the canonical wnt signaling pathway required for axis formation in Xenopus embryos. Cell *120*, 857-871.

Tran, H., and Polakis, P. (2012). Reversible modification of adenomatous polyposis coli (APC) with K63-linked polyubiquitin regulates the assembly and activity of the β-catenin destruction complex. J Biol Chem *287*, 28552-28563.

Umbhauer, M., Djiane, A., Goisset, C., Penzo-Méndez, A., Riou, J. F., Boucaut, J. C., and Shi, D. L. (2000). The C-terminal cytoplasmic Lys-thr-X-X-X-Trp motif in frizzled receptors mediates Wnt/beta-catenin signalling. EMBO J *19*, 4944-4954.

Valvezan, A. J., Zhang, F., Diehl, J. A., and Klein, P. S. (2012). Adenomatous polyposis coli (APC) regulates multiple signaling pathways by enhancing glycogen synthase kinase-3 (GSK-3) activity. J Biol Chem *287*, 3823-3832.

van Amerongen, R., and Nusse, R. (2009). Towards an integrated view of Wnt signaling in development. Development *136*, 3205-3214.

van Bokhoven, H., Celli, J., Kayserili, H., van Beusekom, E., Balci, S., Brussel, W., Skovby, F., Kerr, B., Percin, E. F., Akarsu, N., and Brunner, H. G. (2000). Mutation of the gene encoding the ROR2 tyrosine kinase causes autosomal recessive Robinow syndrome. Nat Genet *25*, 423-426.

van den Heuvel, M., Harryman-Samos, C., Klingensmith, J., Perrimon, N., and Nusse, R. (1993). Mutations in the segment polarity genes wingless and porcupine impair secretion of the wingless protein. EMBO J *12*, 5293-5302.

Vincent, J. P., Oster, G. F., and Gerhart, J. C. (1986). Kinematics of gray crescent formation in Xenopus eggs: the displacement of subcortical cytoplasm relative to the egg surface. Dev Biol *113*, 484-500.

Vinson, C. R., Conover, S., and Adler, P. N. (1989). A Drosophila tissue polarity locus encodes a protein containing seven potential transmembrane domains. Nature *338*, 263-264.

Wallingford, J. B., Fraser, S. E., and Harland, R. M. (2002). Convergent extension: the molecular control of polarized cell movement during embryonic development. Dev Cell *2*, 695-706.

Wallingford, J. B., Rowning, B. A., Vogeli, K. M., Rothbacher, U., Fraser, S. E., and Harland, R. M. (2000). Dishevelled controls cell polarity during Xenopus gastrulation. Nature *405*, 81-85.

Wallingford, J. B., Vogeli, K. M., and Harland, R. M. (2001). Regulation of convergent extension in Xenopus by Wnt5a and Frizzled-8 is independent of the canonical Wnt pathway. Int J Dev Biol *45*, 225-227.

Wang, J., Hamblet, N. S., Mark, S., Dickinson, M. E., Brinkman, B. C., Segil, N., Fraser, S. E., Chen, P., Wallingford, J. B., and Wynshaw-Boris, A. (2006a). Dishevelled genes mediate a conserved mammalian PCP pathway to regulate convergent extension during neurulation. Development *133*, 1767-1778.

Wang, Y., Guo, N., and Nathans, J. (2006b). The role of Frizzled3 and Frizzled6 in neural tube closure and in the planar polarity of inner-ear sensory hair cells. J Neurosci *26*, 2147-2156.

Wehrli, M., Dougan, S. T., Caldwell, K., O'Keefe, L., Schwartz, S., Vaizel-Ohayon, D., Schejter, E., Tomlinson, A., and DiNardo, S. (2000). arrow encodes an LDL-receptor-related protein essential for Wingless signalling. Nature *407*, 527-530.

White, J., Mazzeu, J. F., Hoischen, A., Jhangiani, S. N., Gambin, T., Alcino, M. C., Penney, S., Saraiva, J. M., Hove, H., Skovby, F., Kayserili, H., Estrella, E., Vulto-van Silfhout, A. T., Steehouwer, M., Muzny, D. M., Sutton, V. R., Gibbs, R. A., Baylor-Hopkins, C. F. M. G., Lupski, J. R., Brunner, H. G., van Bon, B. W., and Carvalho, C. M. (2015). DVL1 frameshift mutations clustering in the penultimate exon cause autosomal-dominant Robinow syndrome. Am J Hum Genet *96*, 612-622.

Willert, K., Brown, J. D., Danenberg, E., Duncan, A. W., Weissman, I. L., Reya, T., Yates, J. R., and Nusse, R. (2003). Wnt proteins are lipid-modified and can act as stem cell growth factors. Nature *423*, 448-452.

Wong, H. C., Bourdelas, A., Krauss, A., Lee, H. J., Shao, Y., Wu, D., Mlodzik, M., Shi, D. L., and Zheng, J. (2003). Direct binding of the PDZ domain of Dishevelled to a conserved internal sequence in the C-terminal region of Frizzled. Mol Cell *12*, 1251-1260.

Wu, J., Roman, A. C., Carvajal-Gonzalez, J. M., and Mlodzik, M. (2013). Wg and Wnt4 provide long-range directional input to planar cell polarity orientation in Drosophila. Nat Cell Biol *15*, 1045-1055.

Xu, Q., Wang, Y., Dabdoub, A., Smallwood, P. M., Williams, J., Woods, C., Kelley, M. W., Jiang, L., Tasman, W., Zhang, K., and Nathans, J. (2004). Vascular development in the retina and inner ear: control by Norrin and Frizzled-4, a high-affinity ligand-receptor pair. Cell *116*, 883-895.

Yamamoto, H., Kitadai, Y., Yamamoto, H., Oue, N., Ohdan, H., Yasui, W., and Kikuchi, A. (2009). Laminin gamma2 mediates Wnt5a-induced invasion of gastric cancer cells. Gastroenterology *137*, 242-52, 252.e1.

Yamamoto, S., Nishimura, O., Misaki, K., Nishita, M., Minami, Y., Yonemura, S., Tarui, H., and Sasaki, H. (2008). Cthrc1 selectively activates the planar cell polarity pathway of Wnt signaling by stabilizing the Wnt-receptor complex. Dev Cell *15*, 23-36.

Yan, K. S., Janda, C. Y., Chang, J., Zheng, G. X. Y., Larkin, K. A., Luca, V. C., Chia, L. A., Mah, A. T., Han, A., Terry, J. M., Ootani, A., Roelf, K., Lee, M., Yuan, J., Li, X., Bolen, C. R., Wilhelmy, J., Davies, P. S., Ueno, H., von Furstenberg, R. J., Belgrader, P., Ziraldo, S. B., Ordonez, H., Henning, S. J., Wong, M. H., Snyder, M. P., Weissman, I. L., Hsueh, A. J., Mikkelsen, T. S., Garcia, K. C., and Kuo, C. J. (2017). Non-equivalence of Wnt and R-spondin ligands during Lgr5(+) intestinal stem-cell self-renewal. Nature *545*, 238-242.

Yen, W. W., Williams, M., Periasamy, A., Conaway, M., Burdsal, C., Keller, R., Lu, X., and Sutherland, A. (2009). PTK7 is essential for polarized cell motility and convergent extension during mouse gastrulation. Development *136*, 2039-2048.

Yoshikawa, S., Bonkowsky, J. L., Kokel, M., Shyn, S., and Thomas, J. B. (2001). The derailed guidance receptor does not require kinase activity in vivo. J Neurosci *21*, RC119.

Yu, M., Ting, D. T., Stott, S. L., Wittner, B. S., Ozsolak, F., Paul, S., Ciciliano, J. C., Smas, M. E., Winokur, D., Gilman, A. J., Ulman, M. J., Xega, K., Contino, G., Alagesan, B., Brannigan, B. W., Milos, P. M., Ryan, D. P., Sequist, L. V., Bardeesy, N., Ramaswamy, S., Toner, M., Maheswaran, S., and Haber, D. A. (2012). RNA sequencing of pancreatic circulating tumour cells implicates WNT signalling in metastasis. Nature *487*, 510-513.

Zecca, M., Basler, K., and Struhl, G. (1996). Direct and long-range action of a wingless morphogen gradient. Cell *87*, 833-844.

Zeng, X., Tamai, K., Doble, B., Li, S., Huang, H., Habas, R., Okamura, H., Woodgett, J., and He, X. (2005). A dual-kinase mechanism for Wnt co-receptor phosphorylation and activation. Nature *438*, 873-877.

Zhai, L., Chaturvedi, D., and Cumberledge, S. (2004). Drosophila wnt-1 undergoes a hydrophobic modification and is targeted to lipid rafts, a process that requires porcupine. J Biol Chem *279*, 33220-33227.

Zhang, J., and Carthew, R. W. (1998). Interactions between Wingless and DFz2 during Drosophila wing development. Development *125*, 3075-3085.

Zhang, X., Cheong, S. M., Amado, N. G., Reis, A. H., MacDonald, B. T., Zebisch, M., Jones, E. Y., Abreu, J. G., and He, X. (2015). Notum is required for neural and head induction via Wnt deacylation, oxidation, and inactivation. Dev Cell *32*, 719-730.

Appendix

Figure A1. An antibody derived from peptide B specifically recognizes xWnt8.

Peptide A:

ASAWSVNNFLMTGPKAYLTYSASVAVGAQNGIEECKYQFAWERWNCPESTLQLATHNGLRSAT
RETSFVHAISSAGVMYTLTRNCSMGDFDNCGCDDSRNHHHHHHHHH*

Peptide B:

LQLAEFRDIGNHLKIKHDQALKLEMDKRKMRSGNSADNRGAIADAFSSVAGSELIFLEDSPDYCL
KNISLGLQGTEGRECLQSGKNLSQWERRSCKRLCTDCGLRVEEKKTEHHHHHHHH*

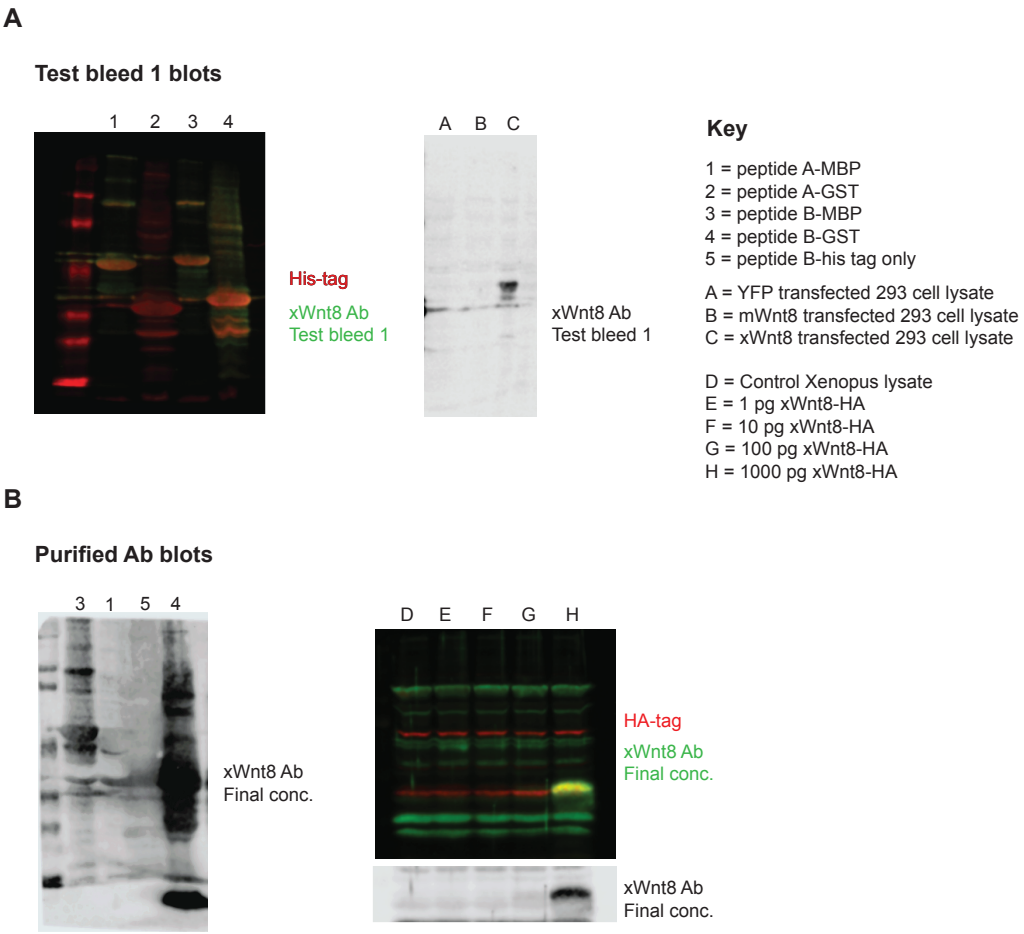

Figure A1. An antibody derived from peptide B specifically recognizes xWnt8.

(A) The xWnt8 antibody Test bleed 1 detects peptide B and xWnt8 with high specificity. Peptides A and B were expressed as both maltose-binding protein (MBP) and glutathione-S transferase (GST) fusion proteins in *E. coli*. MBP constructs were chosen based on their higher solubility and purified over an amylose column using standard methods. On the left Western, purified MBP peptides were run in lanes 1 and 3. Whole cell lysates of *E. coli* expressing GST fusion proteins were run in lanes 2 and 4. Gels were run and transferred and probed with a 1:500 dilution of Test bleed 1 (November, 2013) as well as an anti-His-tag antibody. In the right Western, whole cell lysates derived from 293 cells transfected with 1 ng of plasmid DNA encoding YFP (lane A), mWnt8 (lane B) or xWnt8 (lane C) were probed with a 1:500 dilution of Test bleed 1. To note, mWnt8 expression was previously confirmed in these lysates by IP (experiment date: 1/31/13). (B) The purified xWnt8 antibody detects peptide B and xWnt8 in *Xenopus* lysates. The peptide B-GST construct was expressed in *E. coli*, purified on a GST column using standard methods, and coupled to the column of an EpiMAX Affinity Purification Kit and used for the purification and concentration of the xWnt8 antibody. The resulting Ab (137 μM) was diluted 1:500 and used to confirm peptide B recognition (left). To ensure that the antibody specifically recognizes xWnt8 in *Xenopus* lysates, I injected 1 – 1000 pg of xWnt8-HA into embryos and probed whole cell lysates (right) with both the xWnt8 antibody and an HA epitope antibody.

Figure A2. Notum inhibits both acylated and non-acylated Wnt signaling.

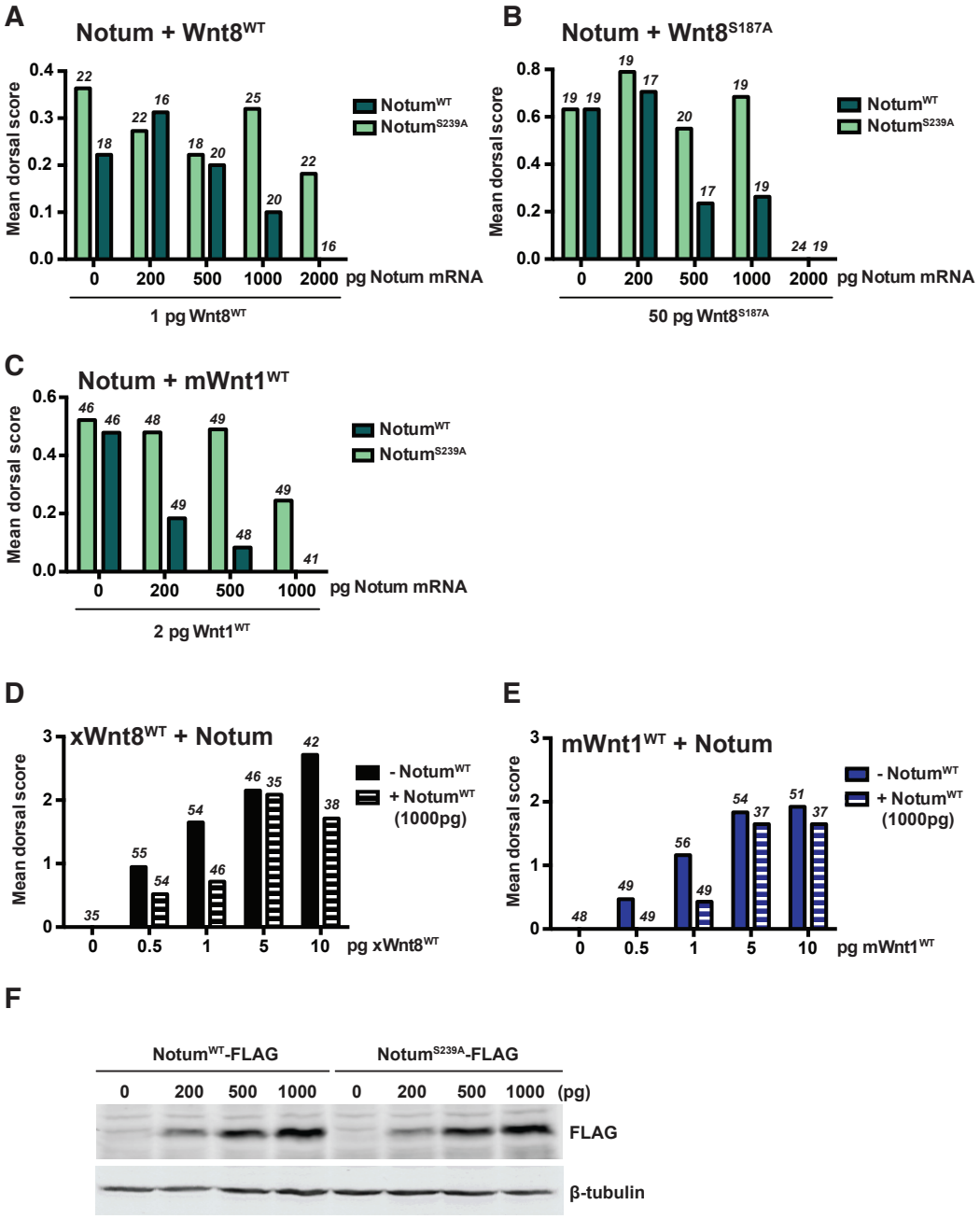

Figure A2. Notum inhibits both acylated and non-acylated Wnts. Notum inhibits xWnt8^{WT}, xWnt8^{S187A} and mWnt1^{WT}. For the experiments shown in A-C, *Wnt* and *Notum* mRNA were co-injected into the VMZ of four-cell stage embryos. The dose of Wnt was held constant and a dose curve of Notum^{WT} (dark green) or Notum^{S239A} (light green) was co-injected. Mean dorsal scores were calculated for all treatment groups at the tailbud stages. Curiously, I found that (A) xWnt8^{WT} – 1 pg (n=1), (B) xWnt8^{S187A} – 50 pg (n=1) and (C) mWnt1^{WT} – 2 pg (n=2) were all inhibited by both Notum^{WT} and Notum^{S239A} (enzymatically inactive version – Kakugawa et al., 2015). To eliminate any interactions between mRNAs or proteins within the cell, I next expressed Notum and Wnt from separate cells of the embryo. In the experiments shown in D – E, I injected *Notum* mRNA into a four-cell stage embryo at one ventral blastomere. Embryos received either *YFP* alone or 1000 pg *Notum^{WT}* mRNA. I let these embryos develop until the eight-cell stage, when I injected both the YFP-only and Notum^{WT}-expressing clutches with doses of either (D) *xWnt^{WT}* (n=3) or (E) *mWnt1^{WT}* (n=3) mRNA concentrations between 0.5 – 10 pg at the neighboring ventral blastomere. Mean dorsal scores were calculated for all treatment groups at the tailbud stages. (F) Notum^{WT} and Notum^{S239A} are expressed equally in *Xenopus* embryos. Whole embryo lysates were obtained from Notum-expressing embryos and probed with an anti-FLAG antibody to detect the epitope tag on Notum.